TECHNICAL REPORT 87-13

GRIMSEL TEST SITE

ANALYSIS OF RADAR MEASUREMENTS PERFORMED AT THE GRIMSEL ROCK LABORATORY IN OCTOBER 1985

L. Falk
K.-Å. Magnusson
O. Olsson
M. Ammann
H.R. Keusen
G. Sattel

FEBRUARY 1988

Nagra
Nationale
Genossenschaft
für die Lagerung
radioaktiver Abfälle

Cédra
Société coopérative
nationale
pour l'entreposage
de déchets radioactifs

Cisra
Società cooperativa
nazionale
per l'immagazzinamento
di scorie radioattive

TECHNICAL REPORT 87-13

GRIMSEL TEST SITE

ANALYSIS OF RADAR MEASUREMENTS PERFORMED AT THE GRIMSEL ROCK LABORATORY IN OCTOBER 1985

L. Falk
K.-Å. Magnusson
O. Olsson
M. Ammann
H.R. Keusen
G. Sattel

FEBRUARY 1988

GRIMSEL TEST SITE / SWITZERLAND
A JOINT RESEARCH PROGRAM BY

- NAGRA — National Cooperative for the Storage of Radioactive Waste, Baden, Switzerland
- BGR — Federal Institute for Geoscience and Natural Resources, Hannover, Federal Republic of Germany
- GSF — Research Centre for Environmental Sciences, Munich, Federal Republic of Germany

Parkstrasse 23 5401 Baden/Schweiz Telephon 056/20 55 11

FOREWORD

Concepts which foresee the disposal of radioactive waste in geological formations lay great weight on acquiring knowledge of the proposed host rock and the surrounding rock strata. For this reason, Nagra has, since May 1984, been operating the Grimsel Test Site which is situated at a depth of 450 m in the crystalline formation of the Aar Massif. The general objectives of the research being carried out in this system of test tunnels include, in particular

- the build-up of know-how in planning, performing and interpreting underground experiments in different scientific fields and

- the aquisition of practical experience in developing, testing and applying test equipment and measuring techniques.

The Test Site (GTS) is operated by Nagra. On the basis of a German-Swiss cooperation agreement, the various experiments are carried out by Nagra, the Federal Institute for Geoscience and Natural Resources (BGR) and the Research Centre for Environmental Sciences (GSF); the latter two bodies are supported in this venture by the German Federal Ministry for Research and Technology (BMFT).

NTB 85-47 gives an overview of the GTS and a review of the status of the investigation programme as at August 1985.

VORWORT

Bei Konzepten, die die Endlagerung radioaktiver Abfälle in geologischen Formationen vorsehen, ist die Kenntnis des Wirtgesteins und der angrenzenden Gesteinsschichten von grundlegender Bedeutung. Die Nagra betreibt deshalb seit Mai 1984 das Felslabor Grimsel in 450 m Tiefe im Kristallin des Aarmassivs. Die generelle Zielsetzung für die Arbeiten in diesem System von Versuchsstollen umfasst insbesondere

- den Aufbau von Know-how in der Planung, Ausführung und Interpretation von Untergrundversuchen in verschiedenen Experimentierbereichen und

- den Erwerb praktischer Erfahrung in der Entwicklung, Erprobung und dem Einsatz von Testapparaturen und Messverfahren.

Das Felslabor (FLG) wird durch die Nagra betrieben. Die verschiedenen Untersuchungen werden aufgrund eines deutsch-schweizerischen Zusammenarbeitsvertrages durch die Nagra, die Bundesanstalt für Geowissenschaften und Rohstoffe (BGR) und die Gesellschaft für Strahlen- und Umweltforschung (GSF) durchgeführt, beide gefördert vom Deutschen Bundesministerium für Forschung und Technologie (BMFT).

Eine Uebersicht des FLG und die Zusammenfassungen der Untersuchungsprogramme sind mit Status August 1985 im NTB 85-47 enthalten.

Der vorliegende Bericht wurde im Rahmen der Zusammenarbeit zwischen den drei Partnern erstellt. Die Autoren haben ihre eigenen Ansichten und Schlussfolgerungen dargelegt. Diese müssen nicht unbedingt mit denjenigen der Nagra, BGR oder GSF übereinstimmen.

AVANT-PROPOS

La connaissance de la roche d'accueil et des couches rocheuses avoisinantes est d'importance fondamentale pour l'élaboration de concepts prévoyant le stockage de déchets radioactifs dans des formations géologiques. C'est pour cela que la Cédra exploite depuis mai 1984 le laboratoire souterrain du Grimsel à 450 m de profondeur dans le cristallin du massif de l'Aar. Les objectifs généraux des travaux menés dans ce complexe de galeries d'essais comprennent notamment:

- la constitution d'un savoir-faire dans la préparation, l'exécution et l'interprétation d'essais souterrains dans divers domaines et

- l'acquisition d'expérience pratique dans le développement, la mise à l'épreuve et l'engagement d'appareillages d'essais et de techniques de mesure.

Le laboratoire souterrain est exploité par la Cédra. Les différentes recherches sont réalisées dans le cadre d'un accord de collaboration germano-suisse par la Cédra, la "Bundesanstalt für Geowissenschaften und Rohstoffe" (BGR) et la "Gesellschaft für Strahlen- und Umweltforschung" (GSF), ces deux dernières instances étant soutenues par le Ministère allemand pour la recherche et la technologie (BMFT).

Un aperçu du laboratoire souterrain et un résumé des programmes de recherches apparaissent dans le rapport NTB 85-47 d'août 1985.

Le présent rapport a été élaboré dans le cadre de la collaboration entre les trois partenaires. Les auteurs ont présenté leurs vues et conclusions personnelles. Celles-ci ne doivent pas forcément correspondre à celles de la Cédra, de la BGR et de la GSF.

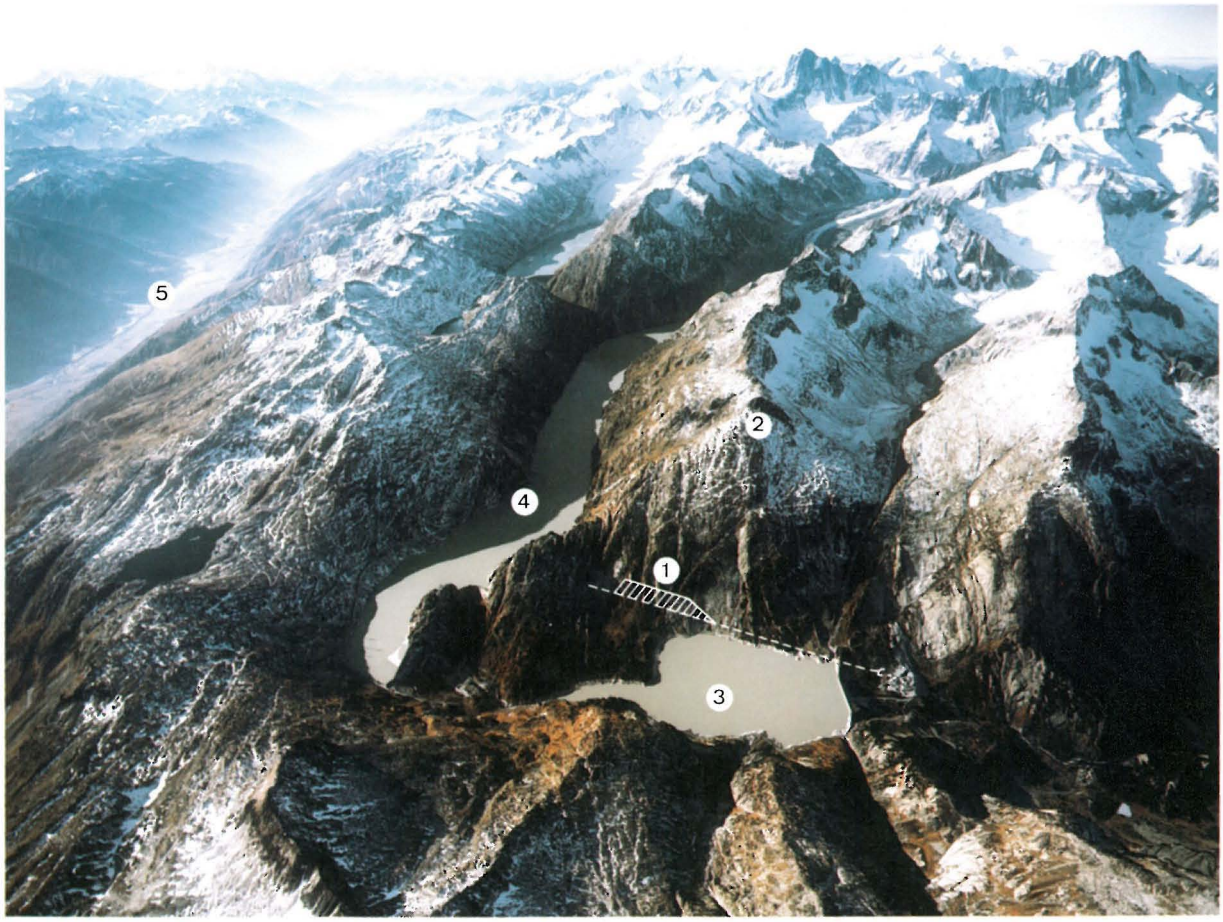

GRIMSEL-GEBIET

Blick nach Westen

1 Felslabor
2 Juchlistock
3 Räterichsbodensee
4 Grimselsee
5 Rhonetal

GRIMSEL AREA

View looking West

1 Test Site
2 Juchlistock
3 Lake Raeterichsboden
4 Lake Grimsel
5 Rhone Valley

FLG FELSLABOR GRIMSEL
GTS *GRIMSEL TEST SITE*

Situation

0 100 m

- Zugangsstollen/*Access tunnel*
- Fräsvortrieb/*by tunnel boring machine*
- Sprengvortrieb/*excavated by blasting*
- Zentraler Aaregranit ZAGR / *Central Aaregranite CAGR*
- Biotitreicher ZAGR / *CAGR with high content of biotite*
- Grimsel-Granodiorit / *Grimsel-Granodiorite*
- Scherzone/*Shear zone*
- Lamprophyr/*Lamprophyre*
- Wasserzutritt/*Water inflow*
- SB Sondierbohrung/*Exploratory borehole*
- US US Bohrung/*US borehole*

ZB	Zentraler Bereich/*Central facilities*
AU	Auflockerung/*Excavation effects*
BK	Bohrlochkranz/*Fracture system flow*
EM	El.magn. HF-Messungen/*-measurements*
FRI	Kluftzone/*Fracture zone investigation*
GS	Gebirgsspannungen/*Rock stresses*
HPA	Hydr. Parameter/*Hydr. parameters*
MI	Migration/*Migration*
MOD	Hydrodyn. Modellierung/*H. modeling*
NM	Neigungsmesser/*Tiltmeters*
UR	Untertageradar/*Underground radar*
US	Seismik/*Underground seismic testing*
VE	Ventilationstest/*Ventilation test*
WT	Wärmeversuch/*Heat test*

A — A Schnitt/*Section*

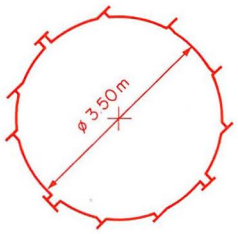

6/88

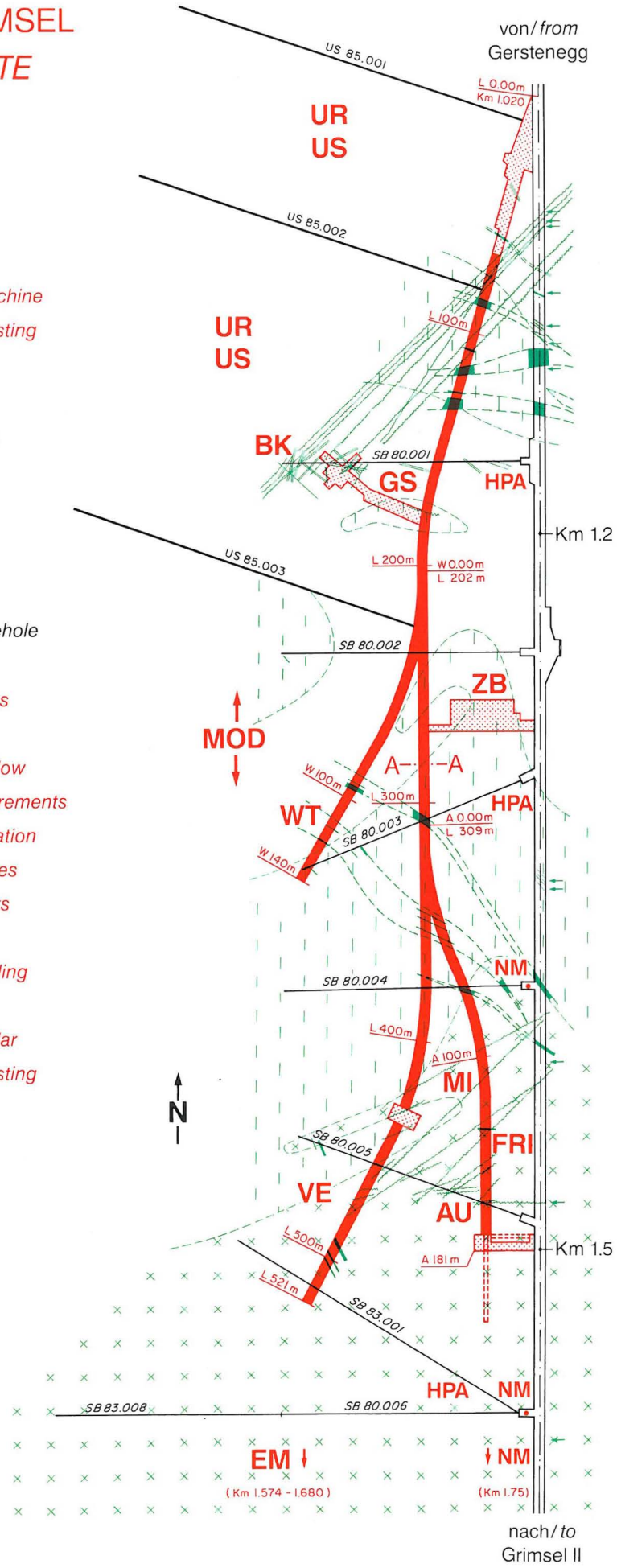

SUMMARY

In october 1985 Swedish Geological Co. conducted a radar reflection survey at Grimsel Test Site to map discontinuities in the rock mass of the Underground Seismic (US) test field. These measurements first designed as a test of the equipment at that specific site allowed a comprehensive interpretation of the geometrical structure of the test field.

The geological interpretation of the radar reflectors observed is discussed and a possible way is shown to construct a geological model of a site using the combination of radar results and geological information. Additionally to these results the report describes the radar equipment and the theoretical background for the analysis of the data.

The main geological features in the area under investigation, situated in the "Zentraler Aaregranit", are lamprophyre dykes and fracture/shear zones. Their position and strike have been determined using single- and crosshole radar data, SABIS data (accoustic televiewer) as well as existing geological information from the boreholes or the drifts under the assumption of steep dipping elements (70 to 90°).

ZUSAMMENFASSUNG

Im Oktober 1985 führte Swedish Geological Co. eine Radar-Messkampagne durch mit dem Ziel, Inhomogenitäten im Untertageseismik-Testbereich des Felslabors Grimsel zu kartieren. Diese Messungen, die zunächst nur Aufschluss über die Einsatzfähigkeit der Radargeräte im Felslabor geben sollten, erlaubten eine umfassende Interpretation der geometrischen Lage der Inhomogenitäten im Testgebiet.

Der vorliegende Bericht beschreibt detailliert die geologische Deutung der gefundenen Radarreflektoren. Der Bericht will einen möglichen Weg aufzeigen, wie die Resultate einer Radarkampagne unter Ausnützung der vorhandenen geologischen Kenntnisse zu einem geologischen Modell eines Standortes verknüpft werden können. Zudem werden die verwendeten Messgeräte sowie die theoretischen Grundlagen für die Auswertung der gewonnen Daten beschrieben.

Das Untersuchungsgebiet liegt im Bereich des Zentralen Aaregranites. Als geologische Inhomogenitäten treten vor allem Lamprophyre und Bruch- bzw. Scherzonen auf. Unter Ausnutzung der Tatsache, dass diese Elemente mit 70 - 90° gegen die Horizontalebene (d.h. nahezu vertikal) einfallen, liessen sich wahre Lagebestimmungen durchführen mittels Auswertung von SABIS - Logs, crosshole - Reflexionen und geologischen Aufschlussverhältnissen.

RESUME

En octobre 1985 la compagnie Swedish Geological a effectué une campagne de mesures radar dans le but de localiser les inhommogénéités dans la zone d'essais sismiques du laboratoire souterrain du Grimsel. Ces mesures, qui devaient d'abord montrer la mise en application des appareils radar sur le terrain, ont permis une interprétation très complète de la position géométrique des inhommogénéités dans le domaine testé.

Ce rapport décrit de façon détaillée la signification géologique des réflécteurs radar détectés. Il contient aussi un cheminement possible pour l'établissement d'une relation entre les résultats d'une campagne radar et un modèle géologique en tenant compte des informations géologiques à disposition. A ce propos les bases théoriques de l'interprétation des données et les appareils de mesure utilisés sont décrits.

Le domaine de recherche se trouve dans la partie centrale du massif de l'Aare. Les inhommogénéités géologiques principales sont des lamprophyres et des zones de fractures ou de cisaillements. La location réelle de ces éléments peut être dérivée en tenant compte du fait que leur pendage est de 70 à 90°, soit pratiquement vertical, et en utilisant les diagraphies SABIS, les réflexions entre puits (crosshole) et les données géologiques existantes (forages, galeries...).

TABLE OF CONTENTS

TABLE OF CONTENTS

TABLE OF CONTENTS Page

LIST OF APPENDICES

Appendix 1: Enclosures

LIST OF APPENDICES

Appendix 2: Tables

LIST OF FIGURES

LIST OF FIGURES

LIST OF TABLES

1. INTRODUCTION

During the last ten years, high frequency electromagnetic investigations also called Radar have become an important factor in mineral exploration (Nickel 1983).

For waste disposal projects in saline and crystalline rocks the application of Radar techniques have been found a suiTable tool for host rock characterization, which means detecting and identifying the extent of discontinuities or the host rock boundaries. Therefore a special Radar System (RAMAC) designed for fracture detection in crystalline rock has been developed and extensively tested in the Stripa mine within the Stripa II project, which is managed by the Swedish Nuclear Fuel and Waste Management Company (SKB).

Impressed by the progressive design of this radar system (fiber optic telemetry) allowing a fast and easy field work and encouraged by the results achieved in the Stripa granite, Nagra decided to test the efficiency of the RAMAC-system in the geological environment of the Grimsel Test Site.

The objective of the test measurements was to investigate the potential of the Radar for fracture mapping in reflection mode and to get basic data on the signal range in transmission mode for a Radar tomography project under consideration.

Single hole and cross hole measurements were performed successfully in the Grimsel Test Site during October 1985. Within the investigation radius of the Radar of about 150 m in the Grimsel Granite, a lot more reflections than expected were recorded from fractured zones and dyke rocks.

Following a presentation at the technical expert meeting (TFG 3) it was recommended to interpret the Radar data extensively and to investigate its potential input for the establishment of a geological site model.

Taking into account the time limits of a standard repository exploration; the task was to work out such a geological model during a three day workshop.

This workshop was held in April 1986 including Radar specialists and scientists familiar with the site.

The interpretations presented in the following report are basically the results of the workshop with some additional detail for presentation purposes.

To give a better understanding on Radar investigations, i.e. advantages and limits of this new method, the first part of this report contains a detailed description of the Radar system as well as some basic information necessary for futher interpretation.

2. GRIMSEL TEST SITE - THE SUBSURFACE SEISMIC TEST AREA (US)

2.1 Site description

The subsurface seismic test area (US) is situated at the northern part of the Grimsel Test Site (**Fig. 1**). It is of nearly rectangular shape with the dimensions of approximately 200 by 450 m. The northern boundary of the area is situated at meter 950 of the main access tunnel while the southern part of the site includes the heat test tunnel (WT). The easterly border is defined by the laboratory tunnel. From here the site under investigation extends approximately 200 m in WNW-direction. The test areas GS (rock stress test) and BK (fracture system flow test) are located within the seismic test zone according to Figure 1. In this area 3 boreholes (BOUS 85.001-85.003) were drilled to perform seismic and electromagnetic (radar) investigations. The maximum depth of these holes is 150 m. The laboratory tunnel and the holes are located in a plane dipping 15° to the horizontal plane in a WNW-direction (290°).

2.2 Geology

2.2.1 Overview

The US area is situated in the Central Aaregranite (ZAGr). The ZAGr is a compact solid rock whose main components are quartz, K-feldspar and plagioclase. The biotite content as well as the degree of the foliation of the ZAGr is variable. Further important rocks in the investigation area are lamprophyres which are aligned mainly in two distinct directions. Information on the discontinuities at the Grimsel Test Site (FLG) is summarized in **Table 1** (see NTB 85-46). The following interpretations are based on the assumption that most of these structures (joint systems, foliations and lamprophyres) dip in a nearly vertical direction.

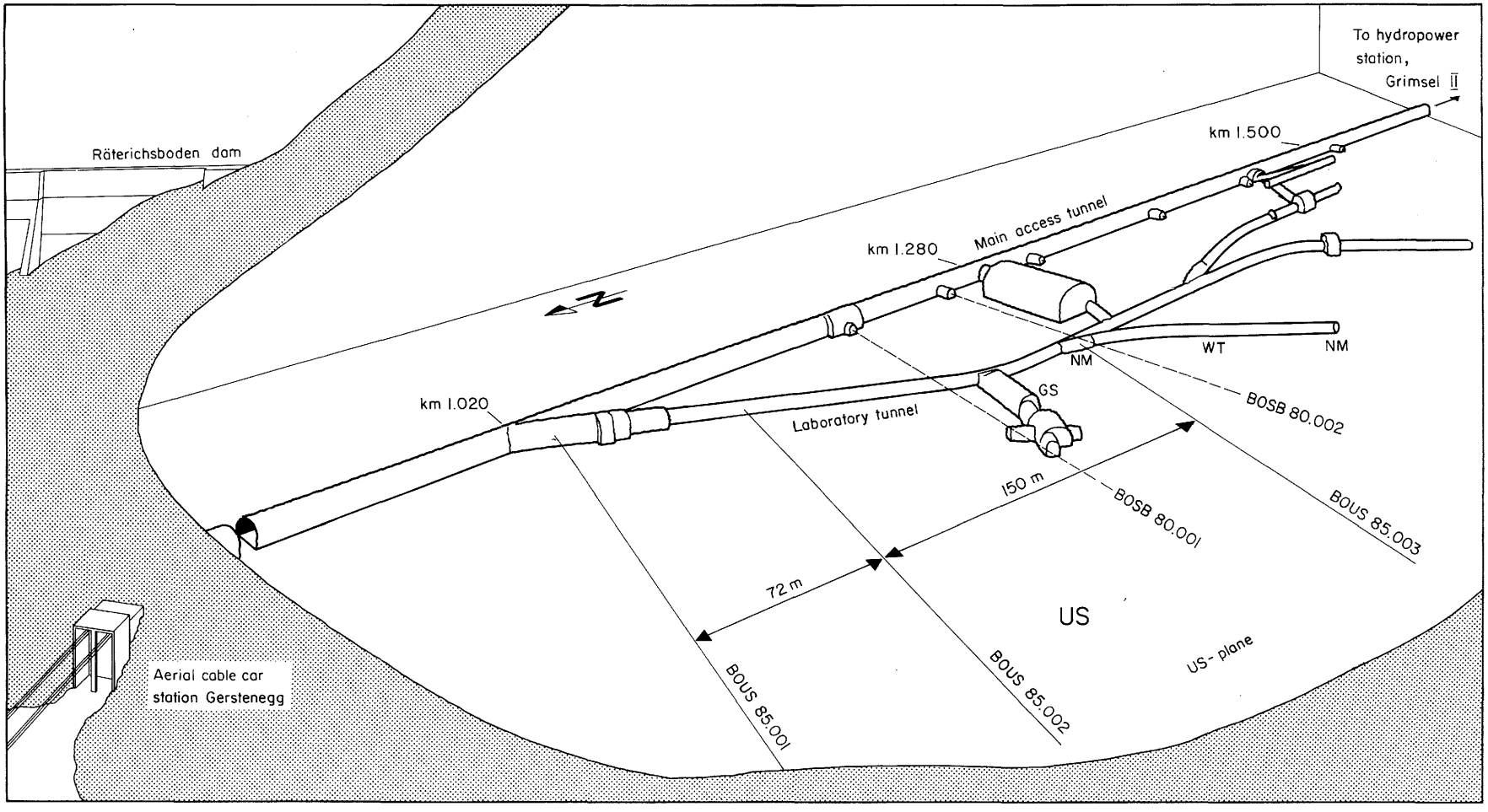

Figure 1: The subsurface seismic test area (US)

LEGEND

BK Bohrlochkranzversuch (Fracture system flow test)

GS Gebirgsspannungen (Rock stress measurements)

NM Neigungsmesser (Tiltmeter test)

US Untertageseismik (Underground seismic testing, subsurface seismic test area)

WT Wärmetest (Heat test)

US-plane Plane built up by the three boreholes BOUS85.001-003

2.2.2 Geological profiles of the drillholes BOUS 85.001-85.003

The investigations were carried out for the 3 drillholes mentioned in Chapter 2.1.
Short description of the boreholes follows:

BOUS 85.001: The entire length of this borehole is comprised entirely of leuco- and mesocratic-ZAGr. Only 1 very narrow zone of lamprophyres was found. The borehole is crossed by two narrow fracture zones at 12 to 13.5 m and 78 to 80 m depth. Only minor water circulation was observed within the drillhole.

BOUS 85.002: Leuco- and mesocratic-ZAGr was found which is similar to the one observed in BOUS 85.001. A zone of lamprophyres is located at a depth of 5 to 6.5 m. The number of fracture zones is larger than in BOUS 85.001. The most important ones are present at 13 to 17 m and 55 to 70 m depth.
A very inhomogenous zone exists between 76 and 86 m depth consisting of quartz dykes, folded rocks and hydrothermally altered ZAGr. This zone is followed by cataclastic to kakiritic deformed rocks. Major amounts of water flow have been observed at 14 to 17 m, 56 m and 112.5 m.

BOUS 85.003: This borehole was drilled through leuco- and mesocratic-ZAGr which is partly porphyritic. 5 lamprophyres were found in this hole. They are 0.1 to 2.4 m thick and partly intensively fractured. Important fracture zones are located between 58 to 64 m and mainly between 90 to 120 m.
In the depth range of 98 and 123 m there are major inflows of water which cannot be exactly located.

Quartz veins and hydrothermally altered ZAGr are observed within all 3 drillholes.

System	Average direction of dipping/dip angle	Number of fabric elements considered	Characteristics	Genetic interpretation
s_1	142/77	639	- Alignment of the rock-forming minerals (stratification of matter) - Shear zones	Youngest, alpine schistosity
s_2	157/75	519		Older schistosity, possibly early alpine
s_3	183/65	271	- Generally rare, readjustment of mica Shear zone in SB 5	Oldest schistosity, possibly hercynian
k_1	53 + 233/80	292		Most important lateral fracture system (age uncertain, alpine and hercynian
k_2	19 + 199/78	124	Rare joints with biotite and chlorite	Possibly hercynian fracture system
k_3	264/84	144	Relatively rare. Joint planes with high degree of separation. Mostly coated with fissure-chlorite	Probably hercynian lateral fracture system
k_4	297 + 117/62	163		
k_5	336/42	singly	Relatively rare, mainly observed at the surface	
k_6/z	subhorizontal	73	Alpine tension fissures partly developed as thin quartz veins (15/20)	Youngest mineral formation +/- 13 mio. years ago at temperatures of 350° - 400° C
ℓ	216/80 and 242/80	186	Lamprophyre contacts	Parallel to k_1, poss. k_2
t	no systematic direction	-	Stress relaxation joints observed to 150 m below ground surface	Youngest fractures caused by stress relaxation

Table 1: Foliations, joint systems and lamprophyres found at Grimsel Test Site (from Nagra, NTB 85-46)

2.2.3 The inventory of geological and geophysical data

Information on the available geological and geophysical data of the US area is given in **Table 2.** The geophysical data consist of the following logs: Sonic, single point resistivity, focussed electric resistivity, spontaneous potential, gamma ray, density, neutron porosity, dipmeter, and acoustic televiewer (SABIS).

	Geophysical data	Geological data
Main access tunnel	-	+
Laboratory tunnel	-	+
US test area		
Boreholes (3)		
BOUS 85.001-003	+	+
GS test area		
Cavern	-	+
Boreholes (2)	+*	+
BK test area		
Cavern	-	+
Boreholes	+*	+
NM test area		
Boreholes (2)		
WT test area		
Tunnel	-	+
Boreholes	-	+
	* partly	

Table 2: Inventory of geological and geophysical data in the US area

3. THE TECHNIQUE OF ELECTROMAGNETIC (RADAR) INVESTIGATIONS

3.1 The RAMAC borehole radar system - description of the equipment

The radar system, RAMAC, used for these measurements, has been developed by the Swedish Geological Co. (SGAB) as a part of the International Stripa Project. Continued development of the system has been funded by the Swedish Nuclear Fuel and Waste Management Company (SKB) in order to construct a system adapted for field work on a production basis.

The radar system can be classified as a short pulse system, which means that the length of the pulse transmitted into the rock will be approximately one wavelength. The system works in principle in the following manner: A short current pulse is fed to the transmitter antenna, which generates a radar pulse that propagates through the rock. The pulse is made as short as possible to maximize the resolution. The receiver antenna is of the same type as the transmitter. The acquired pulse is amplified and registered as a function of time. The receiver may be located in the same borehole as the transmitter or in any other borehole. The borehole radar system can provide data on the distance (travel time) to a reflector, the strength of the reflection, as well as the attenuation and delay of the direct wave between transmitter and receiver (Olsson et al., 1985 b).

The radar system consists of four different parts:

- a microcomputer with two 5 1/4 inch floppy disc units which controls measurements, data storage, data presentation, and signal analysis
- a control unit for timing control, storage and stacking of single radar traces
- a borehole transmitter to transmit short radar pulses
- a borehole receiver to detect and digitize the radar pulses.

A summary of the technical specifications of the system is given in **Table 3.**

General	
Frequency range	20-80 MHz
Total dynamic range	150 dB
Sampling time accuracy	1 ns
Maximum optical fiber length	1000 m
Outer diam. of transmitter/receiver	48 mm
Maximum operating pressure	100 Bar
Operating temperature range	0-40 °C
Transmitter	
Peak power	500 W
Operating time	10 h
Length	4.8 m
Weight	16 kg
Receiver	
Bandwidth	10-200 MHz
A/D converter	16 bit
Least significant bit at antenna terminals	1 µV
Data transmission rate	1.2 MBaud
Operating time	10 h
Length	5.4 m
Weight	18 kg
Control unit	
Microprocessor	RCA 1806
Clock frequency	5 MHz
Pulse repetition frequency	43.1 kHz
Sampling frequency	30-500 MHz
No of samples	256-4096
No of stacks	1-32767
Time window	0-11 µs

Table 3: Technical specifications for the RAMAC borehole radar system

3.2 The procedure of radar measurements

3.2.1 Singlehole measurements (reflection measurements)

In a singlehole reflection measurement the transmitter and receiver are put into the same hole and the distance between the probes is kept constant. The transmitter - receiver array is moved stepwise into the hole and a sequence of equidistant measurements is carried out using 1 m increments. For the measurements performed at Grimsel the probes were separated by 10 m of glass fiber rods, giving a separation of 15 m between the midpoints of the antennas.

The measurement procedure is relatively simple. After initialization of a data disc and selection of input parameters, the borehole probes are put into the borehole and the measurement is started. When the measurement of a trace is completed the computer unit indicates by an audio signal that the operator has to move the probes to the next position. The probes are pushed into the holes using glass fiber push rods with a length of 2 m. The measurement at each position takes about 30-60 s depending on the number of stacks and samples. For 50-100 m interval of a borehole the data acquisition time is about 1 hour if one meter steps between the measurements are used.

The principle of ray propagation for a singlehole measurement is shown by the ray-paths in **Figure 2.** The upper part of this figure illustrates the transmitter-receiver configuration and the raypaths to the reflecting elements (diffractor and planar reflector) while the lower part schematically shows the image of the reflectors in a reflectogram. As indicated by Figure 2 a planar element which intersects the drillhole just gives one linear reflection element in the case of transmitter receiver positions which are exclusively located at one side of the reflector.

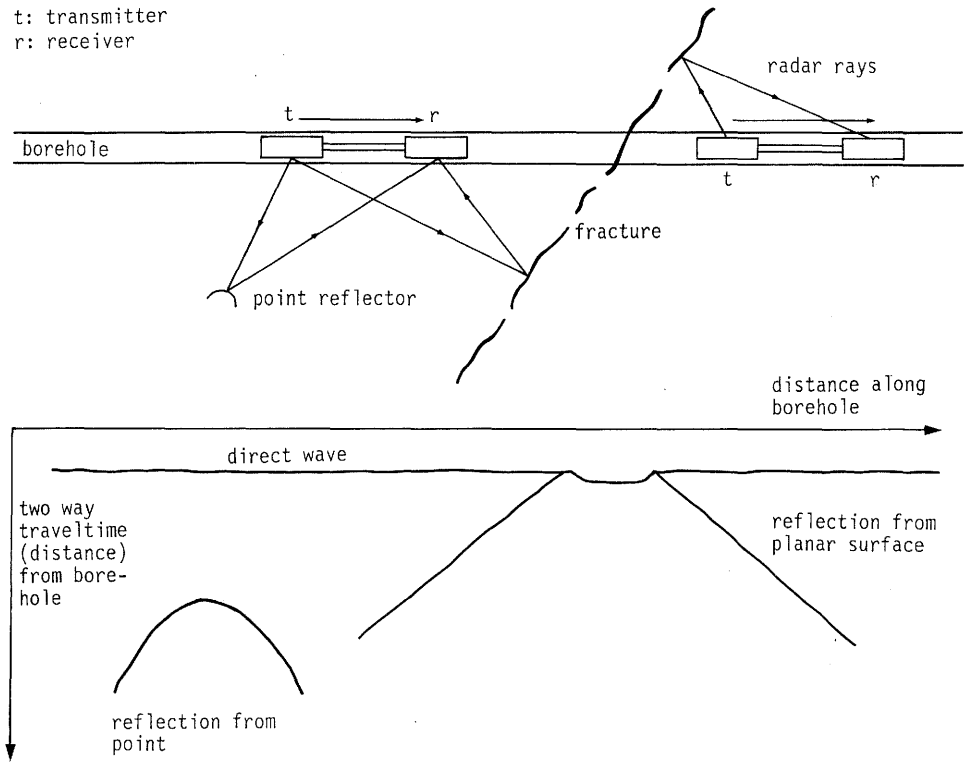

Figure 2: Principle of singlehole measurement

3.2.2 Crosshole measurements

The crosshole measurements were performed as crosshole scans. For crosshole scanning the receiver (or transmitter) is kept at a fixed position in one borehole while the transmitter (or receiver) is moved in small increments in another hole.

The crosshole measurements are used to detect velocity, attenuation and other physical properties of the area under investigation as a function of space. In the case of good azimuthal coverage of the area by the electromagnetic rays it is possible to calculate reliable tomograms as parameter cross sections of the area.

Crosshole measurements are mainly undertaken to observe the attenuation of the transmitted waves but in special cases of source-reflector-receiver positions the observations also show reflected energy (**Fig. 3**).

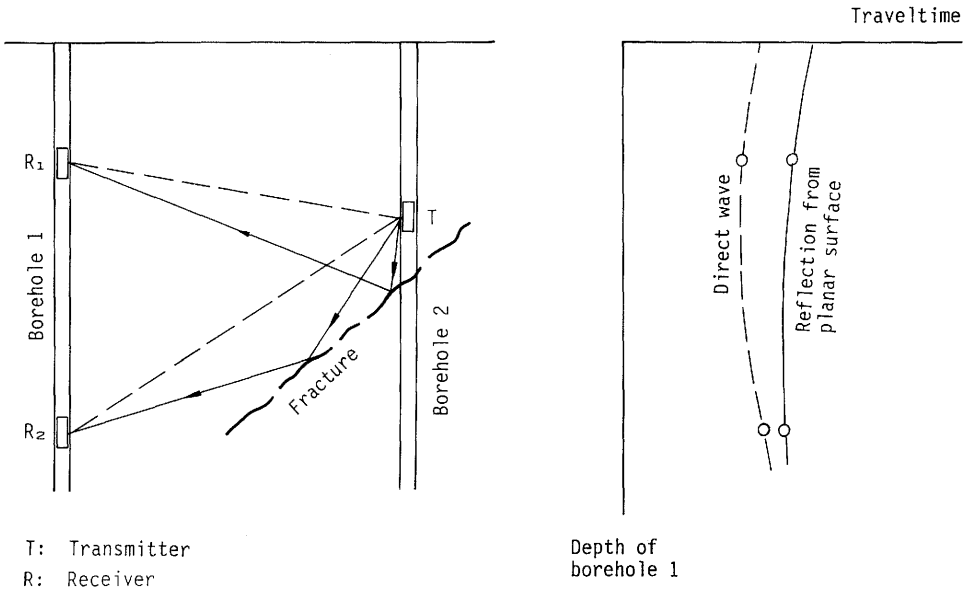

Figure 3: Principle of crosshole measurement

3.3 Data processing

The raw data set contains some spurious signals which should be removed in order to obtain high quality displays of the radar data.

First a DC-level offset is removed from the raw data. This is normally done on site so that the data in the field report (Olsson and Lundmark, 1985) are already corrected for this error. The direct pulse from the transmitter to the receiver causes a low frequency oscillation. This is a nonlinear effect which is not seen as clearly in crosshole as in single hole measurements.

A band pass filter has been applied to remove the low frequency oscillation and some high frequency noise. The upper and lower cut off frequencies of this filter were 10 and 68 MHz respectively. This filter does not essentially affect parts of the spectrum containing significant signals. A high frequency band pass filter, with the cut off frequencies of 25 and 68 MHz, has also been applied to the single- hole data to improve the resolution.

The resulting radar plots after filtering are shown in **Enclosures 1-8.** They are presented as grey scale plots with a time-dependant gain ranging.

In the single hole radar plots it is possible to observe a ringing close to the beginning of the boreholes (laboratory tunnel). The ringing is particularly strong in the hole BOUS 85.003. This is probably caused by guided waves propagating on the electric cables in the laboratory tunnel which are multiply reflected by installations.

There are no guided waves (tube waves) propagating along the boreholes. This is a consequence of the fact that optical fiber cables are used and thus there are no conductors in the holes to guide the waves.

The question has been raised if there are multiple reflections present in the data. There is of course a possibility for the existance of multiples but their presence is not easily detected and their occurrence is less likely than in surface measurement. The reasons for this are mainly geometrical, i.e. in a borehole measurement the geometry of reflectors is quite complex. Most reflections show up very well which implies that the chance to obtain multiples in a complex geometry of reflectors is reduced. The probability to observe a multiple is also reduced by the relatively high (25 dB/100m) attenuation and low reflection coefficient which drastically magnifies the energy loss for multiples.

3.4 Data analysis

3.4.1 Singlehole measurements

Radar measurements allow one to determine the angle of intersection between the hole and a fracture plane as well as the point of intersetion. With the aid of a theoretically computed nomogram **(Fig. 12)** the intersection angle is easily detected. Note that it is sufficient that the fracture plane intersects the extension of the borehole as the visible part of a pattern often can be extended far beyond the end of a borehole. The intersection angles can be determined with varying precision: For fracture planes that intersect the borehole obliquely the angle can be determined with an accuracy of a few degrees while the error for almost orthogonal zones are tens of degrees. When the angle of intersection and the intersection point have been determined the plane still has one degree of freedom. The allowed positions of the normal to the plane will thus make a circle on the unit sphere, which may be represented in a plane by a Wulff projection. When the angle of intersection has been determined from several boreholes, several circles are obtained and their intersection will uniquely determine the orientation of the fracture plane (Olsson et al., 1987).

The geometrical relations are simplified in the case of a parallel configuration of the boreholes as was used for the investigations (e.g. the US investigation area at the Grimsel Test Site).

According to the principle of Fermat, in geometrical optics the reflected radar signal from a distinct point of the reflector has traveled on the shortest possible path which is not necessarily within the plane built up by the two boreholes. For example a dipping reflector (**Fig. 4**) will appear to be closer to the boreholes than the actual distance of the intersection line of the reflector and borehole plane. It can be seen that in this case the actual reflection is offset from the intersection of a perpendicular plane.

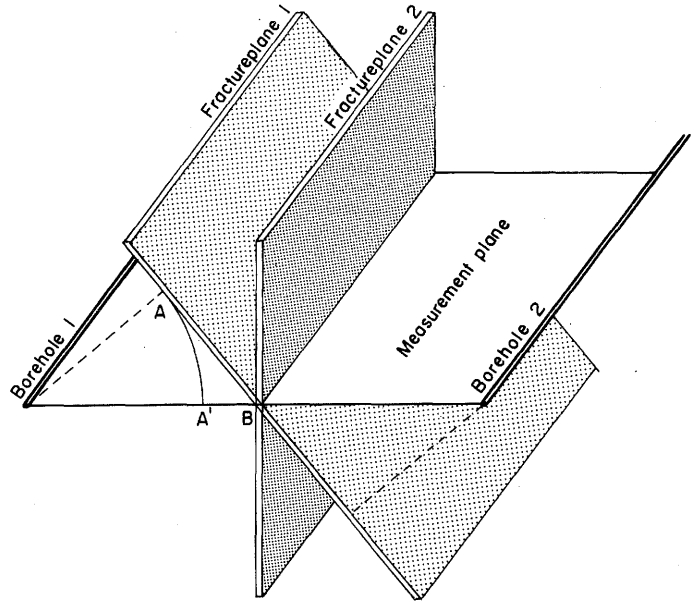

Assumptions: - Fracture planes 1 and 2 are parallel to boreholes

- Boreholes 1 and 2 span the measurement plane

The position of reflection A' is closer to borehole 1 than the intersection of measurement plane and fracture plane 1. If a fracture plane is perpendicular (plane 2) to the measurement plane, reflection point and intersection with measurement plane are identical (A, A', and B are identical).

Figure 4: Sketch of reflector positions from planes with different inclination to the measurement plane

3.4.2 Crosshole measurements

An analysis of the geometrically rather complicated problem to describe reflections of an unknown plane will show that the data can be handled by combining the measured travel distances of the reflected pulse 1' and the direct pulse 1 according to the formula

$$1'^2 - 1^2 = 4\,(\hat{n}\vec{x}_0)(\hat{n}\vec{x}_1) \qquad (3.1)$$

Here $\vec{x}_0$ and $\vec{x}_1$ are the vectors describing the position of the transmitter and receiver if an origin is located in the unknown plane with normal $\hat{n}$ (**Fig. 5**).

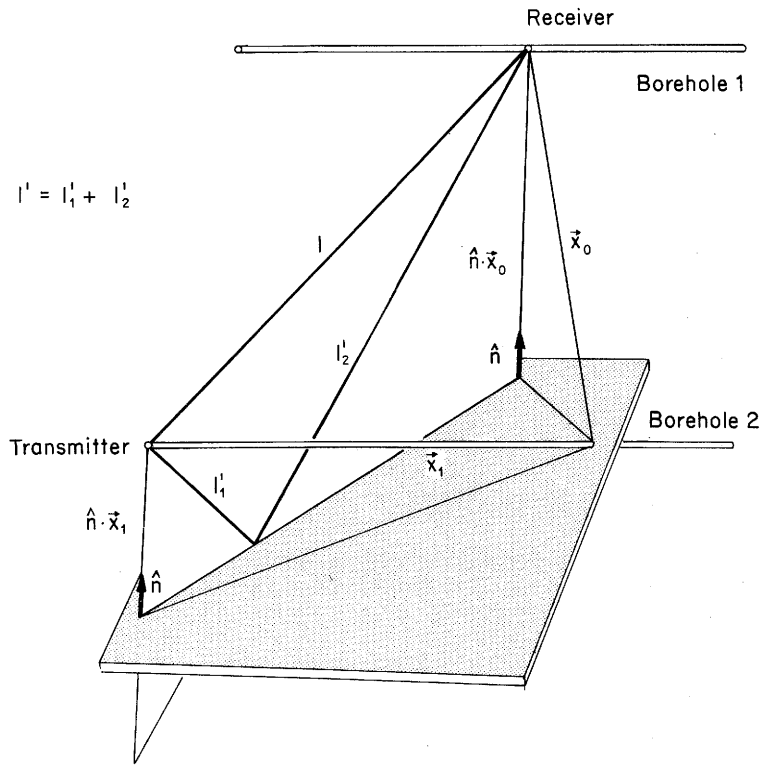

Figure 5: Schematic display of crosshole reflection geometric relationships

The formula becomes useful if several measurements are performed by moving the transmitter along a borehole while the receiver is held fixed in another borehole. Plotting $l'^2 - l^2$ against the borehole depth one will obtain a straight line if the reflector is in fact a plane. At the same time this provides a good check on the procedure used to analyze the data. The point of intersection with the borehole is obtained from the intersection of the line with the abscissa and the slope of the line provides information about the orientation of the plane.

The complete orientation can be derived from several crosshole measurements but in Grimsel this is in principle impossible because only one measurement plane spanned by the boreholes is available. Furthermore it has proved difficult to observe the reflections from a particular zone in more than one measurement. In these cases, the analysis has only been used to check that the results are compatible with information obtained from the single hole measurements.

Planes parallel to the boreholes can not be analyzed in quite the same way as planes that intersect the boreholes. In fact this special case often applies in Grimsel where several of the lamprophyre dykes are parallel to the boreholes. The linear expression is then a constant which can be related to the distances d_1 and d_2 from the plane to the boreholes:

$$l'^2 - l^2 = 4d_1 d_2 \qquad (3.2)$$

Since crosshole measurements have actually been performed between all three boreholes this formula may be used to deduce the distances to parallel lamprophyre dykes by combining several measurements but unfortunately the dykes appear to be more or less vertical and thus often pass between the boreholes causing no crosshole reflections. Still many reflections have been successfully related between themselves and also to single hole reflections (which also provide information about the distances d) and thus contribute significantly to the overall interpretation.

3.4.3 Attenuation and velocity data analysis

The propagation of radar waves through the rock is described by Maxwell's equations. Each frequency component of the electric (or the magnetic) field satisfies the wave equation:

$$\nabla^2 E + k^2 E = 0 \qquad (3.3)$$

where

$$k^2 = \omega^2 \varepsilon \mu + j \omega \mu \sigma \qquad (3.4)$$

ε = dielectric constant
μ = magnetic permeability
σ = conductivity
$\omega = 2\pi f$ = angular frequency.
(A time dependance of exp $(-j\omega t)$ will be assumed throughout this report).

The parameter, k, is termed the wave number and has the dimensions of inverse length. In the high frequency approximation the real and imaginary parts of k become

$$k_{re} = 2\pi/\lambda \qquad (3.5)$$

$$k_{im} = \alpha$$

where λ is the wavelength and α the attenuation constant.
The electric field generated by the borehole radar transmitter is described by the following equation:

$$E(r,t) = c \int a(\theta) \frac{e^{-\alpha r}}{r} e^{j(2\pi r/\lambda - \omega t)} F(\omega)\, d\omega \qquad (3.6)$$

where a (θ) is a function describing the radiation lobes and $F(\omega)$ is the Fourier spectrum of the radiated field.

The exploration task for the borehole radar is to describe the variation of physical properties of the rock in a volume surrounding the boreholes. In a crosshole measurement it is possible to measure the average velocity and the average attenuation along each ray between transmitter and receiver. The velocity and the attenuation depend on the electrical properties of the rock in the following way:

$$v = c/\sqrt{\varepsilon\mu} \qquad (3.7)$$

$$\alpha = \frac{\sigma}{2}\sqrt{\frac{\mu}{\varepsilon}}$$

μ is approximately equal to 1 and does not vary significantly for most rock types.

It should be noted that the electrical properties of the rock correlate with other physical or geological properties of a rock mass which might be of more direct interest. Such properties may be deduced by suitable calibration procedures. For example, an increase in water content (porosity) will normally cause an increase of the dielectric constant and the conductivity, thus, causing a decrease in velocity and an increase of attenuation which can be measured by the radar.

For each transmitter-receiver position (or ray) the electric field at the receiver is registered as a function of time (this is called a trace). The registered signal will generally consist of the direct wave which has followed the fastest path between transmitter and receiver together with later events such as reflections from inhomogeneities in the rock. In the velocity and attenuation analysis only the first pulse is considered. The travel time and amplitude of the direct pulse is obtained through an automatic procedure where the extreme values of each trace are identified. The travel time is the time elapsed to the first maximum or minimum of the signal and the amplitude is defined as the peak to peak amplitude.

In the analysis of this type of data it has proven advantageous to introduce the terms 'residual traveltime' and 'residual amplitude'. This is done to enhance the relatively small variations in velocity and to remove the effects of the radiation lobes in the attenuation data.

The residual travel time, t_r, is defined as the measured travel time, t_m, subtracted by an estimated travel time based on the assumption of a homogeneous medium with an average velocity v_0. The residual travel time thus becomes

$$t_r = t_m - r/v_0 \qquad (3.8)$$

where r is the distance between transmitter and receiver.

In order to simplify the expression for the amplitude variation only one frequency is considered. Based on this assumption the amplitude can be expressed in the following form:

$$E = c \frac{e^{-\alpha r}}{r} a(\theta) \qquad (3.9)$$

The residual amplitude is defined as the quotient (expressed in dB) of the received amplitude, E_r, and the estimated amplitude in a homogeneous medium with constant attenuation α_0. The residual amplitude thus becomes

$$d_T = -20 \log_{10} \left[\frac{E_0}{E_r} \frac{e^{-\alpha_0 r} a(\theta_1) a(\theta_2)}{r} \right] \qquad (3.10)$$

where E_0 is a reference level describing the ratio of transmitted power to receiver gain.

The conversion into residual data makes it possible to look at small variations from a large average value. The residual data are also suitable for detecting systematic errors in the data and are used for calibration of some of the system parameters.

4. RADAR TEST MEASUREMENTS

4.1 Singlehole measurements

Reflection measurements were performed in October 1985 in the three boreholes BOUS 85.001, BOUS 85.002 and BOUS 85.003 with a center frequency of approximately 20 MHz. A sampling frequency of 232 MHz was used and 1024 samples registered for each trace. This corresponds to a registered time window of roughly 4 μs. Each trace was stacked 256 times to improve the signal to noise ratio.

The borehole BOUS 85.001 was also measured with a center frequency of 45 MHz. In this measurement 512 samples were registered corresponding to a time window of 2 μs. The change in center frequency normally requires an exchange of antennas, but in this case a set of spare probes with the center frequency 45 MHz had been brought to the site and were consequently used for the measurement.

Additional reflection measurements were carried out in the 1-tunnel using the 20 MHz recording system. The result of those investigations are presented in a field report. One of the most prominent features in the 1-tunnel data are guided waves propagating along metallic installation in the tunnel.

4.2 Crosshole measurements

To investigate the penetration distance of electromagnetic waves in the ZAGr and to ensure good data quality for the planned crosshole experiment a total of five crosshole scans were measured during October 1985 (**Table 3**). For these scans the probes were located in the holes BOUS 85.002 - BOUS 85.003, BOUS 85.002 - BOUS 85.001 and BOUS 85.003 - BOUS 85.001.

The probes were pushed into the holes by the same glass fiber rods as used for the single hole measurements. The measurements were made with a center frequency of approximately 20 MHz. A sampling frequency of 232 MHz was used and 512 samples were recorded for each trace. This corresponds to a registered time window of 2 μs. The signal position was changed for the different scans in order to keep the received radar pulse within the registered time window.

No	Fixed antenna	Moving antenna
1	BOUS 85.002: 49 m	BOUS 85.001: 0-144 m
2	BOUS 85.002: 121 m	BOUS 85.001: 0-144 m
3	BOUS 85.002: 49 m	BOUS 85.003: 0-145 m
4	BOUS 85.002: 121 m	BOUS 85.003: 0-145 m
5	BOUS 85.003: 51 m	BOUS 85.001: 0-144 m

Table 4: Crosshole scans

5. RESULTS OF THE RADAR MEASUREMENTS GRIMSEL 1985

5.1 Travel time data derived from crosshole measurements

For the interpretation of the data, residual travel-times and amplitudes have to be calculated. These are the time or amplitude differences between the calculated theoretical data for a model with constant velocities or attenuation respectively and the actual data. In the generation of the residual travel time and amplitude the parameters listed in **Table 5** have been used. The zero time correction defines the time instant when the radar pulse was generated by the transmitter. This time varies as different signal positions have been used for the different crosshole scans. These parameters were selected after several tests in order to obtain values as close to the average values as possible.

Sampling frequency	232 MHz
Velocity	114 m/µs
Attenuation	25 dB/100m
Transmitted power (relative)	150 dB
Zero time correction	
US85.002/001	- 10 samples
US85.002/003	- 241 samples
US85.003/001	- 267 samples

Table 5: Parameters used in the generation of residual travel time and amplitude

In **Figure 6** the residual travel time is plotted as a function of the transmitter-receiver separation. In the ideal case the points would make up straight lines passing through the origin. In this case the points outline more or less irregular arcs. A general feature of most of the crosshole scans are that the points make up a bow shaped curve with its sharpest bend at the smallest distance between the holes.

Such curves are typical for errors in the borehole coordinates. It should be noted that the variations in residual travel time are small. The range of values is approximately 60 ns, which corresponds to distances of about 7 m at a velocity of 114 m/µs. This could indicate coordinate errors with a magnitude of a few meters.

Figure 7 shows the residual slowness as a function of the borehole depth for the moving probe. The normal slowness is approximately 8 770 ps/m (corresponding to a propagation velocity in the granite of 114 m/µs) and the variations along the boreholes are on the order of 100 ps/m. This implies that the variations in slowness (or velocity) are roughly 1% of the average value. Furthermore the slowness variations display some correlation with the known geologic structures. Additionally there is an indication for a azimuthal dependence of the velocity. This anisotropy effect is shown in **Fig. 8.**

The quantization error causes the slowness curves to be jagged. The magnitude of the quantization error is on the order of 20 ps/m which corresponds to about 0.2%.

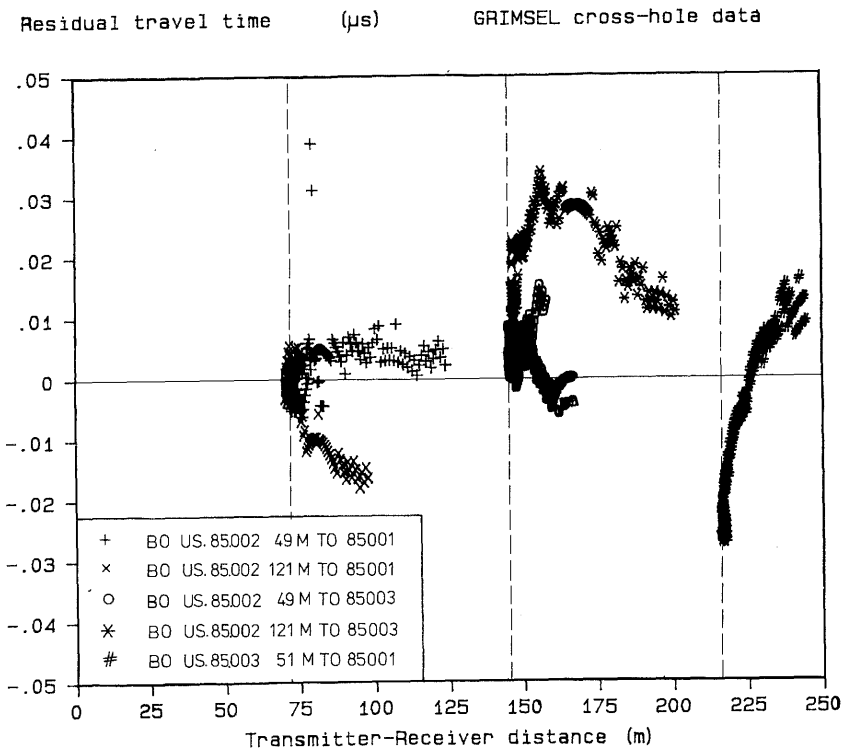

Figure 6: Residual travel time as a function of the transmitter-receiver distance

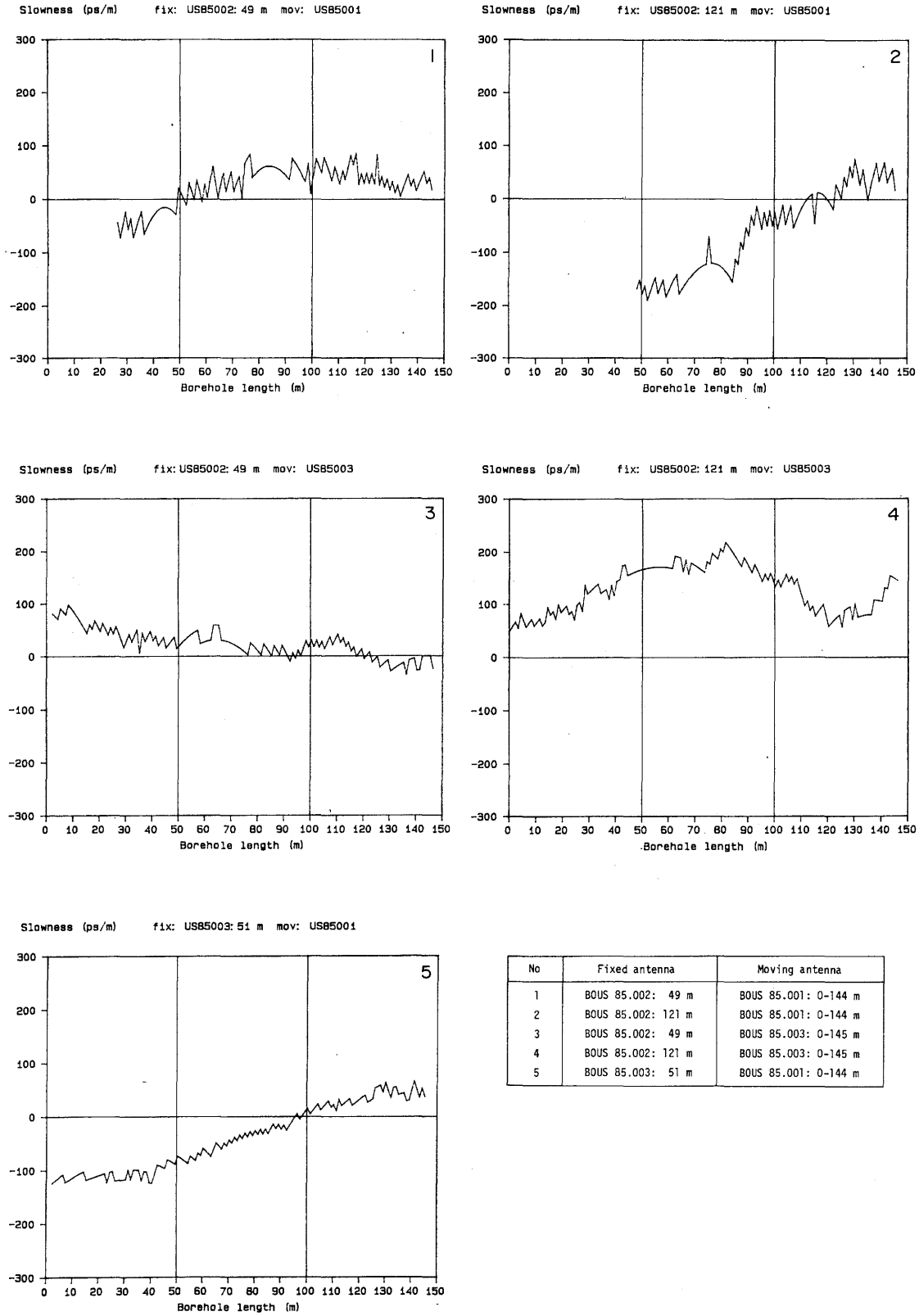

No	Fixed antenna	Moving antenna
1	BOUS 85.002: 49 m	BOUS 85.001: 0-144 m
2	BOUS 85.002: 121 m	BOUS 85.001: 0-144 m
3	BOUS 85.002: 49 m	BOUS 85.003: 0-145 m
4	BOUS 85.002: 121 m	BOUS 85.003: 0-145 m
5	BOUS 85.003: 51 m	BOUS 85.001: 0-144 m

Figure 7: Residual slowness as a function of borehole depth for the moving probe

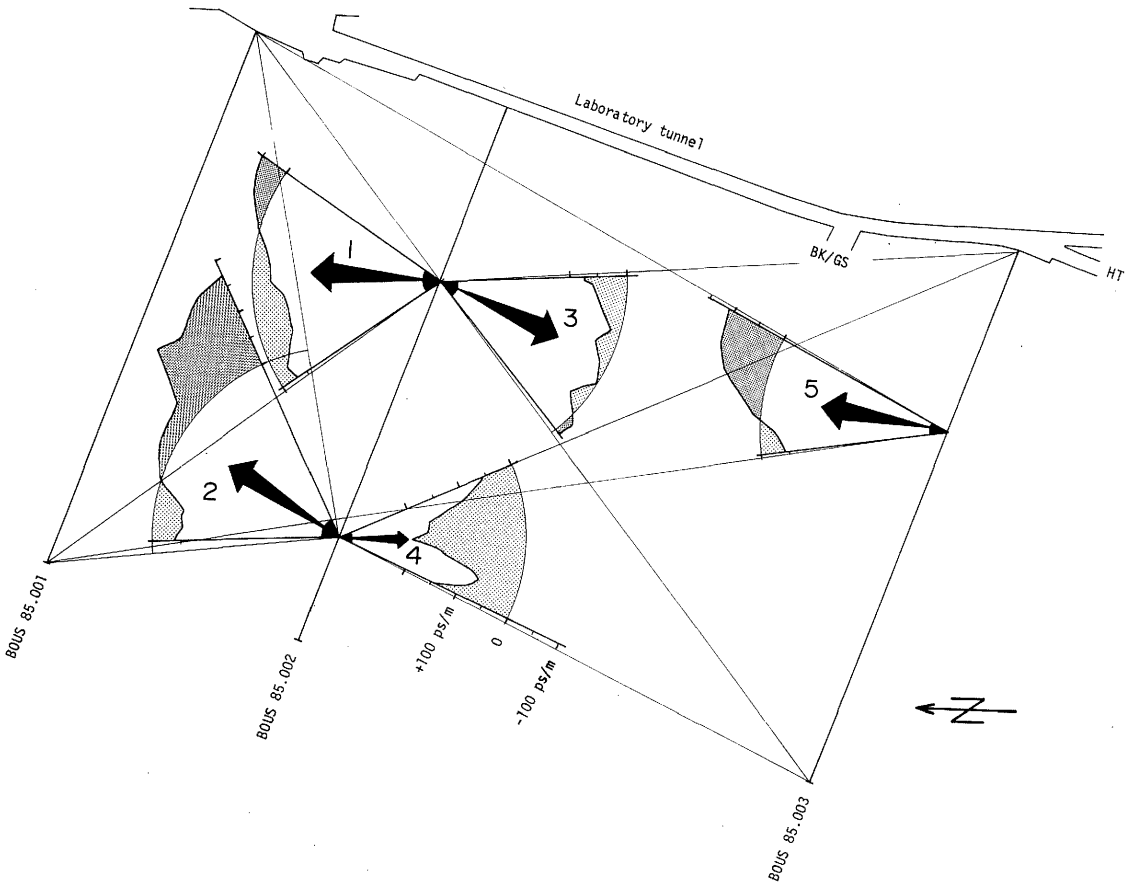

Figure 8a: Residual slowness as a function of ray azimuth for different crosshole scans

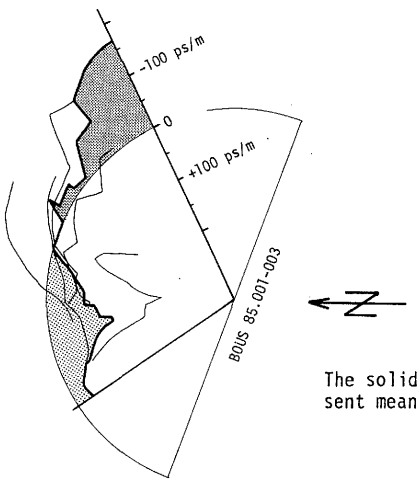

The solid curve and shaded areas represent mean values of all measurements

Figure 8b: Average residual slowness as a function of ray azimuth

5.2 Amplitude data derived from crosshole measurements

The parameters used for the generation of the residual amplitude data are listed in **Table 5.**

In Figure 9 the residual amplitude data are shown as a function of the transmitter-receiver separation, which in the case of a homogeneous medium should be a straight line. In this case the points outline continuous curves for each crosshole scan but the curves display large and apparently unsystematic variations. These variations (on the order of 30 dB) are far too large to be caused by any errors in the borehole coordinates and therefore they have to be interpreted as effects of the inhomogeneous media.

The attenuation is relatively small between the holes BOUS 85.002 and BOUS 85.001 (large residual amplitude corresponds to low attenuation and vice versa) while it is high between BOUS 85.002 and BOUS 85.003. The scan between BOUS 85.003 and BOUS 85.001 takes an intermediate position. The large attenuation between BOUS 85.002 and BOUS 85.003 is probably caused by the large lamprophyre zone which exists between these holes extending in a direction essentially parallel to the holes. From these data in conjunction with the reflection data one might conclude that the average attenuation of the Central Aaregranite is approximately 25 dB/100m and that the higher attenuation values for a large part of the rays are caused by the presence of lamprophyre and fracture zones in the granite.

Figure 10 shows the attenuation as a function of the borehole depth for the moving probe. As could be seen from **Figure 9** the average attenuation varies considerably between the different crosshole scans. A correlation can be observed between geological features intersecting the hole and the increase in attenuation. One example is the zone intersecting borehole BOUS 85.001 at 74-80 m which is associated with an increase in attenuation for both scans to that hole (**Fig. 10**). Although there seems to be some azimuthal dependence of the attenuation (**Fig. 11**) it can not be definitely stated if an anisotropic attenuation exists or not.

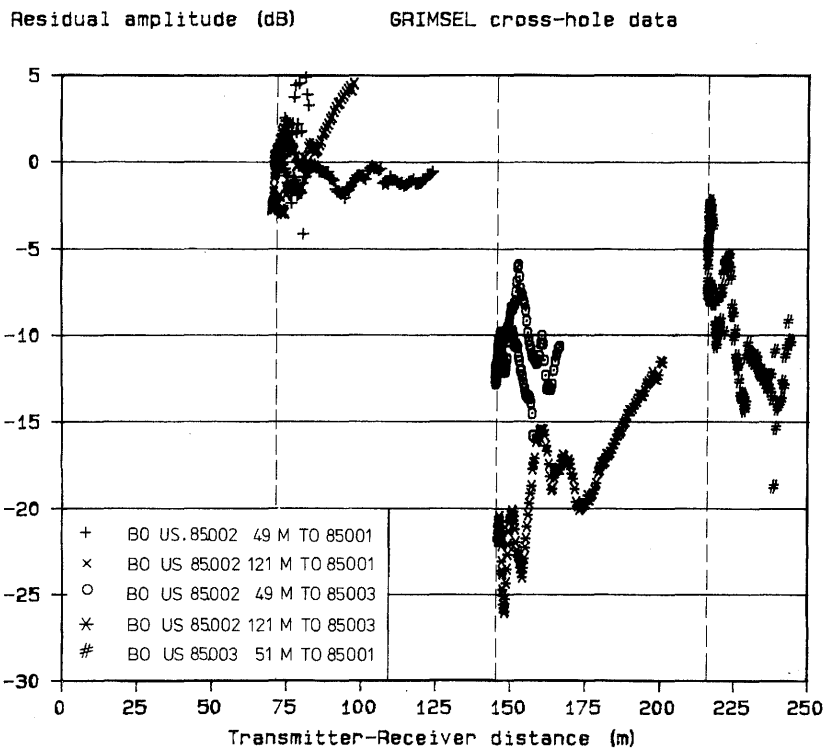

Figure 9: Residual amplitude as a function of transmitter-receiver distance

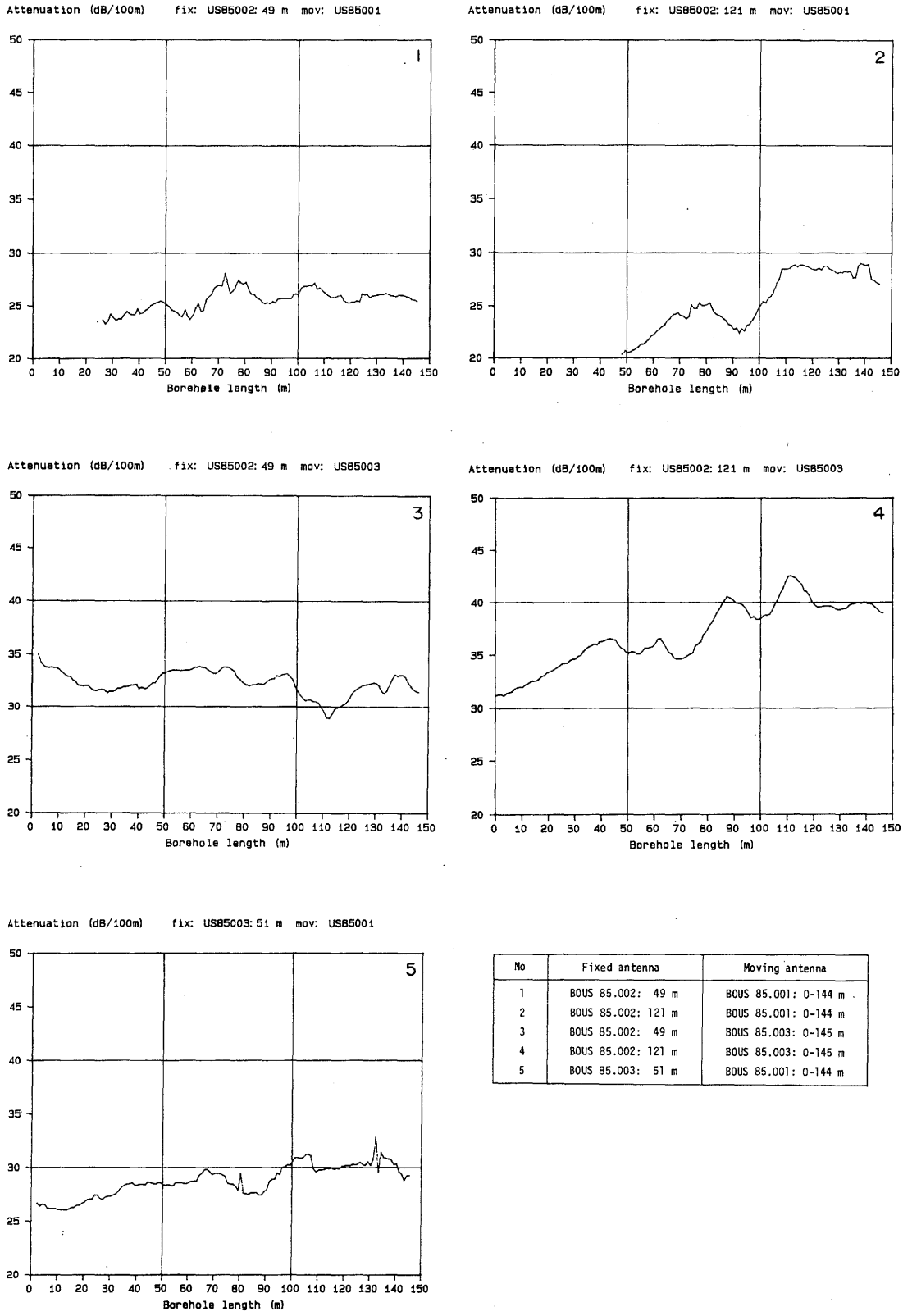

No	Fixed antenna	Moving antenna
1	BOUS 85.002: 49 m	BOUS 85.001: 0-144 m
2	BOUS 85.002: 121 m	BOUS 85.001: 0-144 m
3	BOUS 85.002: 49 m	BOUS 85.003: 0-145 m
4	BOUS 85.002: 121 m	BOUS 85.003: 0-145 m
5	BOUS 85.003: 51 m	BOUS 85.001: 0-144 m

Figures 10: Attenuation as a function of borehole depth for the moving probe

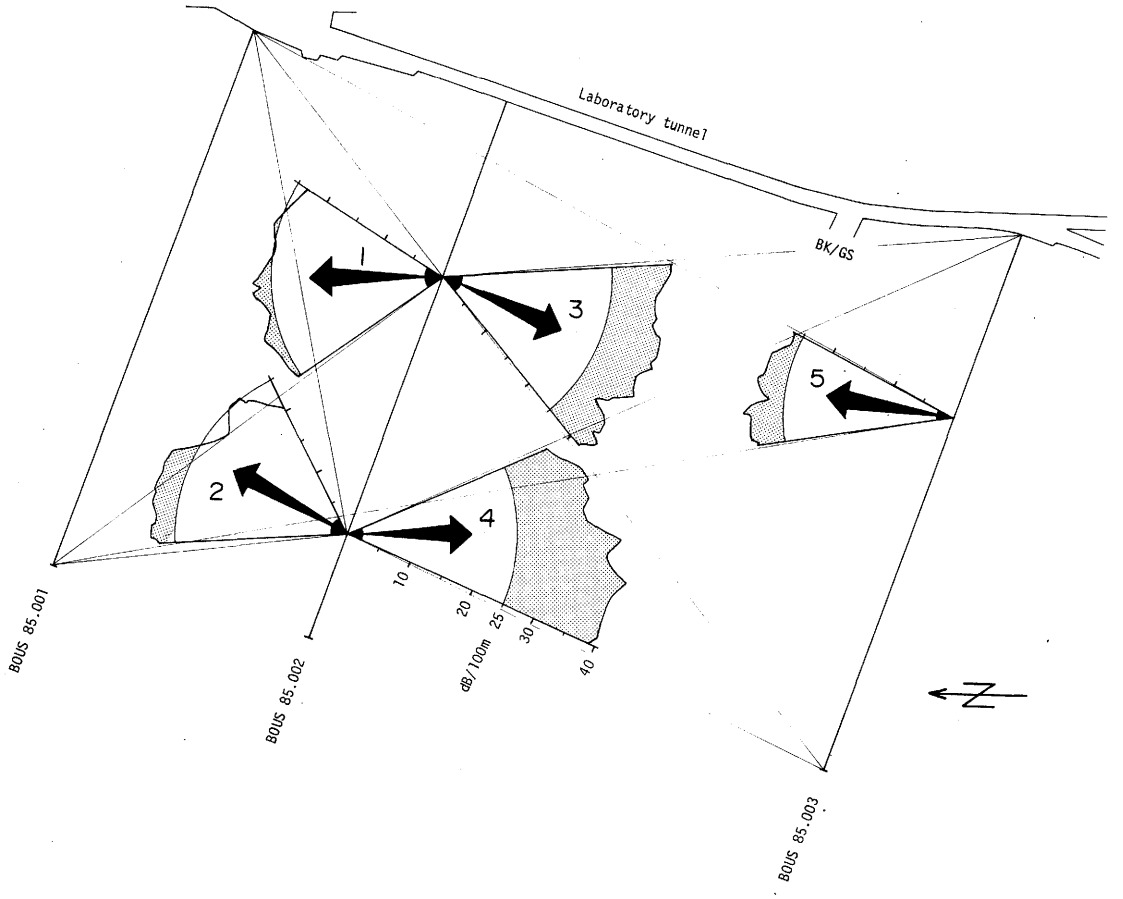

Figure 11a: Attenuation as a function of ray azimuth for different crosshole scans

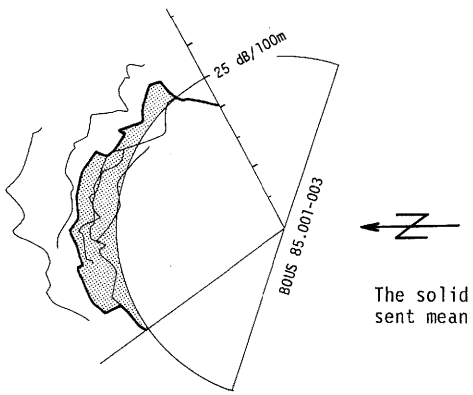

The solid curve and shaded areas represent mean values of all measurements

Figure 11b: Average attenuation as a function of ray azimuth

5.3 Radar reflectograms

5.3.1 Singlehole reflection measurements

In the interpretation of radar reflecting structures two radar reflectograms with different bandpass filters with the respective frequency ranges of 10-68 and 25-68 MHz were used. The two filters give complementary information and enhance different reflecting structures. The filter 25-68 MHz sharpens the reflections in the vicinity of the borehole, but this filter also causes some additional ringing. The other filter enhances structures at larger distance from the borehole, mainly by removing low frequency oscillations. The bandpass filtered radar reflectograms from all boreholes are shown in **Enclosures 1-3.**

For the interpretation of the singlehole measurements the average velocity for the rock mass was taken from the crosshole investigations. Using this information a nomogram (**Fig. 12**) for the Grimsel granite was constructed which allows one to estimate the angle between the borehole and a reflecting plane. Another nomogram was calculated and used for the identification and positioning of local diffractor points at various distances from the boreholes. By overlaying the nomograms on the measured reflectograms the most significant reflectors have been identified for the single hole investigations of the 3 boreholes (Enclosures 1-3). A unique number was assigned to each reflector to simplify data handling. This number together with the angle relative to the hole and the intersection point are listed in a set of Tables (Enclosures 1-3).

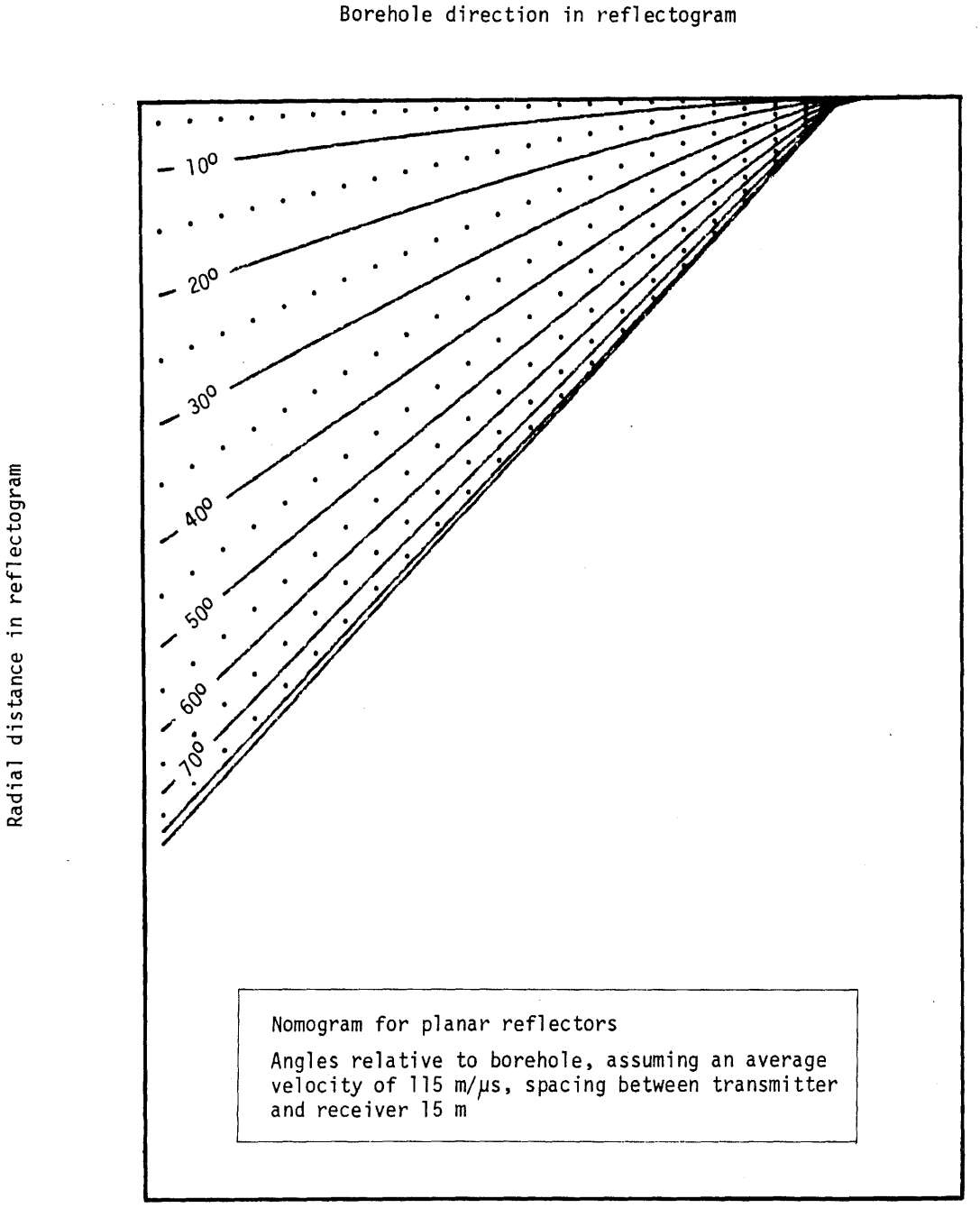

Figure 12: Nomogram for the estimation of angles of reflectors relative to the borehole

5.3.2 Crosshole reflection measurements

Five crosshole measurements were performed between the boreholes using a center frequency of 20 MHz. The corresponding radar reflectograms are shown in **Enclosures 4-8.**

Several reflected pulses can be observed in the crosshole measurements. The interpretation of such reflections is not straighforward and it is complicated in the present case by an unfavorable geometry and the presence of lamprophyre dykes parallel to the boreholes, which tend to obscure other signals by their strong reflections. The analysis is conveniently carried out in two separate steps concerning reflector planes parallel and nonparallel to the boreholes.

The crosshole reflections have been identified and $l'^2 - l^2$ (see **Fig. 5**) plotted to check that a straight line is obtained. The intersection of this line with the abscissa defines the intersection between the borehole and the reflecting plane. The slope of the line is given by the expression $(\hat{n}\vec{x}_0)(\hat{n}t)$, where $\hat{n}$ is the unknown normal vector of the plane and $\vec{t}$ a unit vector along the borehole in which the antenna is being moved.

A check shows that the drift at the beginning of the boreholes can be correctly identified in all maps; since the drift is perpendicular to the boreholes it behaves like a reflecting plane perpendicular to the boreholes and the corresponding reflections are clearly seen.

The lamprophyres parallel to the borehole have been tabulated seperately, since the quantity of interest here is the observed value of the product $d_1 d_2$, the minimum distances from the plane to the boreholes. Identified reflectors are presented in **Enclosures 4-8.**

6. GEOPHYSICAL INTERPRETATION OF THE RADAR TEST MEASUREMENTS GRIMSEL 1985

6.1 Procedure

6.1.1 Detection of the reflectors and migration

The first step of the interpretation of radar reflectograms is the detection and tracing of the reflected energy. A number of conditions have to be taken into account:

Discontinuities which are parallel to the observation borehole or even gently dipping are imaged quite well by the system due to the preferred radial radiation or sensitivity of the dipole antennas. Additionally slight undulations of the reflector surface do not severely affect the ray path of reflected energy, so that still a good alignment is achieved in the radar section. Irregularities of the reflector surface beyond the resolution boundary, the so called roughness, will create some broadening of the observed reflections.

For steeply inclined discontinuous reflections are only received for radiations in the direction near to the dipole axis, which have considerably much lower energy. Furthermore the reflector roughness can create more scattering of incident energy and a poorer line up of the reflections will result.

The unambiguous localization of these inclined reflectors i.e. fracture zones, is additionally made more difficult by the fact that the strong and broad reflection band of parallel reflectors makes the reflections of the steeply dipping ones weak.

Furthermore it has to be taken into account that the reflectograms are not migrated.

The detection of the true angle can be given by a simple geometrical migration or just by overlying precalculated nomograms (**Fig. 12**). **Enclosures 1-3** show the reflectograms and unmigrated reflectors recorded at Grimsel as well as a listing of the recognized reflectors seen in the singlehole experiment. The data taken from the crosshole measurements are similarly shown in **Enclosures 4-8.**

6.1.2 Procedure of the mapping of the reflectors assuming vertical incidence

One difficulty in the analysis of singlehole reflection data is due to the symmetrical radiation characteristics of the dipole antenna. The spatial position of the reflecting element is ambiguous. The possible reflectors are cylindrically symmetric to the measurement borehole. Consequently, it is impossible to obtain a unique orientation of a reflection from radar measurements in just a single borehole. According to a procedure described by Falk et al. (1985) the orientation can exactly be determined by combined interpretation of data taken from several boreholes.

However, this procedure could only be applied at a certain number of the radar data observed at the Grimsel laboratory. The main reason for this restriction is the geometry of the boreholes which were available for the interpretation. First of all the boreholes are parallel (they make up a plane which intersects the laboratory tunnel and dips roughly 15 degrees) and secondly the distances between the holes is quite large. In nearly all cases it is very difficult to localize the same reflector from more than just one borehole.

One assumption made to allow the interpretation of the data is the hypothesis that the reflectors are nearly perpendicular to the plane spanned by the boreholes. This limitation to the data interpretation is based on observations in the area. Nearly all discontinuities at the Grimsel Test Site are dipping steeply (as shown by **Table 1**). The error in locating discontinuities is obviously negligible for a dip larger than 75 degrees.

The assumption of steeply dipping reflectors reduces the possible spatial positions of the reflector to two locations (**Fig. 14**).

The possible locations of all reflectors observed from the boreholes BOUS85.001 to BOUS85.003 are presented in a map (**Enclosure 14**).

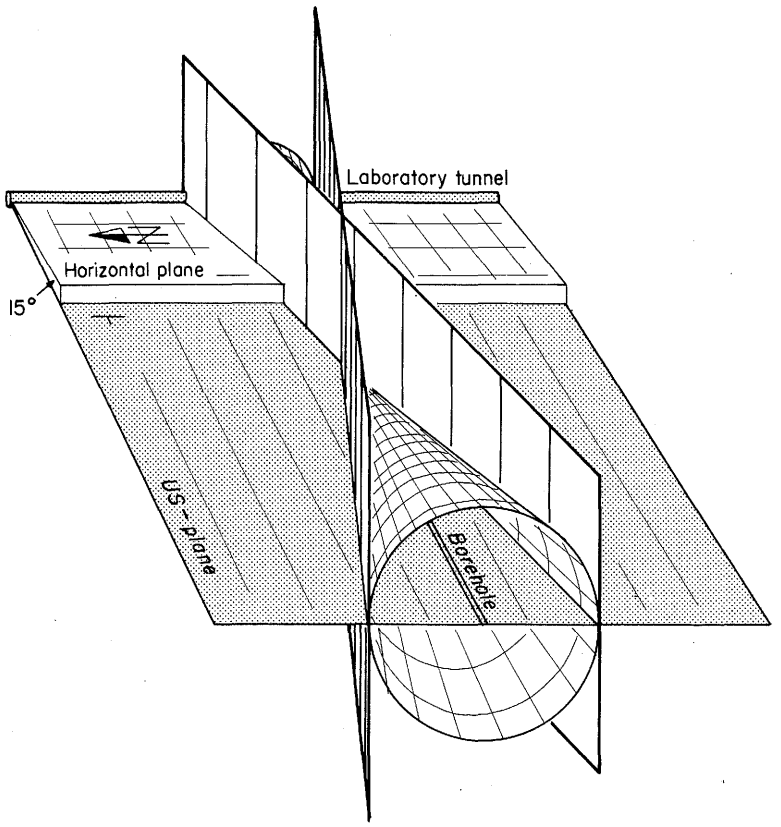

Figure 13: Possible positions of a reflector assuming vertical incidence

6.1.3 Detection of the true position of the reflectors using acoustic borehole televiewer measurements (SABIS) and information of crosshole-radar investigations

The singlehole radar measurements detected a number of reflectors but as it was mentioned above these investigations do not allow a unique positioning of the reflecting elements. Under the assumption of steeply dipping reflectors the real location of the reflector can be sorted out of the two remaining solutions by using additional information from crosshole measurements on one hand or SABIS investigations on the other hand. By applying this technique nearly half of the observed reflectors could become uniquely located. No additional geological information was used in this part of the interpretation.

In the case of the detection of the true position by using crosshole data, secondary arrivals were used because in preferred transmitter-receiver-reflector configurations the direct wave will be followed by the reflected wave. This preferred configuration is given by the geometrical conditions. The theory for this investigation is discussed in chapter 3.4.2.

The other possibility mentioned above holds for the case when the reflector intersects the borehole. This intersection should be recognizable in the SABIS-borehole image. As the SABIS measurements are oriented by a fluxgate magnetometer the detection of the true position of the reflector is possible.

6.2 Mapping of the radar reflectors

The maps which are shown and described in the following chapters are based on basic geophysical data and general geological information of the area under investigation. Detailed geological information (interpretation of the cores) is used later on to characterize the reflectors (see chapter 7).

6.2.1 Map "Possible reflector positions assuming vertical incidence"

The reflectors which were observed in the US-plane lay in an area of approximately 200x450 m. The boundaries are given by the geometrical conditions at the FLG and the technical limits of the methods (eg. attenuation, frequency range etc.). The geometrical conditions are

- the position of the boreholes BOUS 85.001-003 and the laboratory tunnel
- the shadow affect of the laboratory tunnel which cuts off possible raypaths east of the area

The first assumption that the reflectors are nearly vertical to the plane of investigation leads to the possible reflector positions shown in **Enclosure 14.** The two axisymmetrical lines define the possible intersection lines between the US-plane and each migrated planar reflector. The signature of the reflectors shows from which borehole the reflectors are observed. The first part of the labels (1-3) refers to the boreholes, BOUS 85.001 to 85.003 from where the reflectors were detected, while the second part gives the sequential number. The length of the reflectors shown in the graphs is restricted to the real observations. Possible or reasonable continuations of the reflectors are not shown in Enclosure 14.

It should be mentioned that the curvature of the reflectors influences the intensity of the reflection. Reflectors which are of concave shape with respect to the observation hole focus the energy (eg. bell-like reflectors 3/5 and 3/10) while reflections from convex curved elements are weakened. Most of the energy loss due to the geometrical spreading is compensated by a time dependant gain on the amplitudes. Diffracted energy can be identified by the hyperbolic shape of the traveltime curves. In the migrated section these diffraction curves are reduced to point reflectors (e.g. reflectors 1/20, 3/23, 3/24, 3/25). The detection of their positions is done by using a precalculated nomogram (**Fig.12**) for pointlike reflectors.

One very interesting point is the fact that a number of reflectors parallel to the boreholes exist close to boreholes BOUS 85.001 and 85.002.

6.2.2 Map "Reflectors unambiguously localized by geophysical means"

As mentioned above the singlehole reflection investigation still contained uncertainties because of the nonuniqueness of the physical problem. Using acoustic televiewer (SABIS) measurements and crosshole information the true position of nearly half the reflectors could be unambiguously located. These reflectors are marked on the map shown in **Enclosure 15.**

The capability of the SABIS investigation is limited by the fact that only those reflectors can be identified which intersect one of the boreholes. A number of the reflectors located by SABIS were also seen in the crosshole reflectograms. Additionally a number of other reflectors not intersecting the boreholes were positioned by the crosshole interpretation. The nomenclature used for the identification of the reflectors indicate which method was used to locate the true position of the reflector (S = SABIS, CH = crosshole investigations).

The map of Enclosure 15 does not contain the reflectors which can be attributed to caverns and various point reflectors.

7. GEOLOGICAL INTERPRETATION OF THE RADAR TEST MEASUREMENTS

7.1 Procedure

The first step to be performed in the geological interpretation was the collection and listing of all discontinuities found in the cores of the boreholes BOUS 85.001-85.003. Included in this inventory are discontinuities between different rock types as well as joints in the rock mass (e.g. open joints and fissures). The petrophysical and geological characterization of each feature which is a potential reflector or any other anomaly encountered in the borehole are listed in a set of Tables (**Appendix 2, Tables AT 1-4**). This data collection allows an estimation of average physical properties for each category of all features.

The next step consists of the correlation of detected radar reflections which intersect one of the boreholes with the discontinuities listed in the inventory. This procedure allowed in the case of a successful match

- to identify the observed reflectors from the geological and petrophysical point of view
- to make an assumption on the spatial extensions of the discontinuities seen in the cores

Additional geological information was used to orient reflectors which were not uniquely positioned by geophysical means. Geological data from the BOUS-boreholes and the drift and also from the BK-cavern and the BOBK-boreholes were taken into account to identify the reflectors.

These investigations allowed for the identification of a large number of reflectors and to sort out their most likely positions by geological means. The results are summarized to a geological model of the US-area of the FLG (**Enclosure 17**). In this model nearly all reflectors detected in the single-hole experiment are assigned to geologically described discontinuities. Additionally a small number of fracture zones which are nearly perpendicular to the boreholes are shown in Enclosure 17. Due to the

geometrical conditions those structures cannot be distinctively observed in a singlehole reflection survey but the existance of these zones is proven by the geological data analysis. It has to be mentioned that in these cases the spatial extension of the fracture zones is questionable as the information of the geological data is restricted to the area close to the boreholes.

7.2 Geological identification of radar reflections

The final geophysical interpretation (Enclosure 15) still shows uncertainties concerning the true position of a number of reflections. The following geological interpretation was first done separately for every borehole where radar measurements were carried out in the US-area. The synthesis of these separate investigations led to the final geological model of the discontinuities in the US-area. A detailed geological description of the Grimsel Test Site is not included into this report but can be found in several technical reports on the site (for example NTB 81-07, NTB 85-34, and NTB 85-46).

The classification of all major geological and geophysical features encountered in the boreholes BOUS 85.001-003 allowed us to identify three main categories of geological discontinuities (**Appendix 2, Tables AT 1-3**).

- Lamprophyres
- Fracture and shear zones
- Hydrothermally altered granite

In addition, a few other geophysical anomalies are observed from the boreholes. As they do not fit into any of the categories mentioned above, these anomalies were consequently put into a separate class called (**Appendix 2, Table AT 4**)

- other prominent structures.

The detailed explanation of the categories follows in the subsequent chapters. Outcrops seen in the caverns and the drift are not used to set up the inventory of the discontinuities. Nevertheless this additional information was incorporated in the final synthesis and the geological model.

7.2.1 Lamprophyres

- Overview:
Two sets of lamprophyre dykes are observed at the Grimsel Test Site. Both of them are steeply inclined to near vertical but their azimuth is quite different. One set shows an azimuth of 216°/80° (Table 1, page 6). It crosses the laboratory tunnel nearly perpendicular and runs parallel to borehole BOUS 85.002. As mentioned in chapter 7.2 the inventory consists mainly of borehole data which means this set is underrepresented because there are nearly no intersections with the holes.
The second set running in direction 242°/80° cuts through the US-area close to the heat test (WT) drift and intersects the borehole BOUS 85.003. Therefore it is adequately represented in the geological inventory.

- General characterization:
The lamprophyres seen at Grimsel Test Site show characteristic changes in thickness within a distance of a few meters, and in some cases these dykes can pinch-out or split. Furthermore one observes changes of the general direction and undulations. The lamprophyres and their contact zones are often water bearing. They have a very low content of quartz and, depending on the type, they are enriched in biotite, plagioclase, hornblende or epidote (see NTB 81-07).

- Discontinuities (Appendix, Table AT 1):
Within the inventory set up for the three boreholes, the lamprophyres mainly show up in BOUS 85.003. They can be described as follows: The lamprophyre dykes generally exhibit sharp contacts to the surrounding granite and have significant electric but poor sonic response. Their thickness varies from 0.4 to 2.2 m.

Enclosure 9 represents the characteristics of a typical dyke cutting through borehole BOUS 85.003. The density of open fractures rapidly increases in the vicinity of the lamprophyres. In contrast to the sonic log which shows almost no changes, the resistivity as well as the long spaced neutron log show significant changes. This response is due to an increase in hydrogen content due to the presence of clay minerals.

- Radar reflection characteristics:
The lamprophyre dykes show up as broad, often undulating bands of reflectors. The correlation with the geological discontinuities of the boreholes is easily established. Problems arise in particular in the last step of the interpretation - the synthesis of the interpretation of several boreholes. The main reasons for that are:
  - the reflections are mainly caused by the borders of the lamprophyre so that one detects the right or left border depending on which side of the lamprophyre the borehole is situated
  - the border to the undisturbed granitic rocks undulates and is more like a crooked plane
  - the local changes in thickness

It should be mentioned that due to the geometry of the investigated area and the position of the measurement boreholes, the resolution of the spatial orientation and the thickness of the lamprophyres differs in distinct areas. Especially north of borehole BOUS 85.001 and south of BOUS 85.003 the lamprophyres are indicated as very narrow bands (**Enclosure 17**). This interpretation can result from an artifact because only one border of these discontinuities is probably detected. Due to the wavelength of about 5m used in radar measurement, the reflection of the opposite border could be hidden by the first reflection.

7.2.2 Fracture and shear zones

- Overview:
Fracture and shear zones are defined as areas with increased fracture density (see also definitions on page 56). In particular open joints are important for this study. The observed fracture zones show preferred directions which are consistent with the directions of the joints and in other cases with the orientation of the foliation systems. The latter are sometimes present as shear zones.
The US-area exhibits examples of the three foliation systems known for the Grimsel Test Site (Table 1). The most intense foliation system is the s1 system as a major shear zone of this type cuts right through the area under investigations. Foliations in the s2 and s3 direction are less pronounced. The main observed joint systems are the so called k1 and k2 systems.

- General characteristics:
Reliable statements on the aperture of single open joints are not possible. In addition, it is very difficult to approximate the length of a single joint but usually the dimensions are in the range of a few meters. Continuous joints over longer distances could only be observed in the direction of the k3-system (NTB 81-07). Geological investigations suggest that in reality one is dealing with a set of joints rather than with a single joint. This set as a whole extends over larger distances than a single joint. Therefore the reflector seen in the radar experiment represents the "surface" of the set of joints. The overall thickness of such a set can reach up to several meters. In addition to the open joints, a number of healed joints exist whose joint fillings probably show an increased porosity in comparison with the rock mass. The shear zones run parallel to the foliation direction s1, s2 and s3. Characteristic for these zones is the occurrence of slickensides. Biotite, mica and lamellar chlorite are concentrated within the shear zones which often contain water.

- Discontinuities (Table AT 2, Enclosure 10):
The inventory exhibits that mainly the boreholes BOUS 85.002 and 85.003 intersect numerous fracture and shear zones (e.g. s_1, s_2, k_4). The fracture and shear zones have a significantly larger variation in their physical and chemical properties in comparison with the other categories. The transition to the surrounding rock is generally sharp and the sonic responses are significant while the electric responses may be considered as moderate but highly variable.

- Radar reflection characteristics:
The correlation of fracture and shear zones known from the interpretation of the borehole logging with the reflected energy is often quite good. Part of the reflections (esp. the s2-reflectors) could be verified by the results of SABIS. Fracture and shear zones of s_1 and k_4 directions were poorly validated by the reflection measurements. This is due to the geometrical position of the boreholes relative to the s_1 and k_4 directions. As we know

from geological interpretations the orientation of these shear and fracture zones (s_1, k_4) is mainly perpendicular to the boreholes BOUS 85.001-85.003. Therefore we assume that those reflectors (s_1, k_4) are not adequately represented in our models in comparison to the zones s_2.

7.2.3 Zones of hydrothermally altered granite

- Overview and general characterization:
The zones of hydrothermally altered granite are genetically related to hydrothermal processes in the rock. Within the rock mass the hydrothermal processes can be verified by the observation of leached rock and by mineralization of quartz, epidote and chlorite in tension joints or veins.

Tension joints are generally related to the hydrothermally altered zones. They mainly exist in the vicinity of lamprophyres. They are mainly subhorizontally oriented and do not span a simple plane.

- Discontinuities (Table AT 3, Enclosure 11):
Numerous zones of hydrothermally altered granite could be detected in the US-area. They generally exhibit smooth transitions to the surrounding rock and produce significant electric and sonic anomalies (see Enclosure 11). Statements on the spatial orientation of these zones are impossible. The geological interpretation of the cores of all the three boreholes showed no open tension joints but a few quartz veins.

- Radar reflection characteristics:
A correlation of the radar reflectors and the hydrothermally altered granites is impossible as there is no information on the direction and extension of the latter. The reflectors seen in the reflectograms were attributed to other discontinuities. One hypothesis is that the hydrothermally altered zones interfere with other discontinuities or are genetically related to these structures.

7.2.4 Kakirites, cataclasites and mylonites

- Overview and general characteristics
In a few cases kakirites/cataclasites were found in the boreholes of the US-area. The kakirites which consist of brittle deformed rock have undergone a secondary healing process and therefore their detection is very difficult by geophysical means. Similarly the cataclasites as well as the mylonites do not show a pronounced seismic contrast to the surrounding rock.

- Discontinuities
The geological interpretation of the cores of the boreholes BOUS 85.001-85.003 resulted in just one healed kakirite (**Enclosure 12**). One kakirite seen in borehole BOUS 85.002 cannot be separated from other discontinuities such as fracture zones and lamprophyres. Cataclasites and mylonites have not been observed in the investigated boreholes.

- Radar reflection characteristics
The mapped kakirite mentioned above was assigned to a radar reflector. But the correlation is not unique and therefore a general characterization can not be given of the behavior of kakirites as radar reflectors.

7.2.5 Biotite layers

- Overview and general characteristics
A few biotite lamellas were observed in the US-boreholes showing thicknesses of up to a few centimeters. **Enclosure 13** displays a typical biotite lamella. The comparison of geology and petrophysical logging indicates that particularly the resistivity log responds strongly to these features.

- Discontinuities
Initially only minor attention was payed to these biotite layers. The singlehole reflection measurements and the comparison of the radar reflectograms with geophysical logging and geological interpretation finally demonstrated the significance of these lamellas in the interpretation of radar reflections.

- Radar reflection characteristics
In spite of their relative small dimensions, the biotite lamella show up as extremely good radar reflectors.

7.3 Synthesis of the geological model

Enclosure 16 exhibits the preliminary geological model of the US-area based almost exclusively on the result of geological core analysis and informations from outcrops. In contrast the new final model (Enclosure 17) was constructed using the geological as well as the radar reflection and well logging results.

7.3.1 Basic geological data

The geological database used for both models consists of the following data which have been collected in the tunnels, caverns and boreholes of the Grimsel Test Site:

- records of the geological investigation of the main access tunnel, of the laboratory tunnel, of the heat test tunnel, and of the GS/BK cavern
- records of the core analysis of the boreholes BOUS 85.001-85.003
- records of the core analysis of the boreholes BOSB 80.001-80.002

For the construction of the final model (Enclosure 17) additional data were used from investigations of the following borehole cores at the GS/BK site: BOGS 84.041A, BOGS 84.042A, BOBK 85.004, BOBK 85.008 and BOBK 85.010.

7.3.2 Preliminary geological model

The geological model (**Enclosure 16**) used as a preliminary model of the investigated area was developed by GEOTEST immediately after the geological interpretation of the data from BOUS 85.001 - 85.003 had been completed. The model is mainly based on geological data but additional information was taken from previous radar measurements carried out by the Bundesanstalt für Geowissenschaften und Rohrstoffe (BGR, Hannover) before the recent radar investigations.

7.3.3 Final geological model

The final geological model (**Enclosure 17**) displays the results based on all available information at this stage. For a judgment on the reliability of this final model the following problems and sources of errors must be taken into account:

- Due to the general geological interpretation of the Grimsel Test Site it was assumed that most of the reflectors dip nearly vertically and therefore perpendicular to the measurement plane. The spatial position of the detected reflector planes will slightly change if the assumed incidence of the reflector planes differ from the vertical by +/- 20°.

- The position of reflectors which are not uniquely determined in enclosure 15 by geophysical means had to be resolved by comparison of possible positions with geological profiles.

- In the investigated areas (US) there are areas with variable reflector densities. Due to the limits in wave length and resolution of the used radar waves the degree of resolution of reflectors in low density areas is better than in the high density area. Mainly the lamprophyres which run nearly parallel to the boreholes BOUS 85.001-85.003 cover other reflectors.

- Discontinuities oriented approximately perpendicular to the boreholes do not show up distinctly in the radar reflectograms due to geometrical reasons. Therefore the well known foliation and shear zone s1 was not adequately detected in the reflectograms.

The model shown in Enclosure 17 is based on data collected until October 1986. Although now called the final model it has to be taken into account that additional information from seismic and radar crosshole tomography investigations will become available in the future. These results will further improve our knowledge of the geological situation of the US-area at the Grimsel Test Site.

Structure	Character	Thickness	Angle to boreholes	Radar reflection
Lamprophyre	High biotite content, partly water bearing, major structure	Up to several meters	2 sets of lamprophyres, one of them parallel to the boreholes	Very strong, undulating bands
Fracture and shear zones	Partly water bearing, can be followed over larger distances, major structure	Up to several meters	Important systems (s_1, k_4) nearly perpendicular to the boreholes	Depending on angle to borehole, often weak, masked by stronger reflectors
Hydrothermally altered rock	Leached ZAGr	Up to 2m	Orientation uncertain, probably associated with other struct.	Strong
Kakirite	Healed, high RQD, considered to be of minor importance	Up to 2m	Approx. 35°	Fair, (similar character on radar as mylonites and breccias in Stripa)
Biotite layers	Thin, high biotite content	About 0.1m	25-30°	Partly very strong

Table 6: Prominent structures at Grimsel Test Site and their radar response

8. SUMMARY OF RESULTS AND CONCLUSIONS

To test and to optimize experimental techniques for future routine application at potential repository sites is one of the basic objectives of the Grimsel Test Site. In this connection, non-destructive methods for host rock investigations are of special importance.

The acquisition of a significant data set is certainly the first and most important step but the task is only fulfilled when the second step is performed, which consists of the interpretation and processing of information for the applicants, i.e. geologists, safety analysists and construction engineers.

The tests of the new developed SGAB radar system named RAMAC which have been carried out in October 1985 at Grimsel Test Site showed quite promising results. Taking into account the time spent for field data acquisition (here 2 days), the system has been found to be quite capable of performing routine surveys under mining conditions. Singlehole reflection measurements in the three boreholes of the underground seismic (US) area showed, that the range of the radar is approximately 150 m in the granitic rock mass of the Grimsel type. Within that range, more than 20 different reflectors could be detected by each singlehole measurement. The resolution has been found to be of about 2-3 m providing a good separation of adjacent reflecting elements, i.e. rock discontinuities. Using the system in crosshole mode, signals of good quality can be obtained over distances of more than 200 m proving the efficiency of the radar system for tomographic investigations.

Altogether, the radar system has performed throughout the tests much better than expected providing a very useful data set of reflecting discontinuities from the investigated US-area.

Following a presentation of the field results, it was decided to investigate the potential of the radar data for the establishment of a structural model of the crystalline rock. The basic interpretation including a review of other available information such as logging data and geological profiles, was carried out in a workshop. A three day's period was found to be quite sufficient for the compilation of all information and the development of a first geological model based on the above mentioned radar data.

Such a model can be regarded as basic input for construction purposes, safety analysis and other applications of such a physical representation.

The results of the workshop were revised slightly to point out the procedure of reflector identification and the steps of model built-up.

The first step was the compilation of the crosshole reflections obtained from measurements in the three different boreholes of the US-area. Because there is no azimuthal discrimination on reflector position from a singlehole measurement, this procedure allowed us to define on which side of the borehole the reflector is actually situated. Further positioning for reflectors intersecting the boreholes was performed by other geophysical means, such as the acoustic borehole televiewer (SABIS) records.

Geophysical logs and geological profiles of the boreholes were used to define the reflectors observed as well as to characterize their signature in the radar sections. The same was done for reflectors intersecting the laboratory tunnel by using geological profiles only. Based on these results, the geological model for the US-area was developed.

Most of the reflectors seen in the radar sections could be identified. Lamprohyre dykes are producing the strongest reflections due to their low electrical resistivity and therefore high contrast to the granitic rock mass. This relationship also holds for zones with biotite layering. Fracture zones do not show up so distinctively in the reflectograms for several reasons. Firstly, the electrical contrast to the sound granite is more moderate and secondly the boundary of the zones seems to be of a more irregular shape creating some signal scattering. Another problem is the preferential direction of these discontinuities, intersecting more or less perpendicular to the axis of the measuring boreholes. The capability of the radar for imaging rock discontinuities is much better for structures running parallel to the borehole axis. Obviously in this case, measurements from additional boreholes in other directions would improve the geological model with respect to these structures. Tunnel radar measurements carried out for this purpose gave only poor results because of noise signals, i.e. guided waves produced by metallic installations.

To sum up, it can be verified that the radar measurements deliver quite a valuable contribution for the transfer of information gathered from boreholes or tunnels and the construction of a structural or geological model in areas that can not be directly observed.

Throughout the field survey experience was gathered for the application of this new geophysical method in other host rock areas. But finally only the development of an interpretation methodology during the course of this exercise allows other applicants to use the full information potential contained in the radar sections.

Radar investigations as demonstrated here can be performed at potential sites situated in a highly resistive rock mass such as crystalline, saline or carbonate rock. The low operational demand and the relative simple and straightforward interpretation offers a promising tool for nondestructive investigation of rock mass under consideration.

LIST OF ABBREVATIONS

BGR	Bundesanstalt für Geowissenschaften, Hannover BRD
BK	Bohrlochkranzversuch (Fracture system flow test)
BOBK	Borehole in the BK area
BOGS	Borehole in the GS area
BOSB	Boreholes SB (Sondierbohrungen)
BOUS	Borehole in the US area
CH	Crosshole
FLG	Felslabor Grimsel (Grimsel Test Site)
G	Geology
GEOTEST	GEOTEST AG, Bern CH
GS	Gebirgsspannungen (Rock stress measurements)
GSF	Gesellschaft für Strahlen- und Umwelt-forschung Braunschweig BRD
HZS	Hauptzugangsstollen (main access tunnel)
Lamp	Lamprophyre
LAT	Laboratory access tunnel (= Laboratory tunnel = L - Tunnel)
MAT	Main access tunnel
NM	Neigungsmesser (Tiltmeter test)
RAMAC	Radar system developed by SGAB
RQD	Rock quality designation
S	SABIS
SABIS	Scanning acoustic borehole imaging system, trade mark of WBK
SGAB	Swedish Geological AG

SKB	Swedish Nuclear Fuel and Waste
US	Untertageseismik (Underground seismic testing, subsurface seismic test)
US1,2,3	Borehole BOUS 85.001 (002, 003 respectively)
WT	Wärmetest (Heat test, heat test tunnel)
WBK	Westfälische Berggewerkschaftskasse, Bochum BRD
ZAGr	Zentraler Aaregranit ("Central Aaregranite")

Abbreviations in formulas

d_T	Residual amplitude
$k_{re\ im}$	Wave number (re = real part, im = imaginary part)
t_r	Residual travel time
ω	Angular frequency
α	Attenuation constant
ε	Dielectric constant
λ	Wavelength
μ	Magnetic permeability
σ	Conductivity
$a(\theta)$	Function describing the radiation lobes
c	Speed of light
t	Travel time
r	Distance from antenna
tm	Measured travel time
v_o	Average radar velocity
E	Electric field
E_r	Received amplitude
E_o	Reference amplitude

DEFINITIONS

Definitions are given to explain the meaning of the terms used throughout this report. Only those terms are explained which are often used differently by different authors.

For further explanations see RAMSAY and HUBER (1987).

Fractures: Structures developed by brittle failure. Subdivided into joints, faults, and veins.

- **Joints:** No displacement along the fracture planes
- **Faults:** Displacement along the fracture plane ranging from mm up to km
- **Veins:** Fracture filled with crystalline material

Fracture zone: Area with increased fracture density. In this report the term fracture zone is used in this general sense. Brittle shear zones showing displacement along faults are also included.

Shear zone: Planar or curviplanar zones of high deformation which are long relative to their width. They may be subdivided into brittle shear zones (faults, kakirites), brittle to ductile shear zones (cataclasites), and ductile shear zones (mylonites).

- **Kakirite:** Rock type found in brittle shear zones
- **Cataclasite:** Rock type found in brittle-ductile shear zones
- **Mylonites:** Rock type found in ductile shear zones

The term shear zone is used in this report for zones where displacements have been found at the outcrops. The terms kakirite and cataclasite are not only used for the actual rock but also for zones containing these rock types.

BIBLIOGRAPHY

Falk, L., Sandberg, E., and Olsson, O. (1985).
An analysis of the orientation of fracture zones using radar data.
- Stripa Project Quarterly Report January-March 1985, SKB, Stockholm.

Nagra, NTB 81-07 (1981):
Sondierbohrungen Juchlistock Grimsel.

Nagra, NTB 85-34 (1985):
Felslabor Grimsel, Rahmenprogramm und Statusbericht.

Nagra, NTB 85-46 (1985):
Grimsel Test Site, Overview and Test Programs.

Nickel. H., Sender, F., Thierbach, R., and Weichart, H. (1983):
Exploring the Interior of Salt Domes from Boreholes .
- Geophysical Prospecting 31, 131-148.

Olsson, O., Falk, L., Sandberg, E., Carlsten, S. and Magnusson, K.-A. (1985 a):
Results from borehole radar reflection measurements. In: Proc. on "In situ experiments in granite associated with the disposal of radioactive waste".
- OECD, Stockholm.

Olsson, O., Forslund, O., Lundmark, L., Sandberg, E., and Falk, L. (1985 b):
The design of a borehole radar system for the detection of fracture zones. In: Proc. on "In situ experiments in granite associated with the disposal of radioactive waste".
- OECD, Stockholm.

Olsson, O., Falk, L., Forslund, O., Lundmark, L., and Sandberg, E. (1987):
Crosshole investigations - results from borehole radar investigations.
- Stripa Project Report TR 87-11, SKB, Stockholm.

Olsson, O., and Lundmark, L. (1985):
Documentation of radar measurements performed at the Grimsel Rock Laboratory, Switzerland, in October 1985.
- Unpublished.

Ramsay, J.G., and Huber, M.I. (1987):
The Techniques of Modern Structural Geology, Volume 2: Folds and Fractures.
- Academic Press.

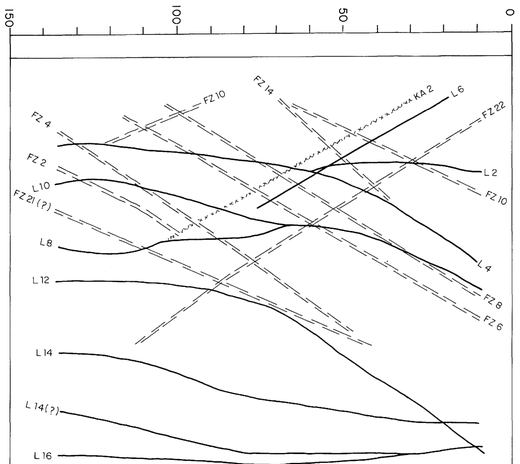

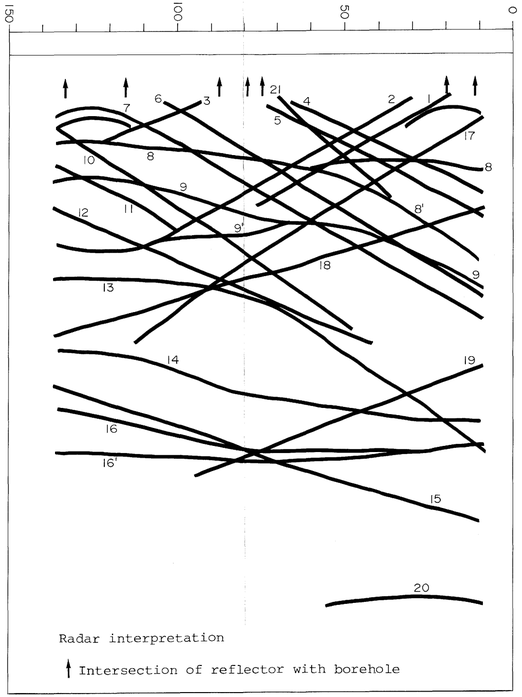

Radar reflecting structures intersecting the borehole					Radar reflecting structures not intersecting the borehole				
No.	Position	Angle Lower/Upper		Comments	No.	Distance to borehole	Angle Lower/Upper		Comments
1/1	12m	35			1/8,8'	20- 55m			Undulating with a apophysis? (8')
1/2	20m	35							
1/3	75m	25			1/9,9'	30- 60m			Including a apophysis? (9')
1/4	79m		30						
1/5	88m		30	Not used for geol. model					
1/6	115m		35		1/10	20- 50m		40	
1/7	132m		35		1/11	25- 50m		30-40	
1/21	79m		65		1/12	40- 75m		25	
					1/13	60-110m		0-45	
					1/14	80-100m		10-20	Undulating
					1/15	90-130m		20	Not used for geol. model
					1/16,16'	100-110m	0-10	0-15	
					1/17	10- 80m	35-45		
					1/18	40- 80m	20		
					1/19	85-120m	25		Not used for geol. model
					1/20	150m			Point source, BK-drift

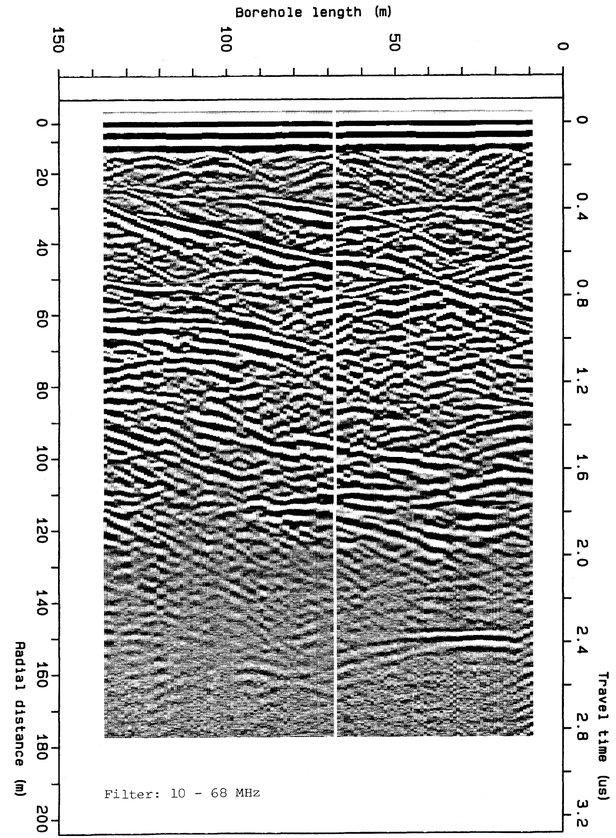

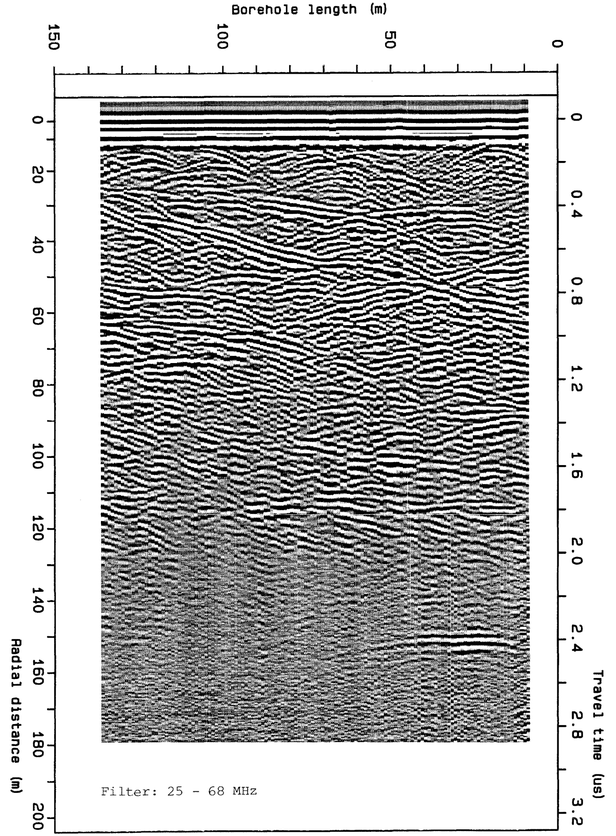

NAGRA TECHNICAL REPORT NTB 87-13

RADAR REFLECTOGRAMS FROM BOUS 85.001 AND INTERPRETATIONS

GRIMSEL TEST SITE | DAT.: | ENCLOSURE 1

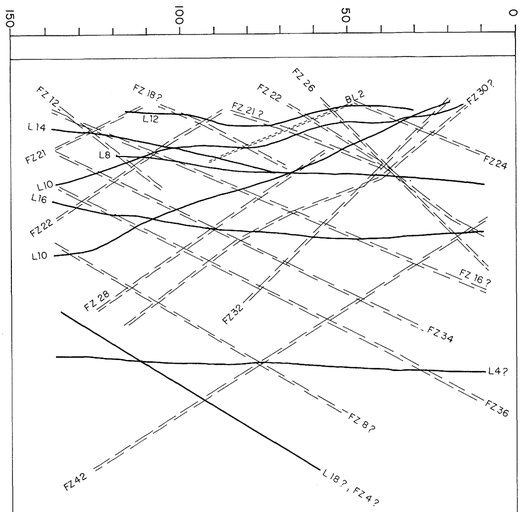

Geological interpretation

- Lamprophyre
- Fracture/shear zone
- Biotite layer

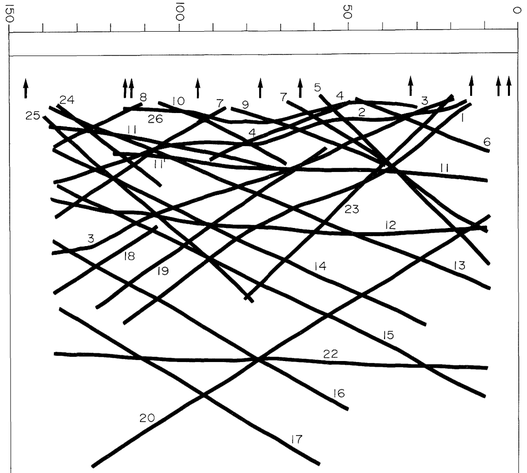

Radar interpretation

Intersection of reflector with borehole

Radar reflecting structures intersecting the borehole					Radar reflecting structures not intersecting the borehole				
No.	Position	Angle Lower/Upper		Comments	No.	Distance to borehole	Angle Lower/Upper		Comments
2/1	3m	25-55		Undulating	2/11,11'	20- 35m		0-10	
2/2	6m	15			2/12	40- 50m		0-10	
2/3	6m	25			2/13	10- 60m		25	
2/4	32m	25			2/14	25- 70m		25-30	
2/5	64m		80		2/15	35- 95m		30	
2/6	64m		25		2/16	45- 95m		35	
2/7	76m	40	40		2/17	70-110m		35	
2/8	95m	35			2/18	45- 65m	40		Not used for geol. model
2/9	114m		20						
2/10	116m		30		2/19	20- 70m	40		
2/23	14m	60-80			2/20	50-110m	40		
2/24	145m		50		2/22	80- 85m		0	
					2/25	15- 65m		55	Not used for geol. model
					2/26	10- 15m		0	

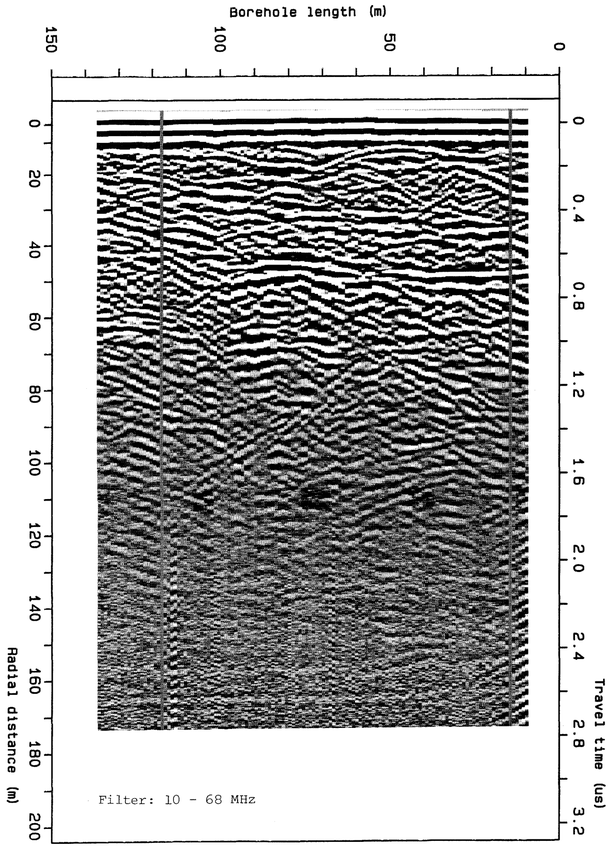

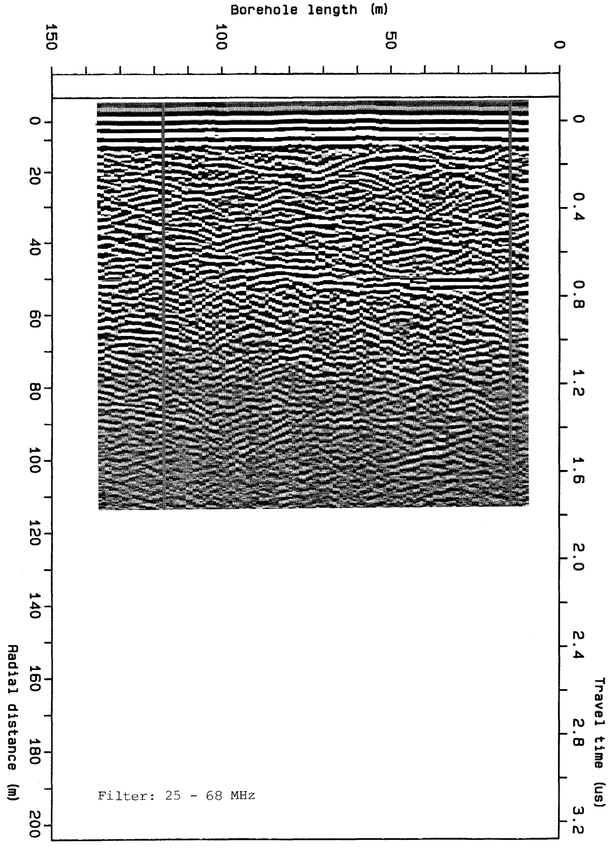

NAGRA TECHNICAL REPORT NTB 87-13

RADAR REFLECTOGRAMS FROM BOUS 85.002 AND INTERPRETATIONS

GRIMSEL TEST SITE | DAT.: | ENCLOSURE 2

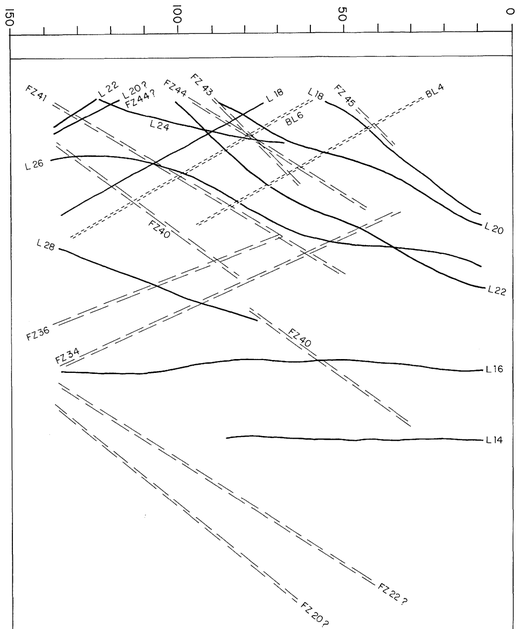

Geological interpretation

Lamprophyre

Fracture/shear zone

Biotite layer

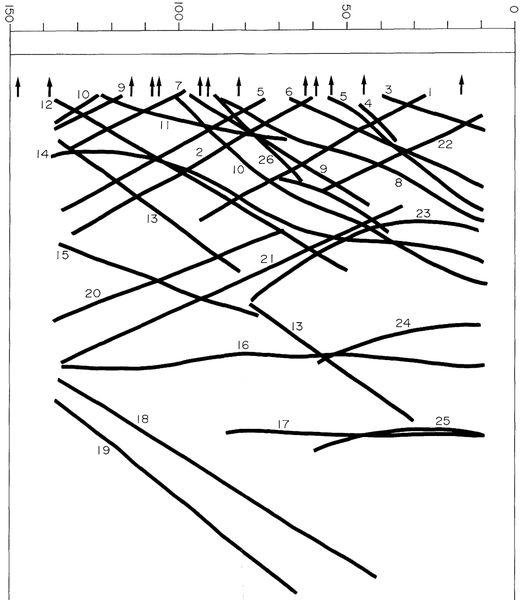

Radar interpretation

Intersection of reflector with borehole

Radar reflecting structures intersecting the borehole					Radar reflecting structures not intersecting the borehole				
No.	Position	Angle Lower/Upper		Comments	No.	Distance to borehole	Angle Lower/Upper		Comments
3/1	16m	30			3/13	20-100m		45	
3/2	45m	35			3/14	25- 55m			Undulating
3/3	55m		20	Not used for geol. model	3/15	50- 7 m		20	
					3/16	85m		0	
3/4	59m		80		3/17	110m		0	
3/5	62m	35	50		3/18	85-150m		40	
3/6	82m		25	Not used for geol. model	3/19	95-150m		50	
					3/20		25		
3/7	91m	30		Not used for geol. model	3/21	40- 85m	25		
				Undulating	3/22	10- 40m	25		Reflection from bore-hole
3/8	106m		(35)						SB 80.002
3/9	108m	30	35						Point sour-ce, BK-drift
3/10	114m	40	(50)						
3/11	138m			Undulating apophysis from 87	3/23	45m			Diffraction pattern
					3/24	75m			
3/12	148m		35						Diffraction pattern
3/26	93m		70-80	Water outflow	3/25	105m			

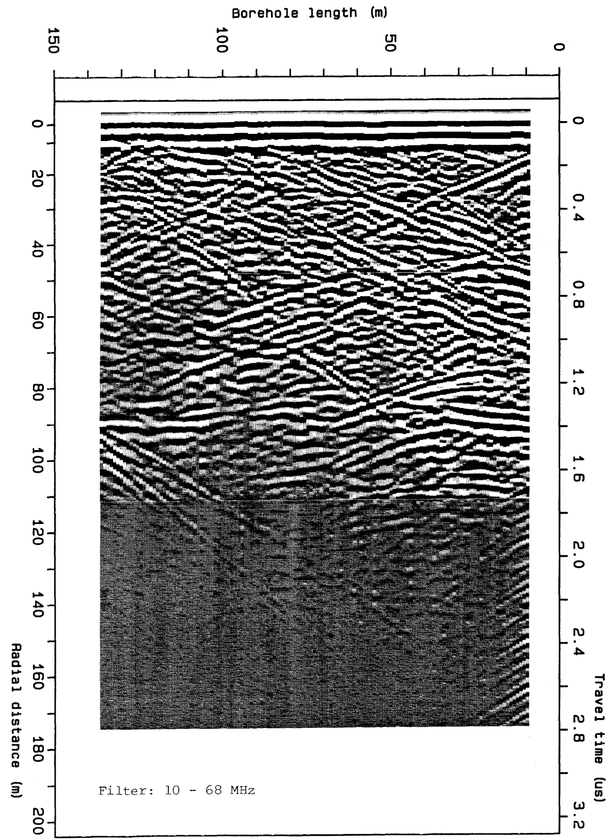

Filter: 10 - 68 MHz

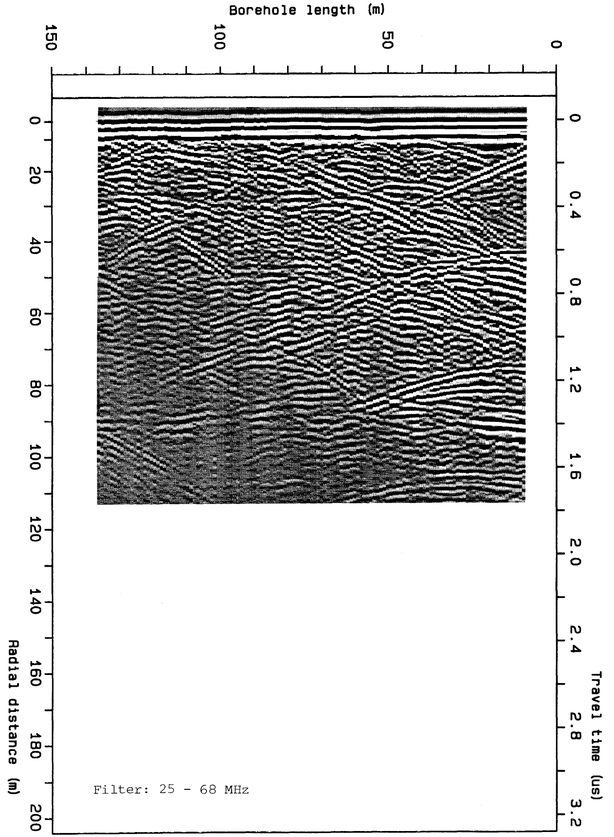

Filter: 25 - 68 MHz

NAGRA	TECHNICAL REPORT NTB 87-13	
RADAR REFLECTOGRAMS FROM BOUS 85.003 AND INTERPRETATIONS		
GRIMSEL TEST SITE	DAT.:	ENCLOSURE 3

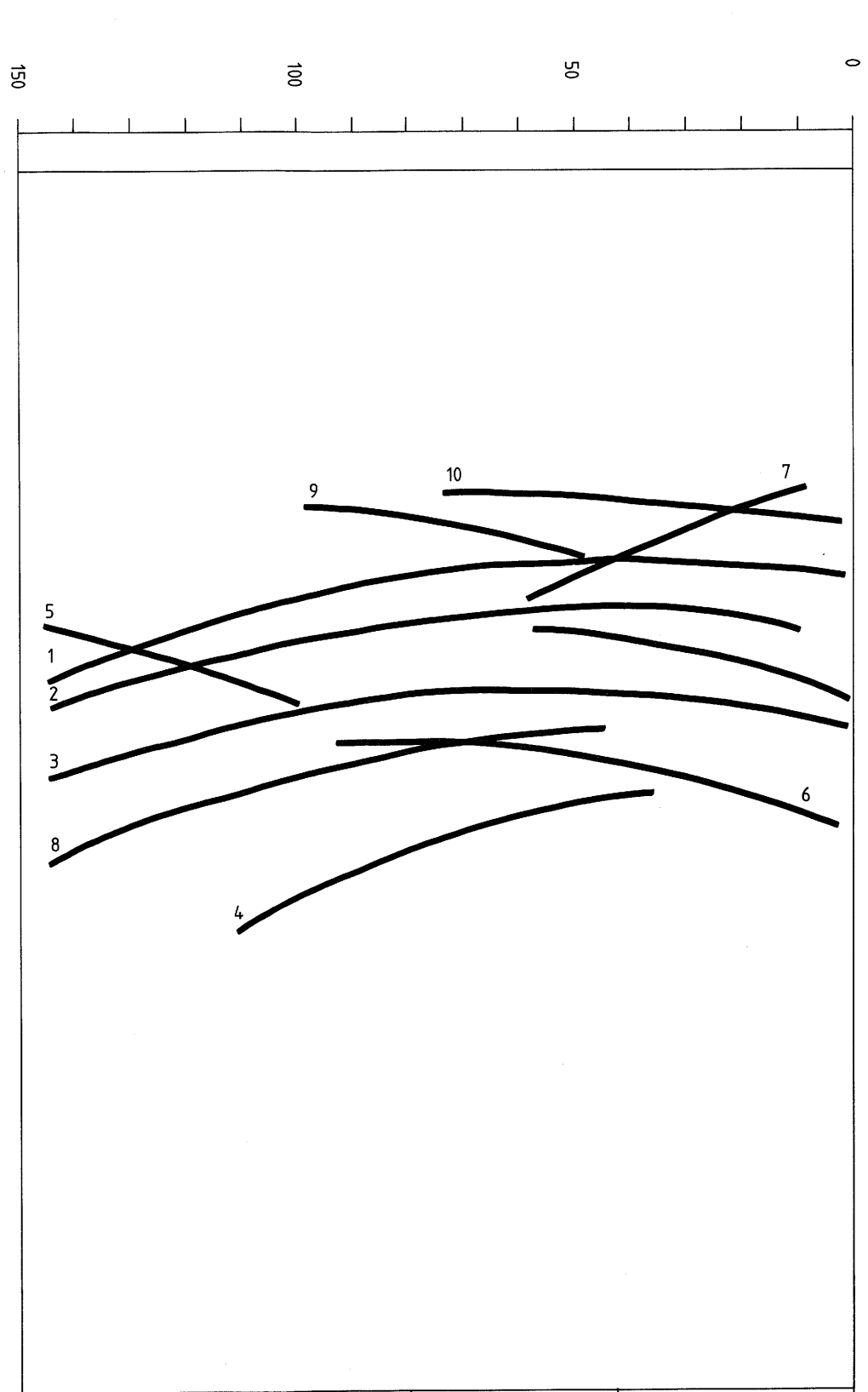

No.	Intersection depth	Slope (m)	Product $d_1 \cdot d_2$ (m^2) (lamprophyres)	Comments (No. singlehole)
C1/1			2100	1/8
C1/2			3200	1/14
C1/3			5100	1/16
C1/4	-100	50		1/18
C1/5	155	-94		1/10
C1/6	213	-44		--
C1/7	0	52		Drift
C1/8			7000	--
C1/9	110	-34		1/6
C1/10	130	-13		--

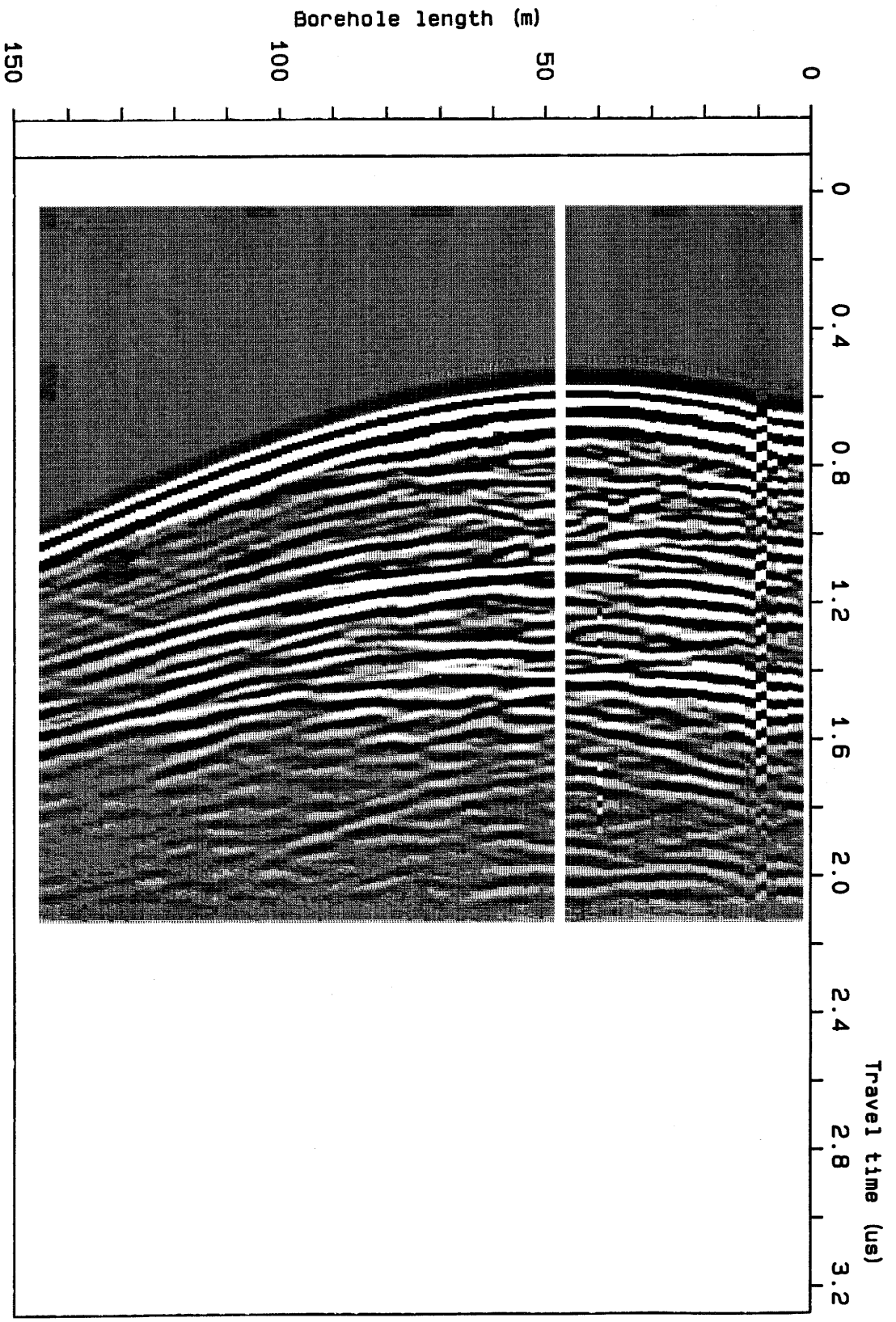

NAGRA **TECHNICAL REPORT NTB 87-13**

CROSSHOLE SCAN 1:
BOUS 85.002 (49 m) — BOUS 85.001

GRIMSEL TEST SITE | DAT.: | ENCLOSURE 4

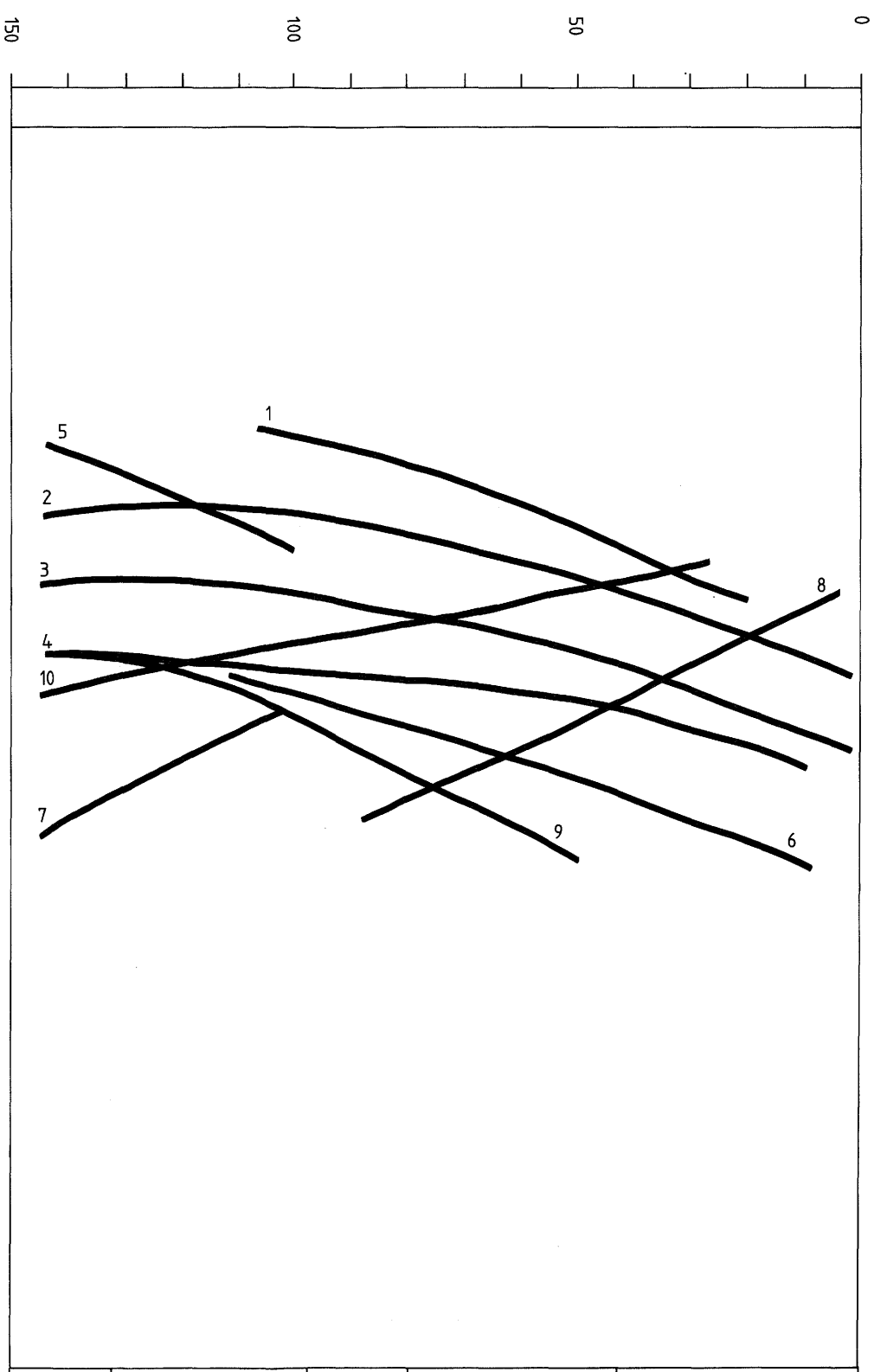

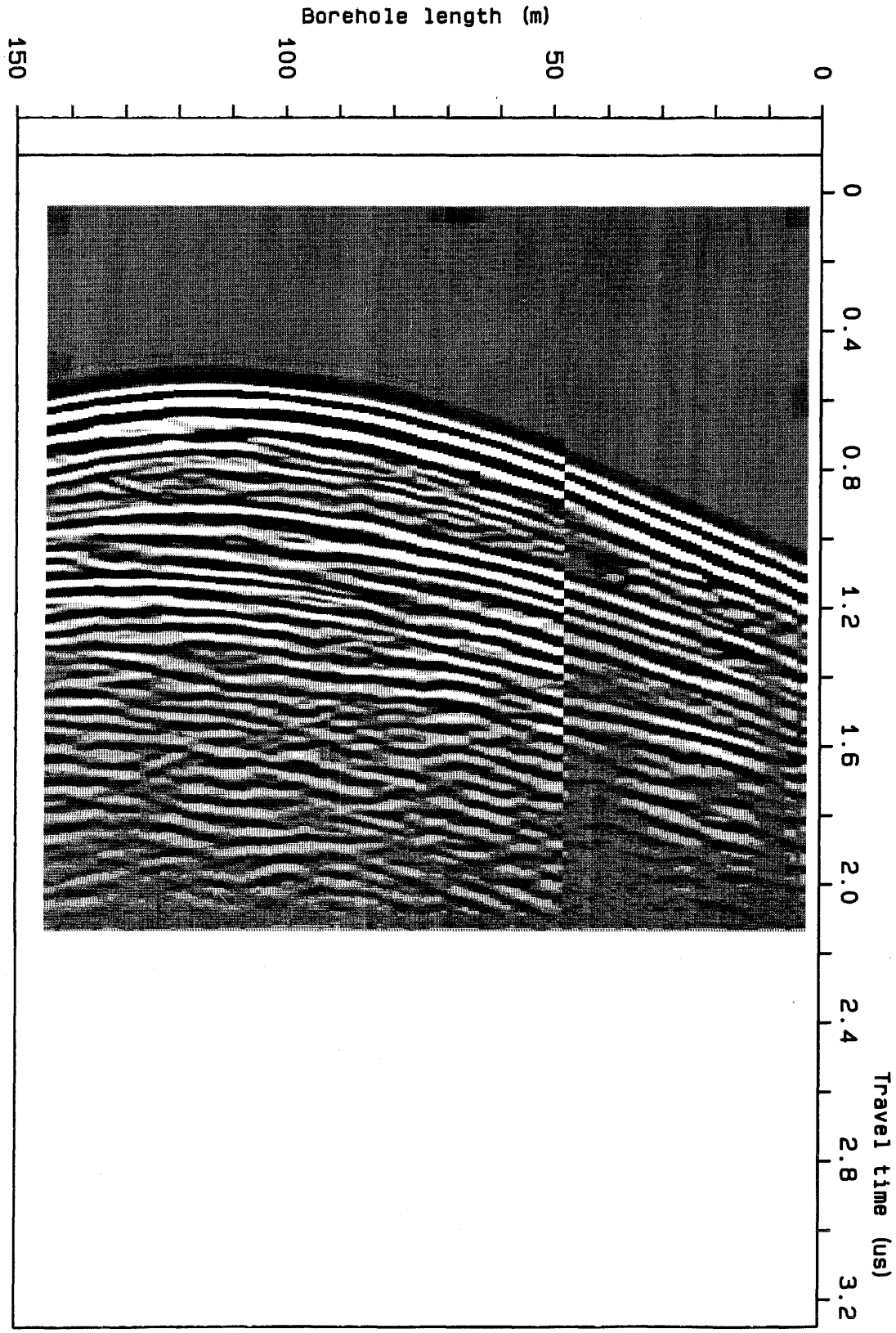

No.	Intersection depth	Slope (m)	Product $d_1 \cdot d_2$ (m^2) (lamprophyres)	Comments (No. singlehole)
C2/1	160	-10		?
C2/2			2100	--
C2/3			3200	--
C2/4			5100	--
C2/5	155	-45		1/10
C2/6	300	-38		--
C2/7	16	80		1/1, lamprophyre, small angle to borehole
C2/8	0	115		Drift
C2/9	195	-72		1/11
C2/10	- 55	31		?

NAGRA **TECHNICAL REPORT NTB 87-13**

CROSSHOLE SCAN 2:
BOUS 85.002 (121 m) — BOUS 85.001

GRIMSEL TEST SITE | DAT.: | ENCLOSURE 5

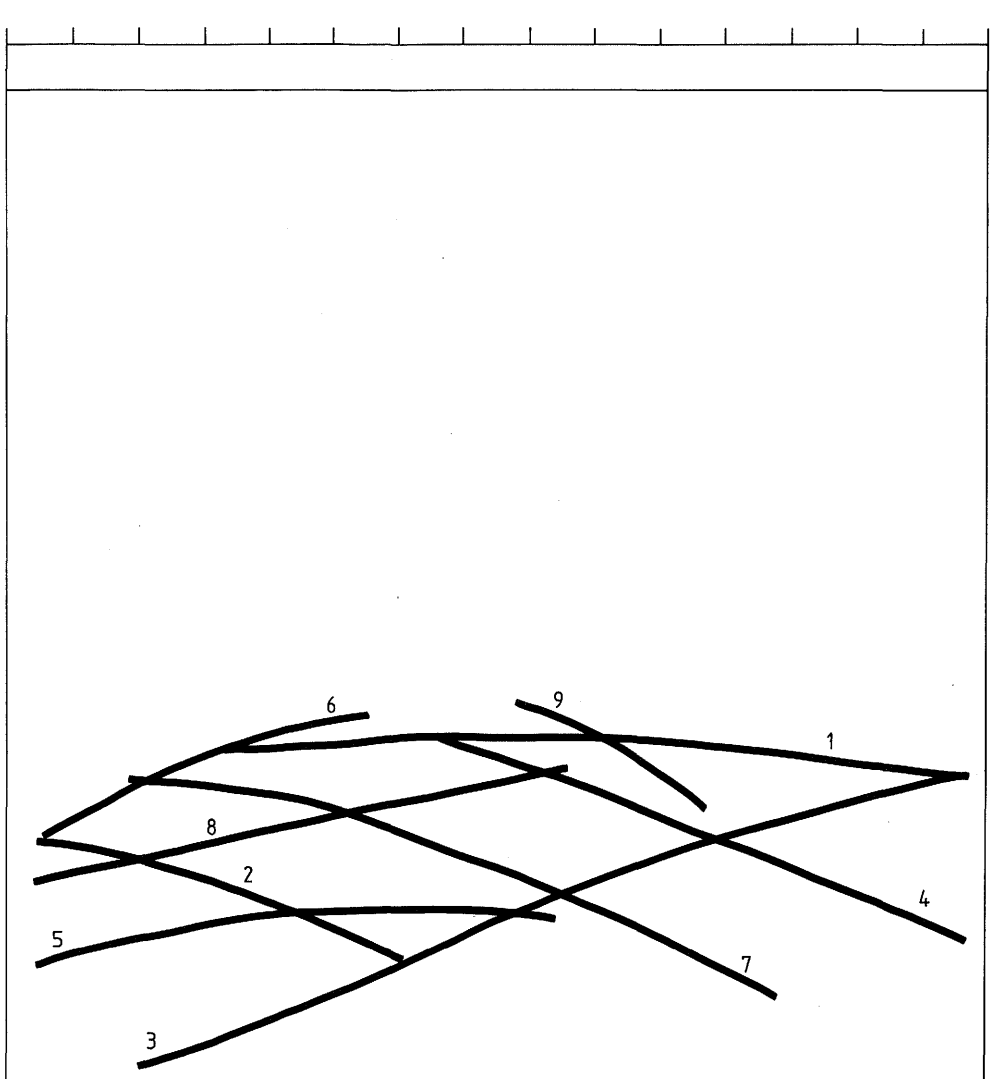

No.	Intersection depth	Slope (m)	Product $d_1 \cdot d_2$ (m^2) (lamprophyres)	Comments (No. singlehole)
C3/1			2100	1/9
C3/2	185	-78		(3/14 ?)
C3/3	- 20	74		Drift
C3/4	118	-59		3/10
C3/5			7000	2/11 ?
C3/7	141	-86		3/11
C3/8	- 95	19		?
C3/9	85	-87		3/6, only mafic lenses seen in borehole (lamprophyre?)

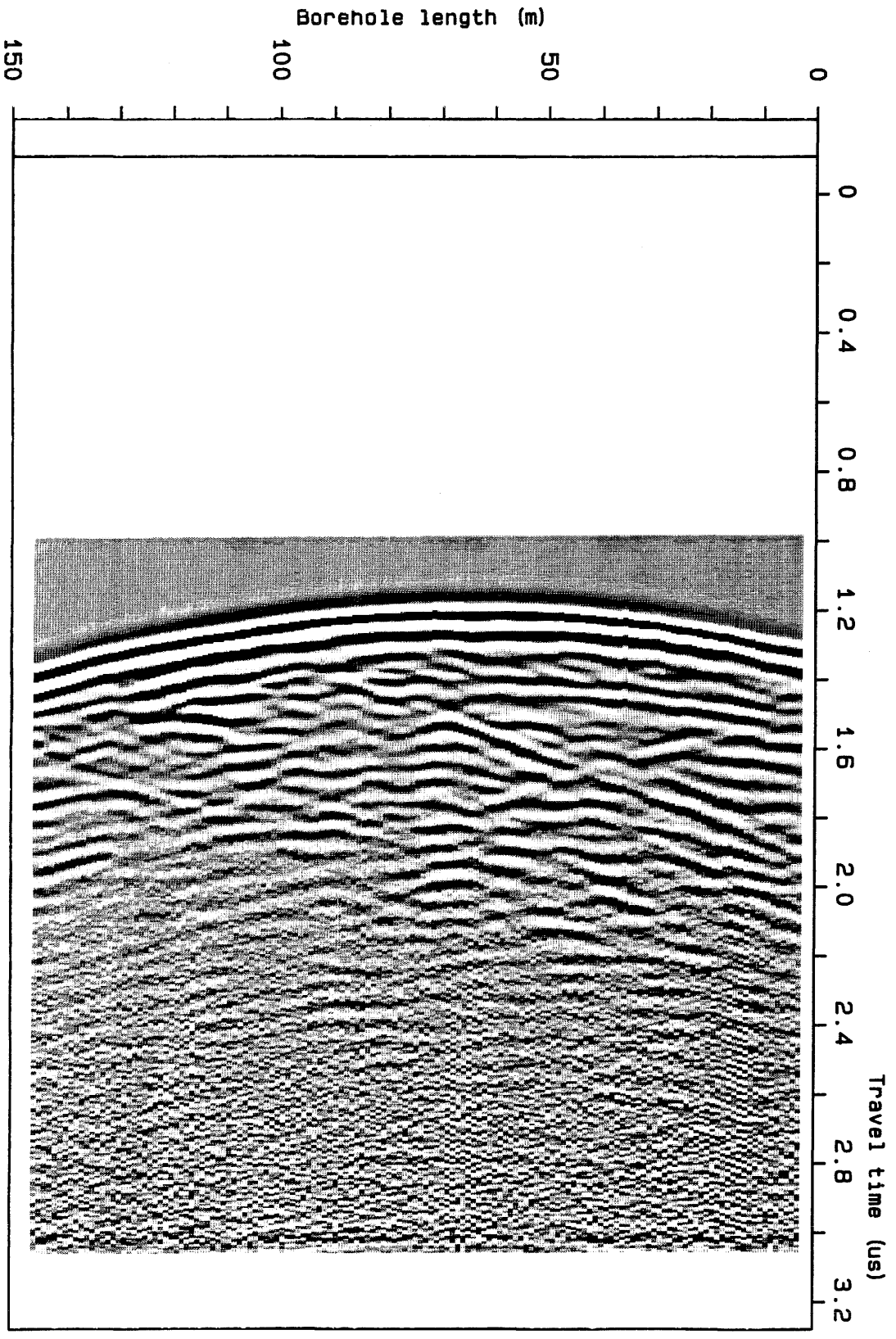

NAGRA **TECHNICAL REPORT NTB 87-13**

CROSSHOLE SCAN 3:
BOUS 85.002 (49 m) — BOUS 85.003

GRIMSEL TEST SITE | DAT.: | ENCLOSURE 6

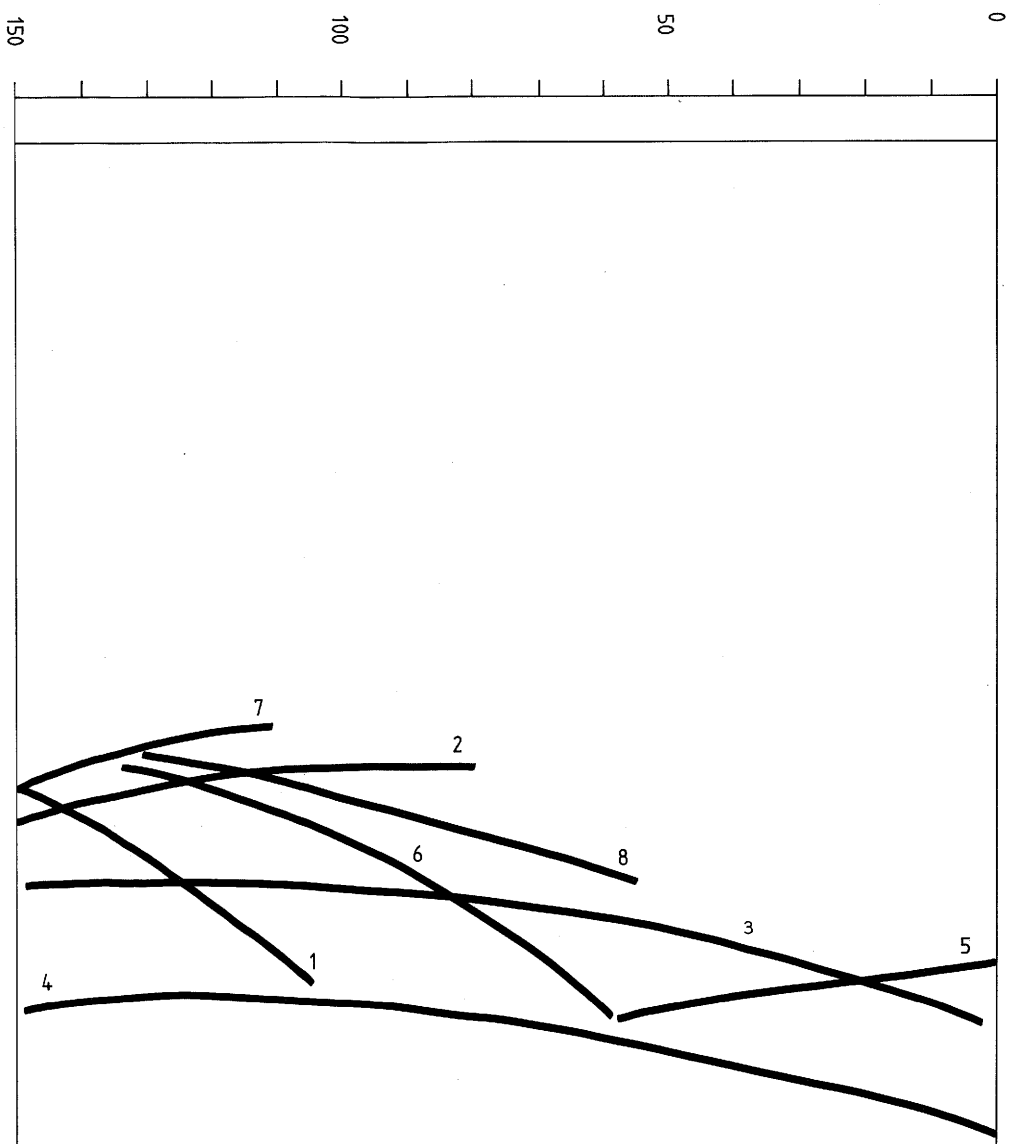

No.	Intersection depth	Slope (m)	Product $d_1 \cdot d_2$ (m^2) (lamprophyres)	Comments (No. singlehole)
C4/1	164	-113		3/13
C4/2	87	45		3/7
C4/3			3400	1/9 (2/2)
C4/4			8000	2/11 ?
C4/5	- 21	84		Drift
C4/6	141	-69		3/11
C4/7	105	40		3/8
C4/8	220	-13		3/19 ?

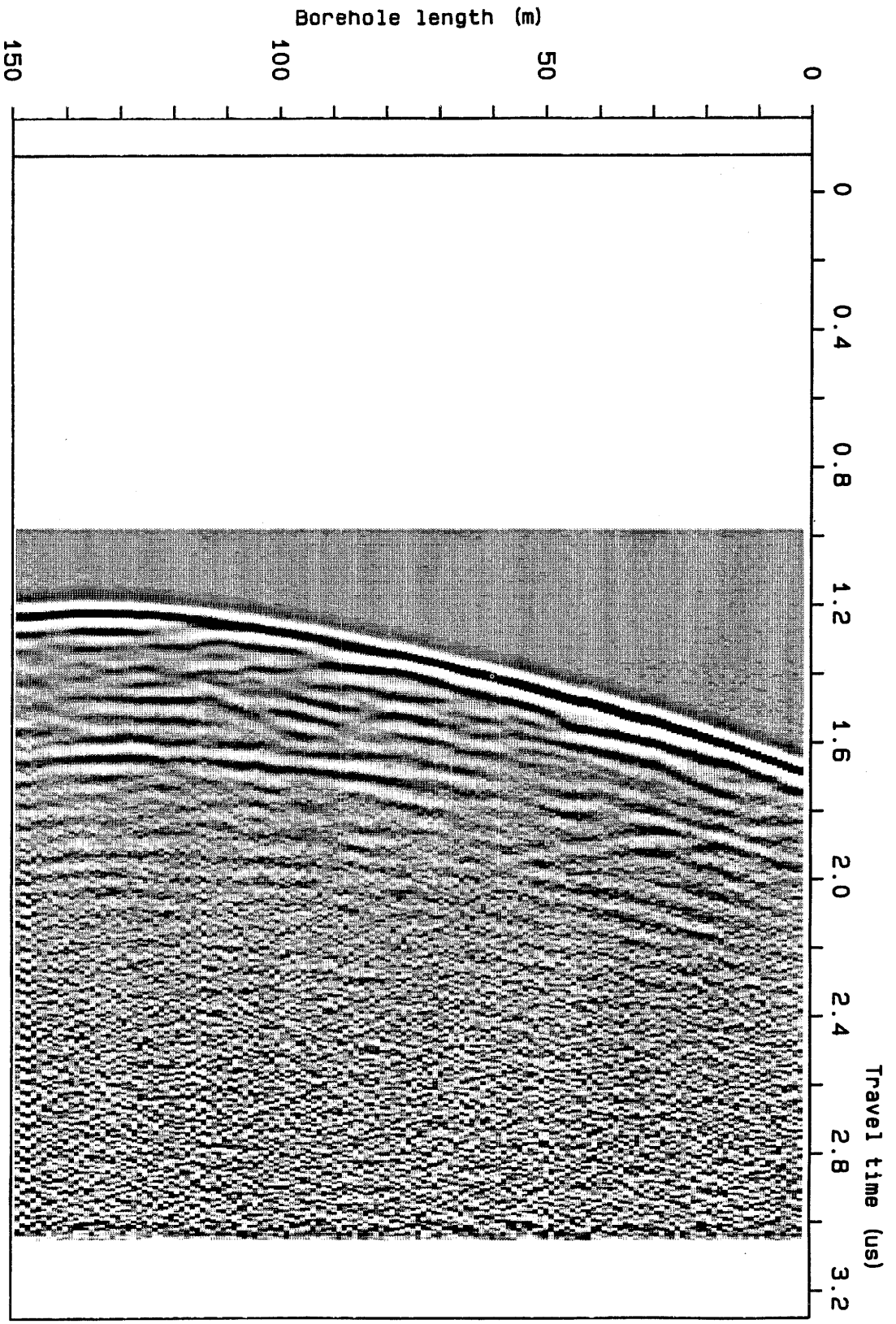

NAGRA **TECHNICAL REPORT NTB 87-13**

CROSSHOLE SCAN 4:
BOUS 85.002 (121 m) — BOUS 85.003

GRIMSEL TEST SITE | DAT.: | ENCLOSURE 7

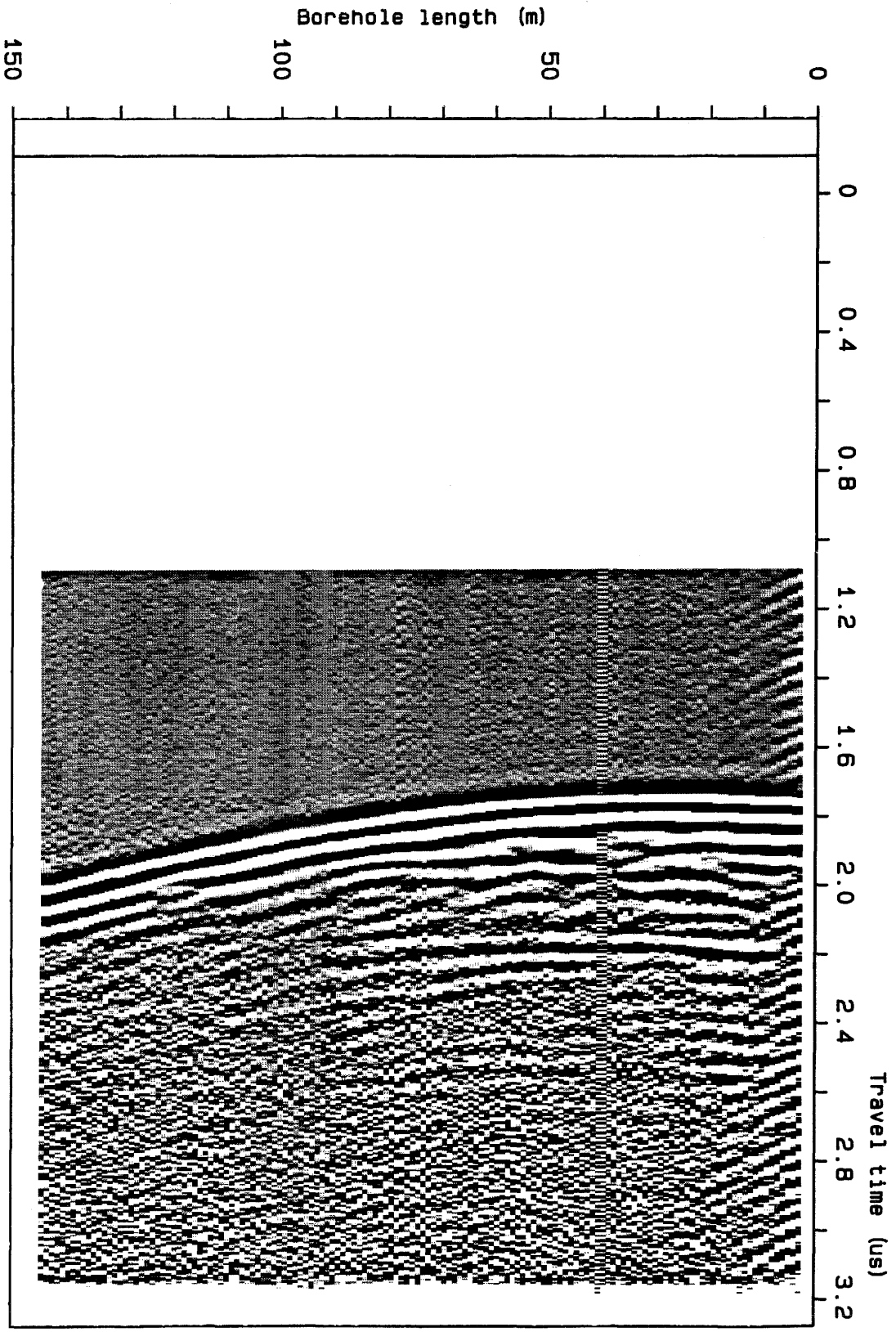

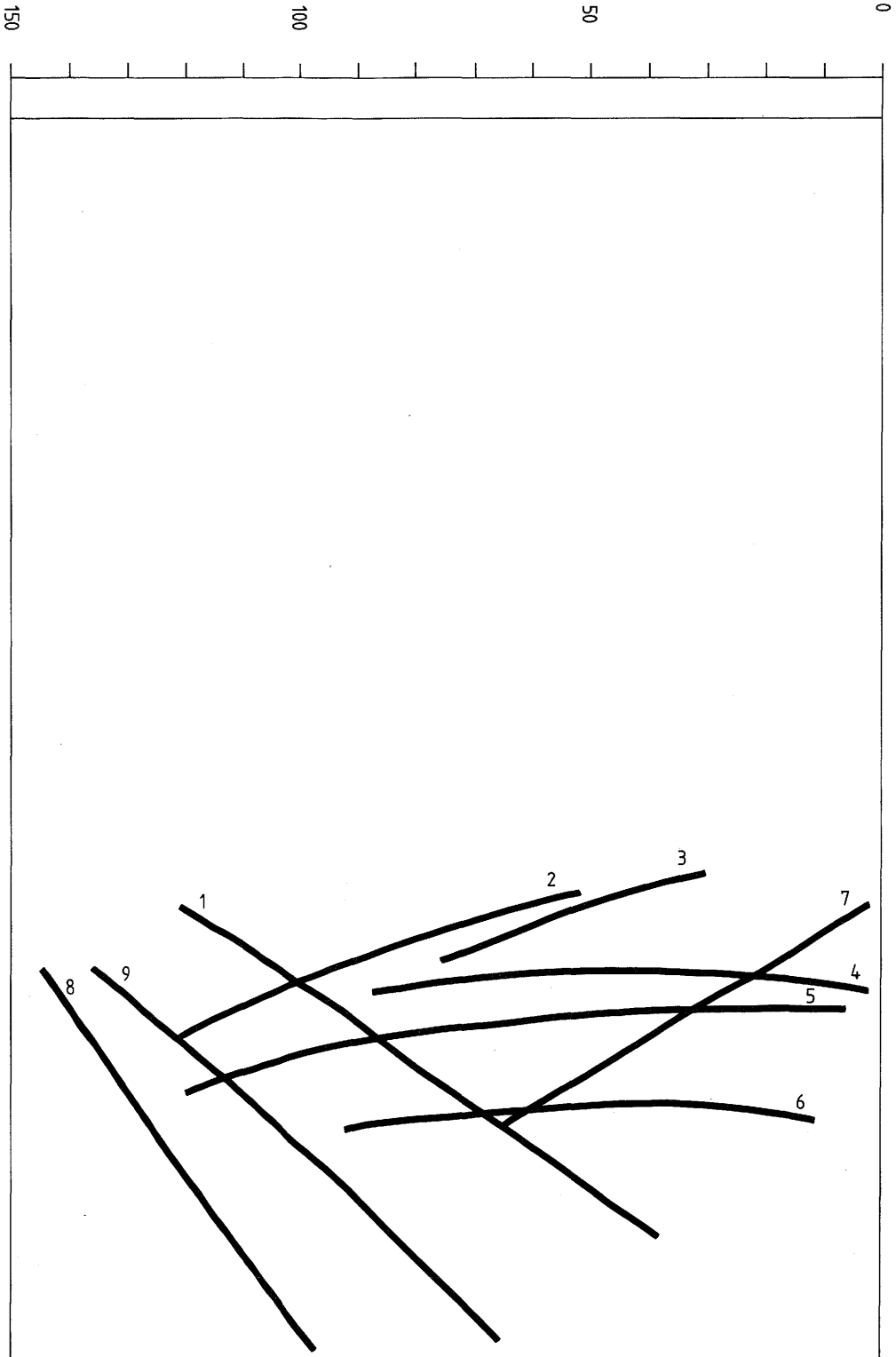

No.	Intersection depth	Slope (m)	Product $d_1 \cdot d_2$ (m^2) (lamprophyres)	Comments (No. singlehole)
C5/1	123	-203		1/6 or 1/7
C5/2	10	48		1/1, lamprophyre, small angle to borehole
C5/3	0	60		Drift
C5/4			5900	1/8
C5/5			7300	--
C5/6			10700	--
C5/7				
C5/8				
C5/9				

NAGRA **TECHNICAL REPORT NTB 87-13**

CROSSHOLE SCAN 5:
BOUS 85.003 (51 m) — BOUS 85.001

GRIMSEL TEST SITE | DAT.: | ENCLOSURE 8

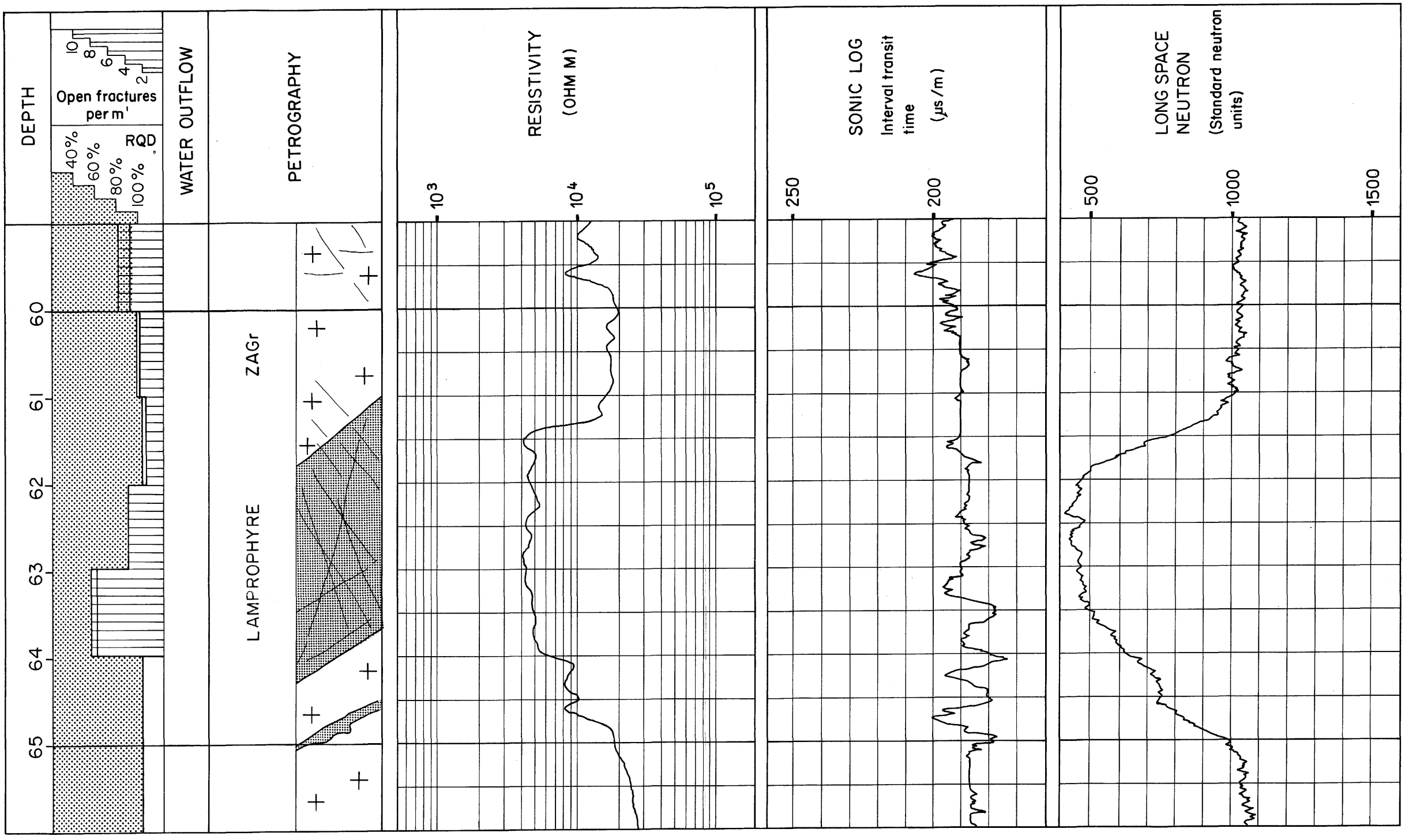

NAGRA	TECHNICAL REPORT NTB 87-13	
LOG RESPONSE LAMPROPHYRE IN BOUS 85.003 AT 61.5 — 64 m		
GRIMSEL TEST SITE	DAT.:	ENCLOSURE 9.

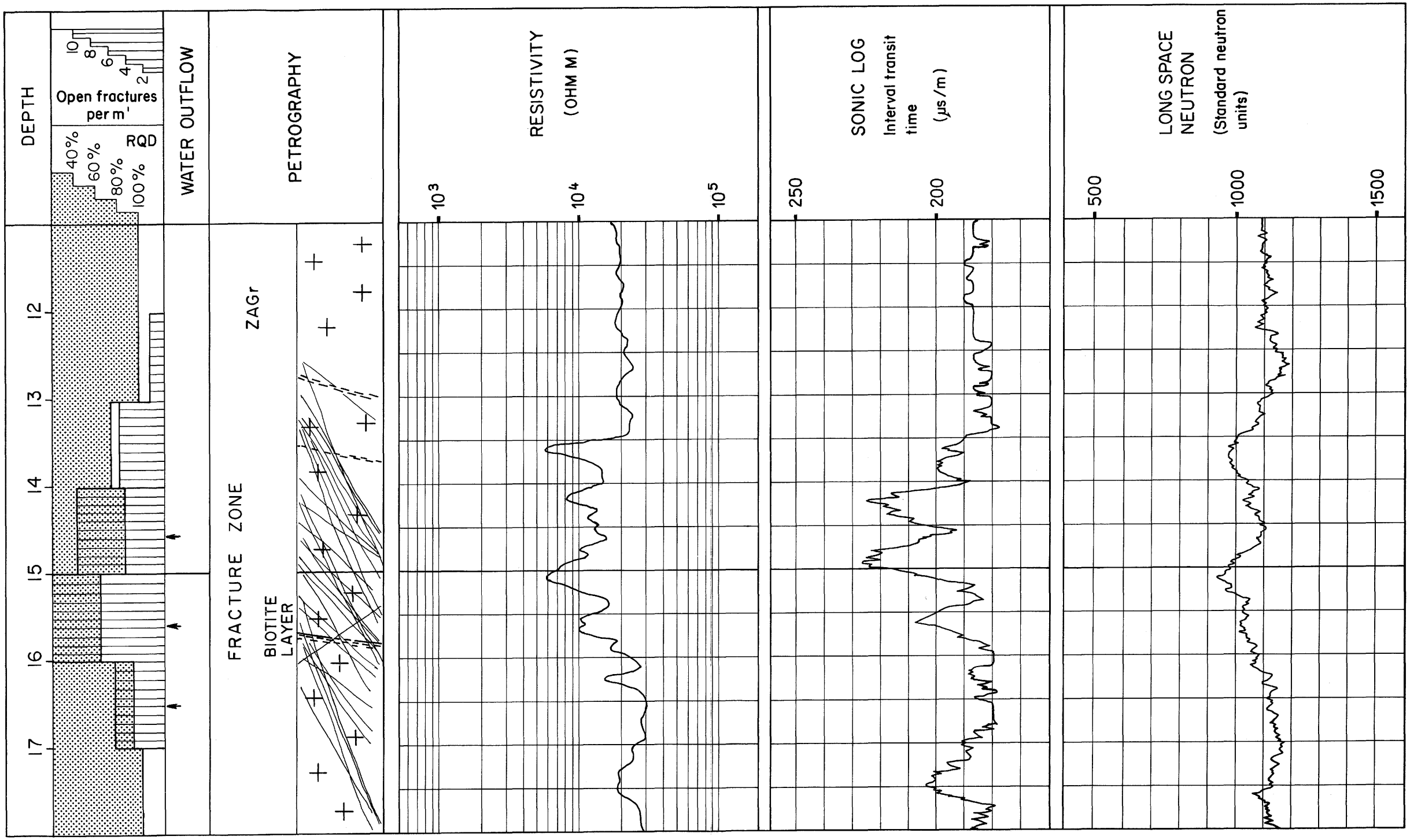

NAGRA	TECHNICAL REPORT NTB 87-13	
LOG RESPONSE FRACTURE ZONE IN BOUS 85.002 AT 13.5 — 16.5 m		
GRIMSEL TEST SITE	DAT.:	ENCLOSURE 10

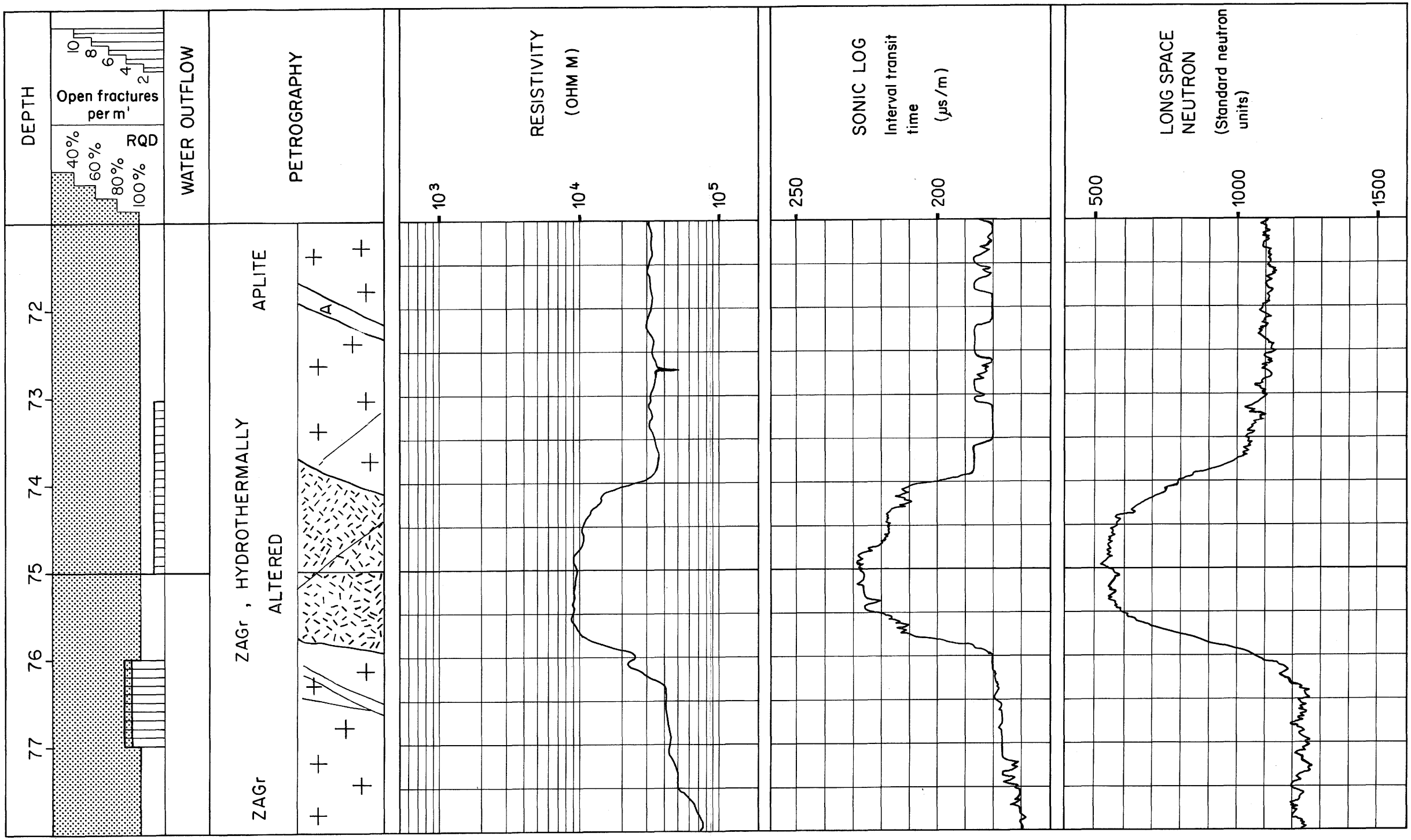

NAGRA	TECHNICAL REPORT NTB 87-13
LOG RESPONSE HYDROTHERMALLY ALTERED GRANITE IN BOUS 85.001 AT 74 — 76 m	
GRIMSEL TEST SITE	DAT.: ENCLOSURE 11

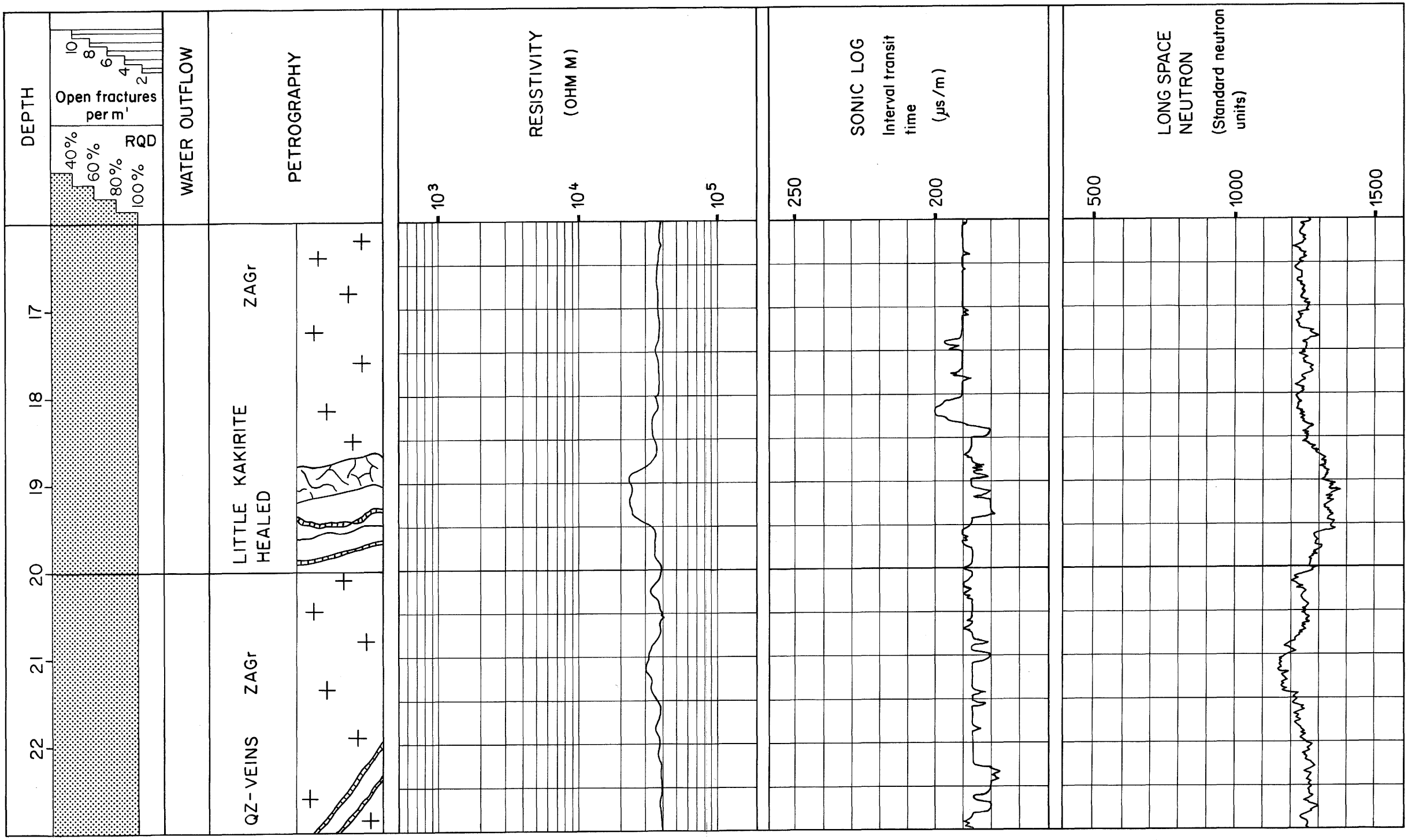

NAGRA	TECHNICAL REPORT NTB 87-13	
LOG RESPONSE KAKIRITE IN BOUS 85.001 AT 19 m		
GRIMSEL TEST SITE	DAT.:	ENCLOSURE 12

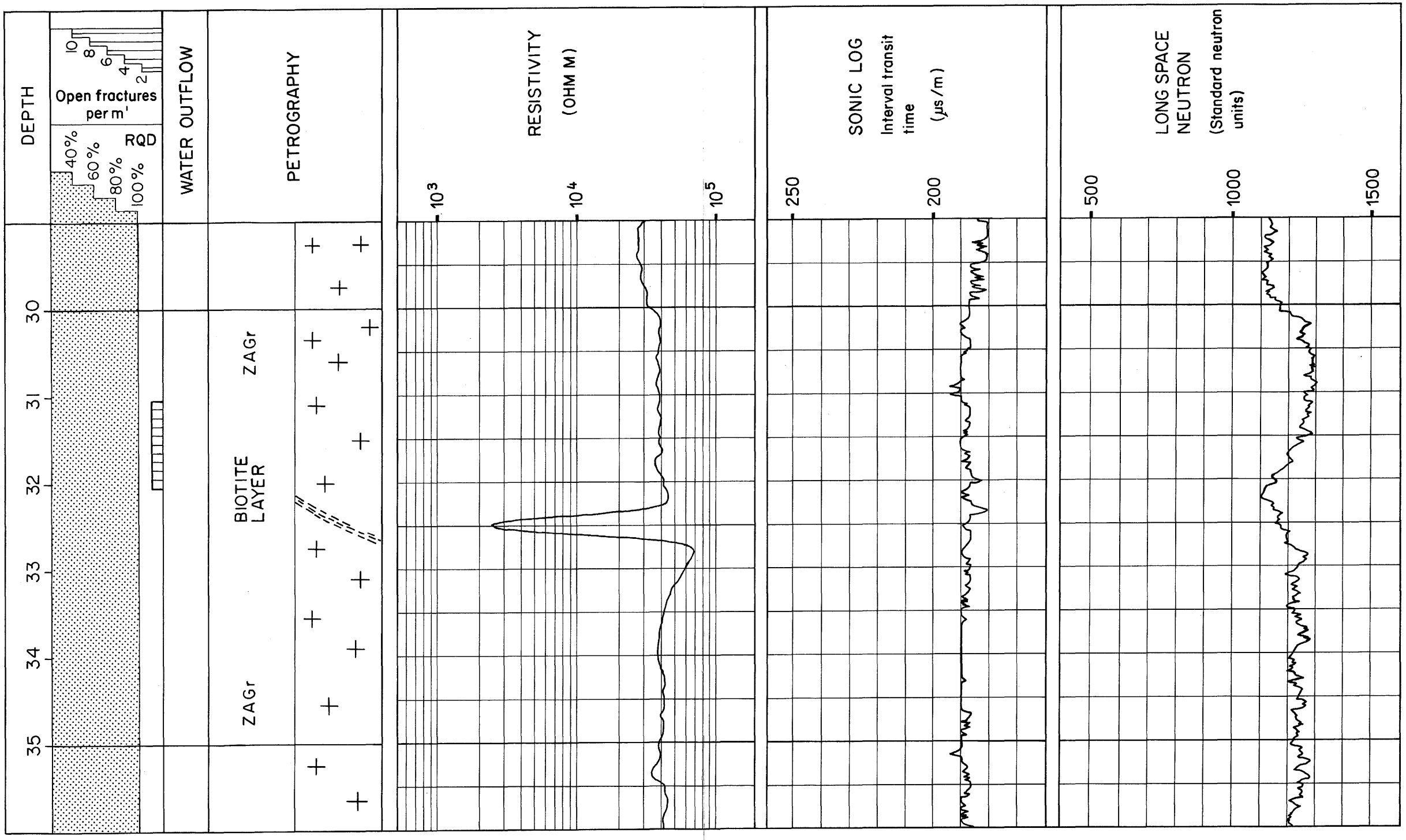

NAGRA	TECHNICAL REPORT NTB 87-13	
LOG RESPONSE BIOTITE LAYER IN BOUS 85.002 AT 32.5 m		
GRIMSEL TEST SITE	DAT.:	ENCLOSURE 13

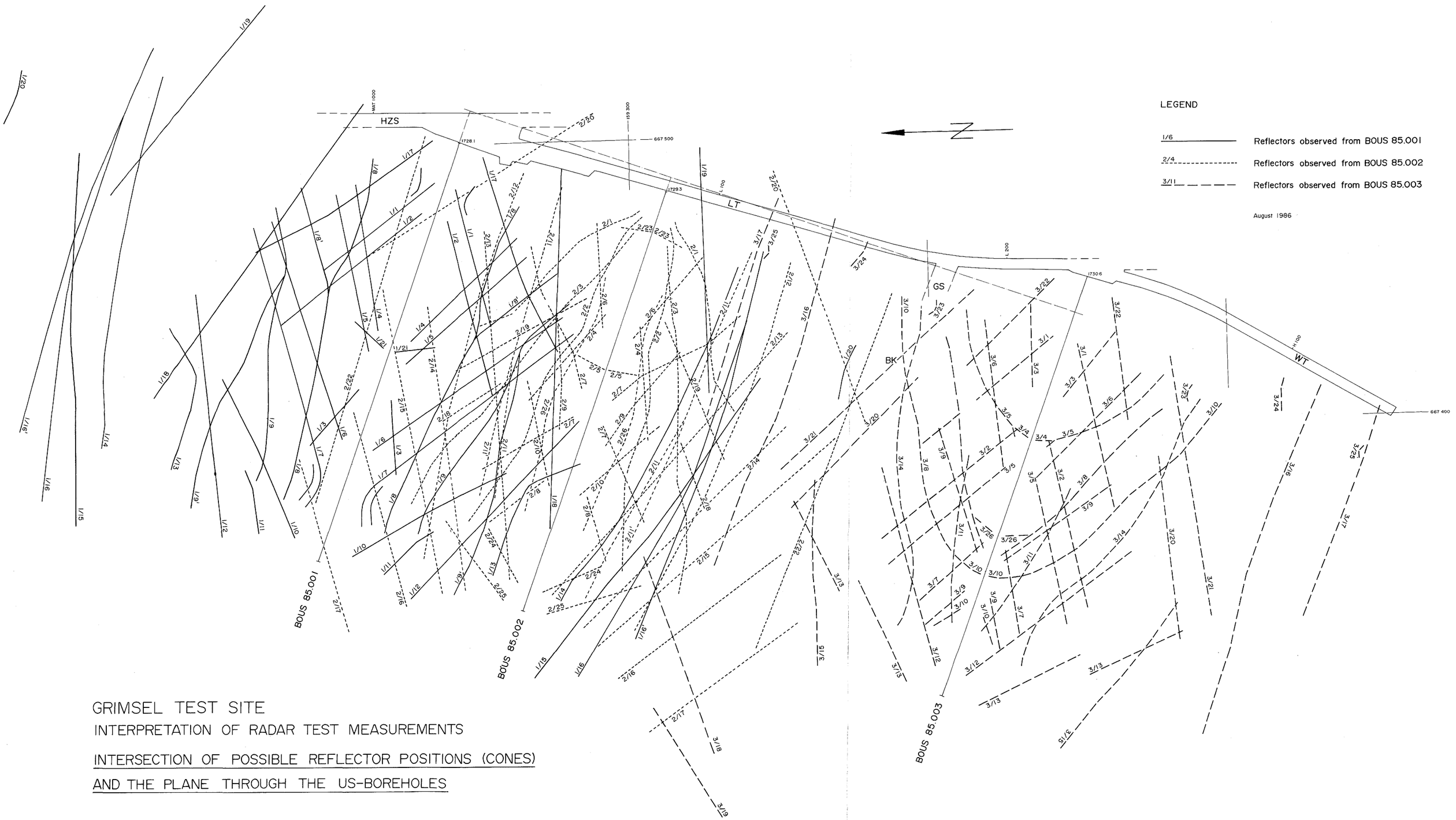

GRIMSEL TEST SITE

INTERPRETATION OF RADAR TEST MEASUREMENTS

INTERSECTION OF POSSIBLE REFLECTOR POSITIONS (CONES)
AND THE PLANE THROUGH THE US-BOREHOLES

NAGRA	TECHNICAL REPORT NTB 87-13	
POSSIBLE REFLECTOR POSITIONS ASSUMING VERTICAL INCIDENCE		
GRIMSEL TEST SITE	DAT.:	ENCLOSURE 14

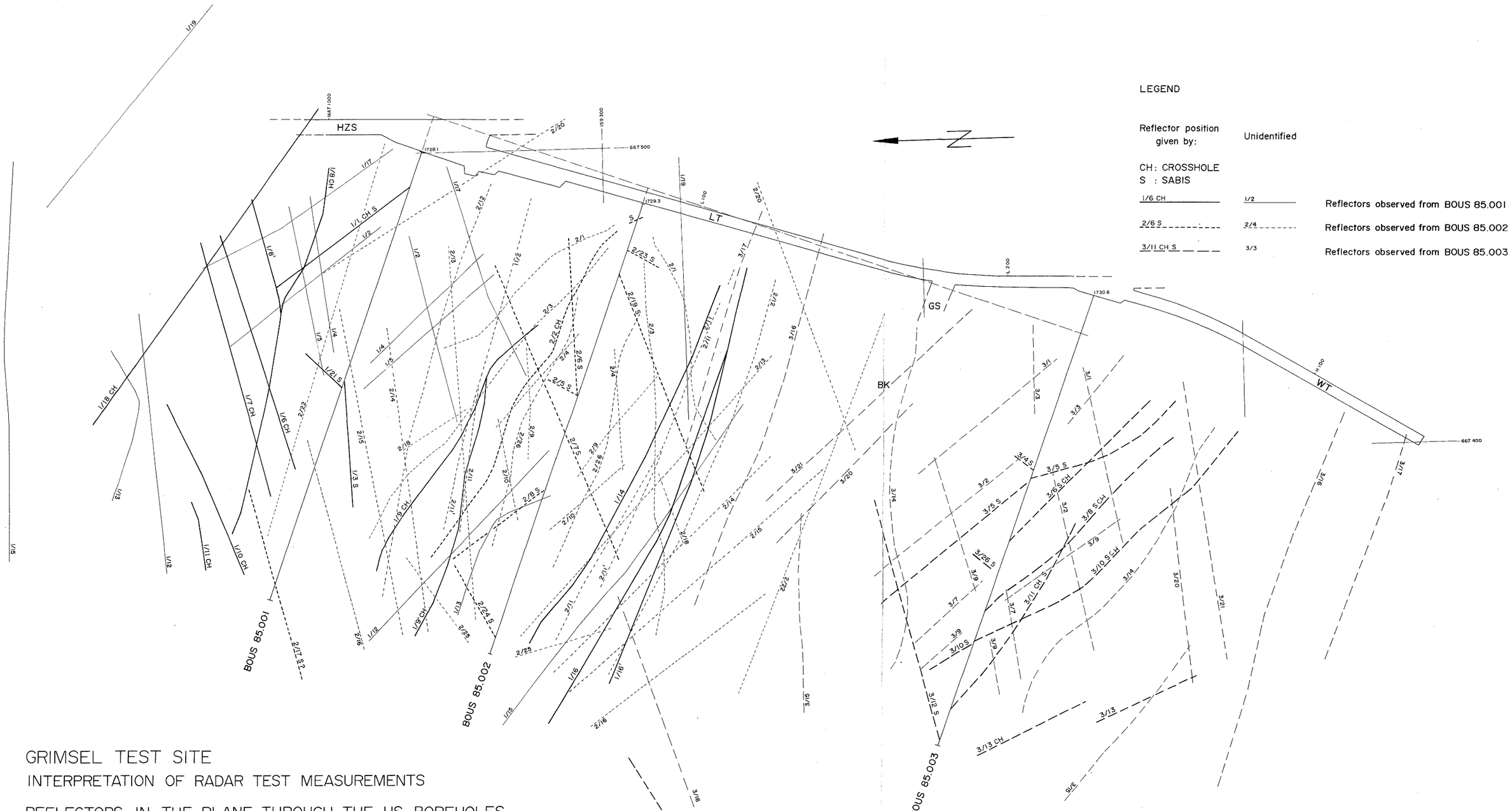

LEGEND

Reflector position given by: Unidentified

CH: CROSSHOLE
S : SABIS

1/6 CH	1/2	Reflectors observed from BOUS 85.001
2/6 S	2/4	Reflectors observed from BOUS 85.002
3/11 CH S	3/3	Reflectors observed from BOUS 85.003

GRIMSEL TEST SITE

INTERPRETATION OF RADAR TEST MEASUREMENTS

REFLECTORS IN THE PLANE THROUGH THE US-BOREHOLES, UNAMBIGUOUSLY LOCALISED BY GEOPHYSICAL MEANS AND POSSIBLE POSITION OF UNIDENTIFIED REFLECTORS

0 50 m

NAGRA **TECHNICAL REPORT NTB 87-13**

TRUE POSITION OF THE REFLECTORS AS DEFINED BY GEOPHYSICAL MEANS

GRIMSEL TEST SITE | DAT.: | **ENCLOSURE 15**

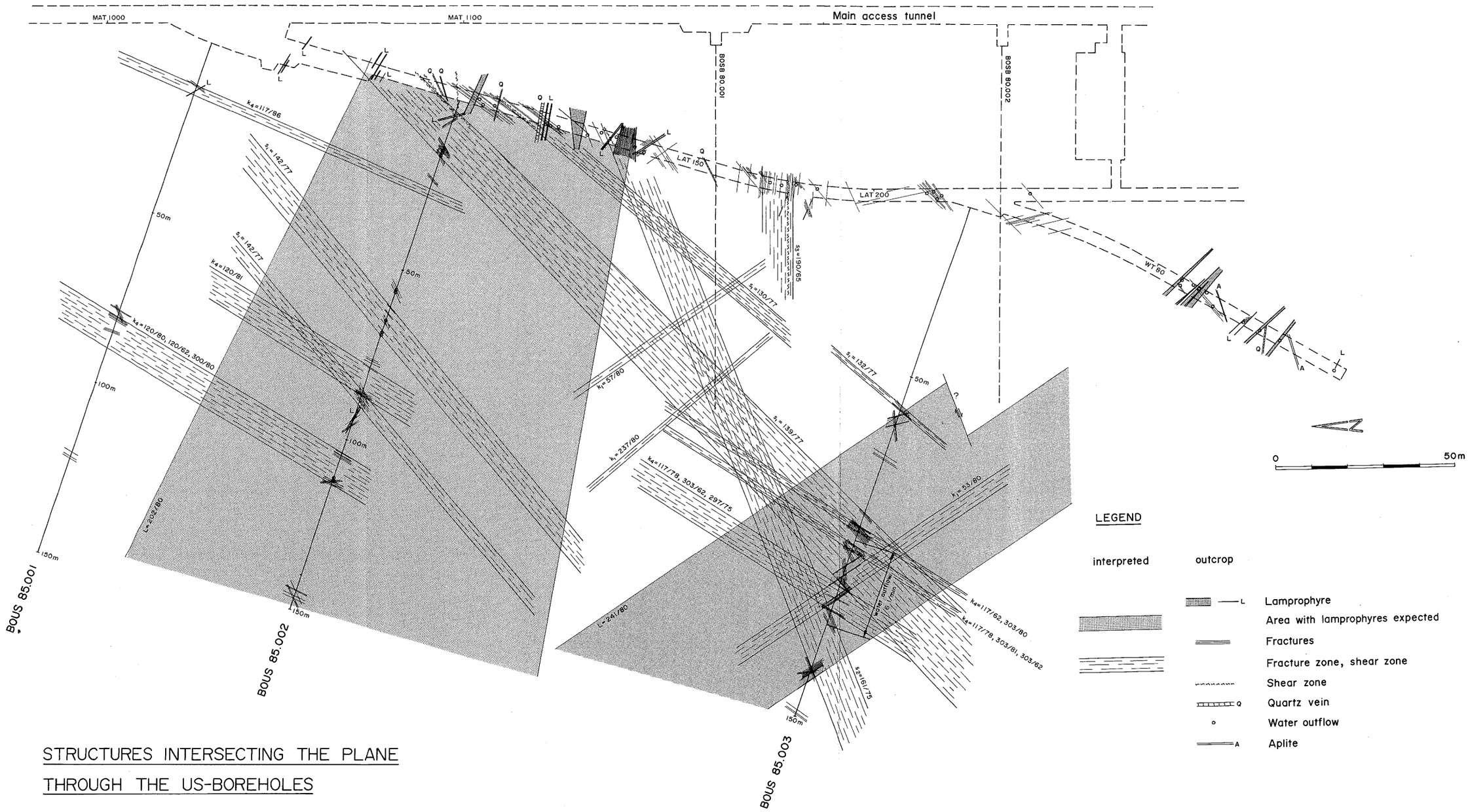

STRUCTURES INTERSECTING THE PLANE THROUGH THE US-BOREHOLES

NAGRA	TECHNICAL REPORT NTB 87-13	
PRELIMINARY GEOLOGICAL MODEL		
GRIMSEL TEST SITE	DAT.:	ENCLOSURE 16

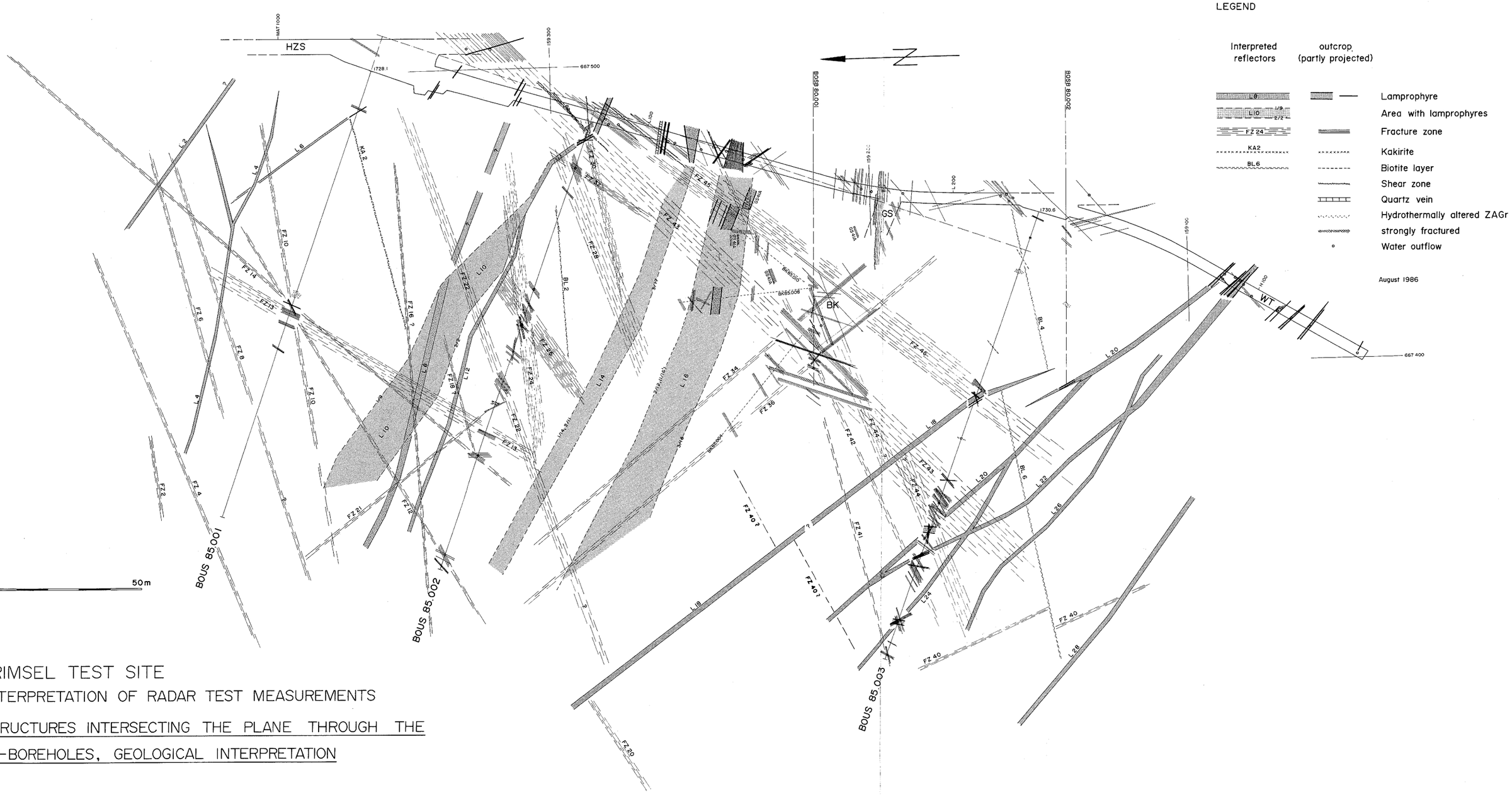

GRIMSEL TEST SITE

INTERPRETATION OF RADAR TEST MEASUREMENTS

STRUCTURES INTERSECTING THE PLANE THROUGH THE US-BOREHOLES, GEOLOGICAL INTERPRETATION

NAGRA	TECHNICAL REPORT NTB 87-13
GEOLOGICAL MODEL BASED ON RADAR REFLECTION INTERPRETATIONS	
GRIMSEL TEST SITE	DAT.: ENCLOSURE 17

	Geometry				Geology			Geophysics					Remarks		
Bore-hole	Pos. m	Width m	Az/Dip deg	Bha deg	Tect. fr/m	Petrography	Transition	Res kohmm	Resw m	T.time µs/m	S-w m	Transition	Hydro-logy	General	No. in final model
001	13.0	0.4	50/80	31	5	Lamp+Qz vein (0.4m) S-side		10.0	0.4	195	0.8	F: flat S: sharp	--	Res two peaks, vein	L 6
002	5.5	0.8	240/80	44	6	Lamp+Qz.vein	F: hydr. alt S: tect cont	7.0	1.5	190	1.0	F: flat	--	Sonic resp. very poor	L 10
003	62.5	2.2	250/80	40	8	Compact lamp	F+S: very sharp tect cont	4.5	3.0	185		F: v sharp S: sharp	--		L 18
	107.0	2.0	255/80	47	>10	Compact lamp	F: v sharp tect S: irreg frac	3.0	4.0	210	0.5	F: v sharp S: v sharp	--	Sonic resp. on frac part (S)	L 20
	115.5	0.7	245/80	39	8	Compact lamp	F+S: sharp	4.0	1.0	180	--	F: fair sh S: extr sh	--	No sonic resp.	L 22
	137.5	1.0	240/80	44	>10	v frac lamp	F+S: sharp	2.7	1.5	190	1.0	F+S: extr sharp	--	Weak sonic resp.	L 24
Average		1.2	--	40	5-10	Lamprophyres	Sharp	5.0	2.0	190	--	Sharp	--	Sonic resp. poor	

alt: altered/alteration
Bha: angle between structure and borehole
cont: contact
deg: degree
extr: extremely
F, S: first and second intersection, respectively
fr, frac: fractured, fracture
irreg: irregular
lamp: lamprophyre
Pos: position of structure in the borehole, middle
Qz: quartz
Resw: width of the resistivity anomaly
Res: resistivity
sh: sharp
S-w: width of the sonic anomaly
Tect: tectonization, open fractures/m
T.time: transit time (1/P-wave velocity), sonic
v: very
w: with

Table AT 1: Lamprophyres identified in the boreholes BOUS 85.001/002/003

	Geometry				Geology			Geophysics					Remarks		
Bore-hole	Pos. m	Width m	Az/Dip deg	Bha deg	Tect. fr/m	Petrography	Transition	Res kohmm	Resw m	T.time µs/m	S-w m	Transition	Hydro-logy	General	No. in final model
001	79.0	1.0	122/62 160/75	73 42	>10	Joints w Clorite	sharp	10.0	4.0	190	4.0	sharp	--		FZ 14 FZ 10 FZ 12
002	3.5	3.0	140/77 160/75 57/80	60 42 38	>10 very frac	Qz, biotite rich	Not sharp	1.0	3.0	250	1.0	Flat	--	Bel. to v promi-nent frac zone in S1	FZ 43 FZ 30
	15.0	3.0	140/77	60	>10	Single joints with-out mine-raliz	Not sharp	7.0	3.0	210	2.0	fairly sh	--	Bel. to S1 biotite layer	FZ 32
	65.0	8.0	142/77	55	4-8	Biotite-chlorite layer	Fairly sh	10.0 (2)	8.0	220	8.0	F: fairly sh S: very sh	--	Bel. to S1	FZ 26
	78.0	0.5	--	--	5	Biotite-chlorite layer	Sharp	9.0	1.0	--	--	Fairly sh	--	Qz vein	
	112.5	0.2	122/70	78	core loss	Joints w chlorite	Very sharp	1.0	0.5	240	0.5	Very sh	water out-flow	Open fracture (hole)	FZ 14
003	90.0	0.5	140/77	60	6	Joints w chlorite	Very sharp	5.0	0.2	200	0.2	Very sh			FZ 43
	99.0	9.0	140/77 303/81	60 64	6	Joint w chlorite and biotite	Not sharp	7.0	9.0	210	9.0	Diffuse borders	water out-flow	Distinct peaks	FZ 43
	148.0	0.5	136/75	64	5	Joints w epidot	Sharp	10.0	0.5	--	--	Sharp			
Min/max		0.2-9			5-10			1-10	0.2-9						
Average		3.0	140/77 303/81	60 64	8	Single joints more or less mi-neraliz with biotite shist	Sharp	6.5	3.0	220	3.5	Sharp	water out-flow	Mostly S1 and K4	

Table AT 2: Fracture and shear zones identified in the boreholes BOUS 85.001/002/003

	Geometry				Geology			Geophysics					Remarks		
Bore-hole	Pos. m	Width m	Az/Dip deg	Bha deg	Tect. fr/m	Petrography	Transition	Res kohmm	Resw m	T.time μs/m	S-w m	Transition	Hydro-logy	General	No. in final model
001	75.0	2.0	250/70	38	1	Qz leached	Fairly sh	9.0	2.0	225	2.0	Fairly sharp	--	Neutron resp.	
002	68.5	0.5	--	--	8	Qz vein + biotite layer	Very sh	3.0	1.5	220	1.5	Fairly sharp	--	Tectonite near neu-tron resp	
	80.2	0.7	--	--	2	Qz leached	Smooth	6.0	0.5	200	0.5	F: fair sh S: smooth	--	Neutron resp.	
	94.5	1.0	--	--	2	Qz leached Cl enriched	F: sharp S: fairly sharp	4.0	3.0	180	--	F: sharp S: fairly sh	--	Neutron resp.	
003	20.0	1.2	--	--	0	Qz leached	Smooth	10.0	1.5	220	1.5	Fairly sharp	--	Stand out in com-pact rock	
	76.5	0.7	--	--	0	Qz leached	F: smooth S: sharp	6.0	0.5	210	0.5	Very sharp	--	Leached zone v dist frac biotite layer	
Average		1.0	--	--	low	Qz leached	Often smooth	6.3	1.5	210	1.0	Fairly sharp	--	Neutron resp.	

Table AT 3: Hydrothermally altered granite identified in the boreholes BOUS 85.001/002/003

	Geometry				Geology			Geophysics					Remarks		
Bore-hole	Pos. m	Width m	Az/Dip deg	Bha deg	Tect. fr/m	Petrography	Transition	Res kohmm	Resw m	T.time µs/m	S-w m	Transition	Hydro-logy	General	No. in final model
001	19.0	0.5	--	--	0	Kakirite	Sharp	25.0	0.5	190	--	Fairly sharp	--	Not dis-dinct	KA 2
002	32.5	0.1	--	--	single joint	Biotite layer	Very sh	5.0	0.2	--	--	Very sharp	--		BL 2
	55.5	--	142/80	58	4	Set of Qz veins	Very sh	9.0	0.3	220	0.4	Sharp	--		

Table AT 4: Other prominent structures identified in the boreholes BOUS 85.001/002/003

	RADAR						GEOLOGY						REMARKS
No.	No. Radar	Orientation	Radar Localisation (m)	∢	Distance from borehole (m)	Intensity	Outcrop (m)	System	Dip Orientation (o)	Petrogr.	Fractures per m	Orientation of zone	
L2	1/8	CH	US1: (-115)	20	35-70	strong	--	--	--	--	--	215/steep	
	--	MAG:G	--	--	--	--	MAT: 990 (?)	--	--	basic patches	--		
L4	1/8,8' (2/22?)	CH	US1	0-35	20-55	strong	--	--	--	--	--	200/steep	apophysys? (1/8')
L6	1/1	CH,S	US1: 12	35	0-30	good	--	--	--	--	--	235/steep	
	--	US1:G	--	--	--	--	US1: 13-13.5	--	--	lamprophyre	--		
L8	1/9'	CH	US1	0-15	40-50	strong	--	--	--	--	--		
	2/11'	--	US2	0- 5	20-25	strong	--	--	--	--	--	200/steep	
	--	LAT:G(?)	--	--	--	--	LAT: 56-59			3 lamp.			
L10	1/9	CH	US1	--	30-60	strong	--	--	--	--	--		
	2/2	CH,S	US1:6	--	0-30	fair	--	--	--	--	--	215/steep	
	2/3	--	US2:6	25	0-50	--	--	--	--	--	--		
	--	US2:G	--	--	--	--	US2: 5-7	--	--	lamp.	--		
	--	MAT:G	--	--	--	--	MAT: 84.5-86	--	--	lamp.	--		
L12	1/13	--	US1	0-45	60-110	strong	--	--	--	--	--		missing in enclosure 14+15
	2/26	--	US2	0	10-15	fair	--	--	--	--	--	200/steep	
L14	(1/16?)												
	1/14	CH	US1	10-20	80-100	strong	--	--	--	--	--		
	2/11	--	US2	0-10	20-35	strong	--	--	--	--	--	205/steep	
	3/17	--	US3	0	110	good	--	--	--	--	--		
		LAT:G	--	--	--	--	LAT:106-107.5	--	--	2 lamp.	--		
							LAT: 113.5-117	--	--	lamp.	--		

Table AT 5: Final geological model - lamprophyres

	RADAR						GEOLOGY						REMARKS
No.	No. Radar	Orientation	Radar Localisation (m)	∠	Distance from borehole (m)	Intensity	Outcrop (m)	System	Dip Orientation (o)	Petrogr.	Fractures per m	Orientation of zone	
L16	(1/16')	CH	US1	0-10	100-110	strong	--	--	--	--			
	2/12	--	US2	0-10	40-50	strong	--	--	--	--	--	200/steep	
	3/16	--	US3	0	85	--	--	--	--	--	--		
	--	LAT:G	--	--	--	--	LAT:127-132	--	--	lamp.	--		
	--	BOBK:G	--	--	--	--	BOBK85.008 30-32 and 40-40.5	--	--	lamp.	--		
	--	BOBK:G	--	--	--	--	BOBK85.010 30.5-35.5	--	--	lamp.	--		
	--	BOGS:G	--	--	--	--	BOGS84.041 A: 182-	--	--	lamp.	--		
L18	3/5	S	US3:62	35-50	0-40	strong	--	--	--	--	--		
	2/17(?)	--	--	35	70-110	strong	--	--	--	--	--	235/steep	
	--	US3:G	--	--	--	--	US3:61.5-65	--	--	lamp.			
L20	3/8 3/9(?)	CH,S	US3:106	0-40	0-40	strong	US3: 107	--	--	--	--		
	--	WT:G	--	--	--	--	WT:87-88	--	--	lamp.	--	230/steep	water out-flow
	--	SB2:G	--	--	--	--	BOSB80.002 95.5-96.5	--	--	2 lamp.	--		
L22	3/10	CH,S	US3:114	40-50	0-60	strong	--	--	--	--	--	230/steep	
	--	WT:G	--	--	--	--	WT:92-95	--	--	3 lamp.	--		water outfl.
	--	US3:G	--	--	--	--	US3-115.5-116.5	--	--	lamp.	--		water outfl.
L24	3/11	CH,S	US3:138	10-20	0-20	strong	--	--	--	--	--	220/steep	
	--	US3:G	--	--	--	--	US3:137.5-138.5	--	--	lamp.	--		
L26	3/14	--	US3	0-30	20-50	strong	--	--	--	--	--	220/steep	
L28	3/15	--	--	20	50-80	strong	--	--	--	--	--	220/steep	

Table AT 5: Final geological model-lamprophyres (continuation)

	RADAR						GEOLOGY						REMARKS
No.	No. Radar	Orientation	Radar Localisation (m)	∢	Distance from borehole (m)	Intensity	Outcrop (m)	System	Dip Orientation (o)	Petrogr.	Fractures per m	Orientation of zone	
FZ2	1/11	CH	US1	30-40	25-50	strong	--	--	--	--	--	175/steep	
FZ4	1/10	CH	US1: (157)	40	20-50	weak	--	s_2	--	--	--	160/steep	cross-hole can be observed over a long distance
	(2/17?)	(S)											
FZ6	1/7	CH	US1:133	35	0-60	good	--	s_2		--	--	165/steep	
FZ8	1/6	CH	US1:115	35	0-50	good	--	--	--	--	--	165/steep	
	2/16?	--											
FZ10	1/4	--	US1:79	30	0-30	good	US1:78.5-79.5	--	160	fract.Z.	>10(?)	170/steep	
	1/3	S	US1:76	25	0-15	good				fract.Z.			
FZ12	2/24	S	US2:145	50	0-30	weak	US2:144-147	--	140-155	fract.Z.	2:	150/steep	
		US1:G	--	--	--	--	US1:78.5-79.5	--	160	fract.Z.	>10(?)		
FZ13	--	US1:G	--	--	--	--	US1:80.5-85	k_4	115	fract.Z.	3	120/steep	
	--	US2:G	--	--	--	--	US2:104-106		115	fract.Z.	3		
FZ14	1/21	S	US1:79	65	0-15	very weak	US1:78.5-85	--	110-135	fract.Z.	>(10)?		
	--	US2:G	--	--	--	--	US2:112-113.5	--	125	fract.Z.	4	130/steep	water out-flow
	--	MAT:G	--	--	--	--	MAT:900-925		117-130	fract.Z.	2(?)		
FZ16?	2/13?	--	US2:(160	25	10-60	strong	--	s_3	--	--	--	175/steep	

Table AT 6: Final geological model - fracture and shear zones

	RADAR						GEOLOGY						REMARKS
No.	No. Radar	Orientation	Radar Localisation (m)	∢	Distance from borehole (m)	Intensity	Outcrop (m)	System	Dip Orientation (o)	Petrogr.	Fractures per m	Orientation of zone	
FZ18	2/10?	--	US2:116	30	0-30	strong	--	--	--	--	--	170/steep	
FZ20	3/19?	CH?	US2:(260)	50	95-150	rel.strong	--	--	--	--	--	150/steep	
FZ21	1/12?		US1:(220)	25	40-75	good	--	--	--	--	--	--	
	2/8 (2/9?)	S	US2:95	30	0-25	fair	US2:96	k_1	240	fract.Z.	3	230/steep	
FZ22	1/17	--	US1:(-10)	35-45	10-80	strong	--	--	--	--	--		
	2/7	S	US2:76	40	0-40	strong	--	--	--	--	--	160/steep	
	3/18?	--	US3:(280)	40	85-150	strong	--	--	--	--	--		
	--	US2:G	--	--	--	--	US2:85-92	s_2	160	fract.Z.	2		
FZ24	2/6	S	US2:64	25	0-25	v. strong						175/steep	
	--	US2:G	--	--	--	--	US2:65+69	s_3	175	fract.Z.	2		
FZ26	2/5	S	US2:64	80	0-60	strong						145/steep	water outfl.
	--	US2:G	--	--	--	--	US2:61-70	--	140	fract.Z.	2		
FZ28	2/19	S	US2:(27)	40	20-70	good						160/steep	water outfl.
	--	US2:G	--	--	--	--	US2:14-23	s_2	160	fract.Z.	1		
FZ30	2/1(?)	(Sabis fehlt)	US2:3	25-55	0-75	good						170/steep	
	--	US2:G	--	--	--	--	US2:1.5	--	170	fract.Z.	>10(?)		
		LAT:G	--	--	--	--	LAT:80	--	180	shear Z.	--		
FZ32	2/23	S	US2:14	60-80	0-70	weak	--	--	--	--	--	125/steep	water outfl.
	--	US2:G	--	--	--	--	US2:14.5-16.5	--	125	fract.Z.	5		
FZ34	2/14	--	US2: (190)	25-30	25-70	strong	--	--	--	--			
	3/21	--	US3: (-50)	25-30	70-85	strong	--	--	--	--	--	230/steep	
	--	BK:G	--	--	--	--	BK	k_1	230	fract.Z.	?		

Table AT 6: Final geological model - fracture and shear zones (continuation)

	RADAR						GEOLOGY						REMARKS
No.	No. Radar	Orientation	Radar Localisation (m)	∢	Distance from borehole (m)	Intensity	Outcrop (m)	System	Dip Orientation (o)	Petrogr.	Fractures per m	Orientation of zone	
FZ36	2/15	--	US2: (200m)	30	35-95	strong	--	--	--	--	--		
	3/20	--	US3: (-40m)	25	50-75	strong	--	--	--	--	--	230/steep	
	--	BK:G	--	--	--	--	BK	k_1	230	fract.Z.	?		
FZ38 =L18													
FZ40	3/13	CH	US3: (162)	45	20-100	strong	--	--	--	--	--		(FZ28?) faulted
FZ41	3/12	S	US3:148	35	0-60	--	--	--	--	--	--		
	--	US3:G	--	--	--	--	US3:136-139	--	165	fract.Z.	3		
FZ42	--		US3:148	35	0-60	strong	--	--	--	--	--		faulted?
	2/20	--	US2:(-55)	40	40-110	strong	--	--	--	--	--	165/steep	
	--	LAT:G	--	--	--	--	LAT:123	--	165	fract.Z.	3(?)		
	--	BOGS:G	--	--	--	--	BOGS:141-143	s_2	160	fract.Z.	4		
	--	US3:G	--	--	--	--	US3:117-125	--	165	fract.Z.	2		
FZ44	3/9	--	US3:108	30-35	0-40	fair	--	--	--	--	--	160/steep	faulted?
	--	BK:G	--	--	--	--	BK	--	160	fract.Z.	?		water outflow
	--	US3:G	--	--	--	--	US3:106-109 (117-125?)	--	--	fract.Z.	>10(?)		water outflow

Table AT 6: Final geological model - fracture and shear zones (continuation)

	RADAR						GEOLOGY						REMARKS
No.	No. Radar	Orientation	Radar Localisation (m)	∢	Distance from borehole (m)	Intensity	Outcrop (m)	System	Dip Orientation (o)	Petrogr.	Fractures per m	Orientation of zone	
FZ43	/26	S	US3:93	70	0-35	weak	--	--	--	--	--		
	--	MAT:G	--	--	--	--	MAT:1055-1075	s_1	135	fract./shear Z.	2?		water outflow
	--	LAT:G	--	--	--	--	LAT:74-75	s_1	140	shear Z.	--		water outflow
	--	BK:G	--	--	--	--	BK	s_1	135	fract.Z.	?	135/steep	water
	--	SB1:G	--	--	--	--	SB1:80-90	s_1	145	fract.Z.	2		outflow
	--	US2:G	--	--	--	--	US2:2-5	?	?	fract.Z.	>10		
	--	US3:G	--	--	--	--	US3:86-104	--	130	fract.Z.	3		water outflow
FZ45	3/4	S	US3:59	75	0-20	--	--	--	--	--	--		
	--	LAT:G	--	--	--	--	LAT:83-107	s_1	130	fract./shear Z.	2		water outflow
	--	SB1:G	--	--	--	--	SB1:66-69	s_1	140	fract.Z.		130/steep	
	--	BK:G	--	--	--	--	BK	s_1	130	fract.Z.	?		
	--	US3:G	--	--	--	--	US3:58-62	s_1	140	fract.Z.	3		

Table AT 6: Final geological model - fracture and shear zones (continuation)

	RADAR						GEOLOGY						REMARKS
No.	No. Radar	Orientation	Radar Localisation (m)	∢	Distance from borehole (m)	Intensity	Outcrop (m)	System	Dip Orientation (o)	Petrogr.	Fractures per m	Orientation of zone	
KA2	1/2 --	-- --	US1:20 --	35 --	0-40 --	fair --	-- US1:18.5 -19	-- --	-- --	-- Kakirite	-- 0	165/steep	
BL2	2/4 --	-- US2:G	US2:32 --	25 --	0-25 --	fair --	-- US2:32.5	-- s_3	-- 170	-- biotite layer	-- 0	180/steep	
BL4	3/1 -- --	-- US3:G LAT:G	US3:16m -- --	30 -- --	0-45 -- --	weak -- --	-- US3:14.7	-- s_3	-- SE	-- biotite layer	-- 0	170/steep	
BL6	3/2 --	-- US3:G(?)	US3:45 --	30-35 --	0-45 --	good --	-- US3:45.5	-- s_3	-- SE	-- biotite layer	-- 0	170/steep	

Table AT 7: Final geological model - biotite layers and kakirites